

Dissertation
submitted to the
Combined Faculties for the Natural Sciences and for Mathematics
of the Ruperto-Carola University of Heidelberg, Germany
for the degree of
Doctor of Natural Sciences

presented by
Diplom-Biologin
Michaela Söhn
born in: Wiesbaden
Oral-examination:

The function of the lipid phosphatase MTMR7 in anti-EGFR therapy resistance of colorectal cancer (CRC)

Referees: Prof. Dr. Stefan Wölfel
Prof. Dr. Jonathan Sleeman

Acknowledgement

Firstly, I would like to express my sincere gratitude to Prof. Matthias Ebert for giving me the opportunity to perform this work at the II. Medical Department of the Medical Faculty Mannheim, University of Heidelberg.

Furthermore, I would like to thank the supervisors of this thesis Prof. Dr. Stefan Wöfl and Prof. Jonathan Sleeman.

I especially want to thank PD Dr. rer. nat. Elke Burgermeister for the development of the scientific research concept, for the continuous support and supervision, her motivation and the scientific discussions.

I would like to thank the “Deutsche Krebsforschungszentrum” (DKFZ) and the Israel Ministry of Science, Technology and Space (MOST) for the joint research funding granted to Prof. Rony Seger (PhD) and PD Dr. Elke Burgermeister (DKFZ-MOST Ca158), which made the realization of my work possible.

I further would like to thank our Israeli cooperation partner Prof. Rony Seger for the exchange of ideas and reagents (plasmids).

Furthermore, I want to thank Prof. Dr. Carsten Schultz, Dr. Norbert Ponielies for carrying out the proteasome assay and Dr. med. Xiaobo Zhou for examining the patch-clamp measurements.

My sincere thanks also goes to Prof. Dr. med. Norbert Gretz, Prof. Dr. med. Timo Gaiser, Dr. med. vet. Kränzlin, Bettina, Dr. rer. nat. Julia Bucher, Stefanie Uhlig, who gave access to the laboratory and research facilities.

I thank my fellow labmates for the friendly working atmosphere and stimulating discussions. In particular, I am grateful to Dr. med. Philip Weidner for the good cooperation within the research project, Fagr Eladly, a medical student, for her help with the microscopic analysis, and Frank Herweck and Sandra Schneider for their perfect technical assistance.

I would like to thank my family and friends for their support and motivation throughout writing this thesis and my life in general.

Table of contents

ZUSAMMENFASSUNG	1
SUMMARY	2
1. INTRODUCTION	3
1.1. Colorectal cancer	3
1.1.1. <i>Epidemiology</i>	3
1.1.2. <i>Environmental factors</i>	3
1.1.3. <i>Molecular pathways of colorectal cancer</i>	4
1.1.4. <i>Classification of colorectal cancer</i>	5
1.1.5. <i>Treatment</i>	7
1.2. Myotubularins	9
1.2.1. <i>Structure and substrate specificity</i>	10
1.2.2. <i>Association with human disease</i>	11
1.2.3. <i>Inactive myotubularins, protein complex formation and cellular functions</i>	12
1.2.4. <i>MTMR7 and PPARγ</i>	13
1.3. Aim of the thesis	14
2. MATERIAL AND METHODS	16
2.1. Materials and Equipment	16
2.2. Software and Bioinformatics	21
2.3. Cell culture	21
2.3.1. <i>Growth conditions</i>	21
2.3.2. <i>Transient transfection of human cell lines</i>	21
2.3.3. <i>Cell stimulation</i>	21
2.4. Protein preparation and analyses	22
2.4.1. <i>Total cell lysate</i>	22
2.4.2. <i>Total tissue lysate</i>	22
2.4.3. <i>Subcellular fractionation of cells</i>	23
2.4.4. <i>Coimmunoprecipitation</i>	23
2.4.5. <i>Ras pulldown activity assay</i>	23
2.4.6. <i>Western Blot</i>	24
2.4.7. <i>Luciferase reporter gene assay (SRE, PPRE)</i>	25
2.5. Nucleic acid preparation and analysis	26
2.5.1. <i>RNA extraction and purification of cells</i>	26
2.5.2. <i>RNA extraction and purification of tissue</i>	26
2.5.3. <i>cDNA-synthesis</i>	26
2.5.4. <i>qPCR</i>	26
2.5.5. <i>Agarose gelelectrophoresis</i>	27
2.6. Immunohistochemical methods	27
2.6.1. <i>Preparation of mouse tissue</i>	27
2.6.2. <i>Immunofluorescence staining of cells</i>	27
2.6.3. <i>Immunofluorescence staining of tissue</i>	28
2.6.4. <i>Immunohistochemistry</i>	28
2.7. Proximity ligation assay	29
2.8. Molecular cloning	30
2.9. Patch-clamp	31
2.10. Ubiquitin Immunoblotting and Proteasome Activity	32
2.11. Data collection and Statistics	33

3. RESULTS	34
3.1. Expression of MTMR7 in colorectal cancer cell lines and tissues	34
3.1.1. <i>mRNA expression in human CRC cell lines and mouse organs</i>	34
3.1.2. <i>Protein expression in human colorectal cancer cell lines and mouse organs</i>	35
3.2. Subcellular localization of MTMR7	37
3.3. Interaction between PPAR γ and MTMR7	38
3.3.1. <i>MTMR7 forms a complex with PPARγ</i>	38
3.3.2. <i>MTMR7 reduces nuclear amount of phosphorylated PPARγ protein</i>	40
3.3.3. <i>MTMR7 activates transcriptional response of PPARγ</i>	41
3.3.4. <i>MTMR7 enhances PPARγ target gene expression</i>	42
3.3.5. <i>MTMR7 promotes membrane retention of EGFR and reduces nuclear EGFR</i>	43
3.3.5.1. <i>MTMR7 influences EGFR and pan-RAS protein expression</i>	46
3.4. Down-regulation of KRAS by MTMR7	46
3.4.1. <i>MTMR7 reduces the activity and total protein levels of pan-RAS in KRAS-mutated CRC cells</i>	46
3.4.2. <i>RAS is not degraded by the proteasome</i>	48
3.4.3. <i>RAS is not degraded by the lysosome</i>	50
3.4.4. <i>Changes in membrane potential promote RAS down-regulation</i>	51
3.4.4.1. <i>KCl promotes RAS reduction and P-ERK 1/2 inhibition in colorectal cancer cell lines</i>	51
3.4.5. <i>PPARγ drug agonist does not promote MTMR7-mediated RAS down-regulation</i>	56
3.5. Effect of MTMR7 on therapy-resistance	57
3.5.1. <i>Knockdown of MTMR7 promotes proliferation of human colorectal cancer cell lines</i>	57
3.5.2. <i>MTMR7 sensitizes human KRAS-mutated CRC cells to mTOR-/RAF kinase-inhibitors</i>	58
3.5.3. <i>Influence of MTMR7 on cetuximab treatment</i>	59
3.5.4. <i>MTMR7 peptide inhibits proliferation of human KRAS-mutated CRC cell lines</i>	60
3.5.4.1. <i>Effect of MTMR7 peptide on RAS-ERK 1/2 signaling</i>	61
3.5.4.2. <i>MTMR7-peptide reduces serum response element activation</i>	62
3.6. <i>In vivo</i> analysis of KRAS signaling in <i>Apcmin/+</i> x <i>Cav1-KO</i> mice	63
3.6.1. <i>Therapy of Apcmin/+ x Cav1-KO mice with an HSP90 inhibitor</i>	63
3.6.2. <i>Therapy influence on PPARγ-target gene expression</i>	64
3.6.2.1. <i>17-DMAG therapy decreases P-ERK 1/2 levels in Apcmin/+ x Cav1-KO mice</i>	65
3.6.3. <i>Therapy of Apcmin/+ x Cav1-KO mice with rosiglitazone</i>	67
4. DISCUSSION	68
4.1. Outlook	77
5. ABBREVIATIONS	78
6. REFERENCES	81
7. APPENDIX	94
7.1. Interaction between MTMR7-PPAR γ and HSP90 (CoIP)	94
7.2. Melting curves of realtime PCRs	94
7.3. RAS down-regulation does not take place on the mRNA level	97
7.4. Colocalization between MTMR7 and PH-domains of AKT and PLC δ	97

Parts of this study were already published in:

1. Myotubularin-related protein 7 inhibits insulin signaling in colorectal cancer.

Weidner P*, **Söhn M***, Gutting T, Friedrich T, Gaiser T, Magdeburg J, Kienle P, Ruh H, Hopf C, Behrens HM, Röcken C, Hanoch T, Seger R, Ebert MP, Burgermeister E. Oncotarget. 2016 Aug 2;7(31):50490-50506. doi: 10.18632/oncotarget.10466.

2. Subcellular compartmentalization of docking protein-1 contributes to progression in colorectal cancer.

Friedrich T*, **Söhn M***, Gutting T, Janssen KP, Behrens HM, Röcken C, Ebert MP, Burgermeister E. EBioMedicine. 2016 Jun;8:159-72. doi: 10.1016/j.ebiom.2016.05.003. Epub 2016 May 5.

*co-shared 1st author

Zusammenfassung

Dickdarmkrebs ist eine der häufigsten Tumorerkrankungen weltweit. Die größte Schwierigkeit bei der Behandlung dieser Art von Tumoren ist die intrinsische und / oder erworbene Resistenz gegen Chemotherapeutika oder gezielte Therapien. Dieser mangelnde Therapieerfolg ist oft auf Mutationen im *KRAS*-Gen zurückzuführen, die zur dauerhaften Aktivierung des RAS-Signalweges und damit zur unkontrollierten Proliferation und zum Überleben der Tumorzellen führen. Die Expression des Peroxisomen-Proliferator-aktivierten Rezeptors gamma (PPAR γ) korreliert mit einer guten Prognose bei Patienten mit kolorektalem Karzinom und kann durch die Aktivierung von RAS inhibitorischen Proteinen, wie beispielsweise PTEN, DOK1 oder Caveolin-1 eine Hemmung der RAS-Aktivität hervorrufen.

In dieser Arbeit wurde die Beziehung zwischen PPAR γ und seinem neuen Bindungspartner, dem Myotubularin-verwandten Protein 7 (MTMR7), hinsichtlich seiner hemmenden Wirkung auf den RAS-Signalweg untersucht. Die Interaktion der beiden Proteine im Zytosol von kolorektalen Karzinomzelllinien konnte durch Co-Immunopräzipitation, „Proximity Ligation Assay“ sowie Immunfluoreszenz-Co-Färbung verifiziert werden. Darüber hinaus konnte als Folge der Transfektion des MTMR7 Plasmids eine erhöhte Expression von PPAR γ -Zielgenen, wie TFF3, sowie eine erhöhte transkriptionelle Aktivität von PPAR γ festgestellt werden. Im Gegensatz dazu zeigte die subzelluläre Fraktionierung keinen Einfluss von MTMR7 auf die PPAR γ -Lokalisation.

Dieser positive Einfluss von MTMR7 auf die PPAR γ -Aktivität wurde anschließend näher differenziert, indem der Einfluss der MTMR7-Überexpression auf den RAS-Signalweg untersucht wurde. Bemerkenswerterweise reduzierte MTMR7 sowohl das aktive RAS als auch den Gesamtproteingehalt von RAS. Dieser Effekt konnte durch proteasomale / lysosomale Inhibitoren (MG132 / Chloroquin) nicht verhindert werden. Die Behandlung der Zellen mit KCl verstärkte sogar die Abnahme des RAS Proteingehalts, während Amilorid, ein epithelialer Natriumkanalblocker, diese Abnahme des RAS Proteins verhinderte.

Die Untersuchung der Wirkung von MTMR7 auf die Therapie-Resistenz zeigte, dass eine Kombinationstherapie mit Everolimus und Sorafenib die Lipidphosphatase nicht ersetzen konnte. Die Behandlung der Zellen mit einem MTMR7-Peptid verringerte jedoch die Zellproliferation signifikant. Eine weitere Untersuchung des MTMR7-Peptids zeigte, dass es in der Lage ist, die Aktivierung des „Serum-Response-Elements“ zu reduzieren, und dass es eine Tendenz zur RAS-Inhibierung besitzt.

Zusammenfassend lässt sich feststellen, dass der Tumorsuppressor MTMR7 die Abnahme des RAS Proteingehalts fördert, was zu einer geringeren ERK1/2-Aktivität führt und als Folge die transkriptionelle Aktivität des nukleären Rezeptors, PPAR γ , erhöht. Dies wiederum führt zu einer Aktivierung von Tumorsuppressorgenen wie *CAV-1*, *DOK1* oder *PTEN*.

Daher könnte die MTMR7-PPAR γ -Interaktion ein neues Ziel für die Behandlung von kolorektalen Karzinomen darstellen, bei denen mutiertes *KRAS* zu einem Therapieversagen der EGFR-Therapie führt.

Summary

Colorectal cancer (CRC) is one of the most common types of cancer worldwide. The most important difficulty of treating this type of cancer, is the intrinsic and/or acquired resistance to chemotherapeutic drugs or targeted therapies. This unresponsiveness is often due to mutations in the *KRAS* gene, leading to constitutive activation of the RAS signaling pathway and in turn to the proliferation and survival of the tumor cells. The expression of the peroxisome proliferator activated-receptor (PPAR γ) is correlated with a good prognosis in CRC patients and it is one of the candidates to inhibit RAS through the upregulation of Ras-inhibitory proteins like PTEN, DOK1 or Caveolin-1.

In this thesis, the relationship between PPAR γ and its new binding partner, myotubularin-related protein 7 (MTMR7), was evaluated concerning its inhibitory effect on RAS signaling. The interaction of the two proteins in the cytosol of colorectal cancer cell lines could be verified using coimmunoprecipitation, proximity ligation assay as well as immunofluorescence co-staining. Furthermore, the expression of PPAR γ target genes like TFF3 were upregulated and PPAR γ -responsive-element (PPRE) activity significantly enhanced upon MTMR7 transfection. In contrast, subcellular fractionation revealed no influence of MTMR7 on PPAR γ localization. This positive influence of MTMR7 on PPAR γ activity was then further elucidated by assessing the impact of MTMR7 overexpression on RAS signaling. Notably, MTMR7 reduced active RAS as well as total protein levels of RAS. This effect could not be prevented by using proteasomal/lysosomal inhibitors (MG132/Chloroquine). Treating the cells with KCl facilitated RAS reduction, whereas amiloride, an epithelial sodium channel blocker prevented its reduction.

Studying the effect of MTMR7 on therapy resistance indicated that a combination therapy using everolimus and sorafenib could not substitute for MTMR7 *in vitro*. Treating the cells with a MTMR7-peptide, though, reduced cell proliferation significantly. Further investigation of the MTMR7-peptide showed that it is capable to reduce serum response element activation and displayed a tendency of RAS-inhibition.

Conclusively, the tumor suppressor MTMR7 promotes RAS down-regulation, which leads to a reduced ERK 1/2 activation and a transcriptional activation of the nuclear receptor PPAR γ . This in turn results in the activation of tumor suppressor genes like *CAV1*, *DOK1* or *PTEN*. Thus, the MTMR7-PPAR γ crosstalk might be a new target for the treatment of colorectal cancer, where mutant *KRAS* leads to treatment failure of EGFR therapy.

1. Introduction

1.1. Colorectal cancer

1.1.1. Epidemiology

Colorectal cancer (CRC) is one of the most common types of cancer worldwide. Due to nearly one million new diagnosed cases, colorectal cancer ranks third as the most common cancer, second in terms of incidence and mortality, and fourth in cause of death with 500.000 per year (IARC Press 2014). It is a gender independent type of cancer and affects both men and women similarly (Boyle and Langman 2000, Marmol, Sanchez-de-Diego et al. 2017).

Although, colorectal cancer is not equally common throughout the world. Cases of colorectal cancer range from 9.4 % in men and 10.1 % in women worldwide. However, incidences in men and women are much higher in western countries (men 12.6 %; women 14.1 %) compared to colorectal cancer patients in non-western countries (men 7.7 %; women 7.9 %) (Boyle and Langman 2000).

Therefore, colorectal cancer has a geographical variation with 63 % of cases in developed western countries (Hagggar and Boushey 2009). For example, the incidence rate ranges from more than 40 out of 100.000 people in Australia, New Zealand, the United States, and Western Europe compared to less than 5 out of 100.000 people in Africa and some parts of Asia (Hagggar and Boushey 2009).

However, the incidence rates of colorectal cancer change with time. Recently, North America confronted a reverse trend as the incidence rate decreased. The rates declined from the mid-1980s to the mid-1990s, followed by a short period of stabilization and another declining period from 1998 to 2005 (Jemal, Thun et al. 2008). This decline could be due to new screening methods that improved the detection of polyps (Jemal, Clegg et al. 2004). This trend is not seen in Western Europe, although the incidence might be stabilizing (Jemal, Thun et al. 2008, IARC Press 2014). There is a rapid increase in incidence rates in former low-income countries that have become high-income economies like Singapore, Japan, and other Eastern European countries (Boyle and Langman 2000, Janout and Kollarova 2001).

1.1.2. Environmental factors

There are many lifestyle related habits known to be associated with an increased risk for developing polyps or colorectal cancer. The most important risk factor of developing CRC is age. Most of the tumors occur beyond the age of fifty whereas below that age the development of a carcinoma is rare (Levin, Lieberman et al. 2008).

In addition to age there might be a personal history for diseases like inflammatory bowel disease (Eaden, Abrams et al. 2001, Canavan, Abrams et al. 2006). These diseases lead to a chronic inflammation which often produces dysplasia, an abnormal cell growth. These dysplastic cells are not per se malignant, but the risk of developing into a tumor is very high.

Another risk factor that can be included in this group is a genetic predisposition for developing CRC because of a positive familial history of CRC in relatives which can be due to inherited mutations or the environment (Johns and Houlston 2001).

Lifestyle factors are also important to take into consideration. For example, a sedentary lifestyle can increase the risk of CRC development. The relationship has to be further assessed but it has been proven, that a moderate physical activity increases metabolic rates as well as gut motility and in a long term view metabolic efficiency (Robertson 2012).

In addition, a sedentary lifestyle could be the cause for obesity, another important risk factor which can be related to food intake on the one hand and high levels of visceral adipose tissue (VAT) on

the other hand. The latter is secreting proinflammatory cytokines which can cause inflammation in the colon and rectum as well as insulin resistance (Martinez-Useros and Garcia-Foncillas 2016).

In this context, nutritional habits or diet represent another risk factor. People whose diet is not balanced, meaning the intake of high animal fat (e.g. red meat), high calories and poor vegetables and fibers have a 70 % higher chance to develop colorectal cancer than patients with healthy nutritional habits. In contrast, a low fat, high vegetable and high fiber diet has a protective effect (Willett 2005, IARC Press 2014).

Furthermore, long-term smoking and alcohol intake have also been suggested to increase CRC risk (Poschl and Seitz 2004). In case of smoking the high content in carcinogens like nicotine can easily reach the intestine and promote the formation of polyps so that the chances to suffer from colorectal cancer may increase by up to 11 %. However the relationship between alcohol consumption and CRC has to be further elucidated (Botteri, Iodice et al. 2008, Cross, Boca et al. 2014).

1.1.3. Molecular pathways of colorectal cancer

There are three molecular pathways of colorectal cancer: (1) chromosomal instability (CIN), (2) microsatellite instability (MSI), and (3) CpG island methylator phenotype (CIMP).

- (1) The classical pathway is the CIN pathway which causes about 80-85 % of all colorectal cancer cases (Geigl, Obenaus et al. 2008, Grady and Carethers 2008). This pathway is characterized by imbalances in the number of chromosomes, resulting in aneuploidic tumors and loss of heterozygosity (LOH), which is due to alterations in chromosome segregation, telomere dysfunction, and defective DNA repair mechanisms. These alterations affect genes like adenomatous polyposis coli (*APC*), kirsten ras (*KRAS*), phosphatidylinositide 3-kinase (*PI3K*) and *TP53* (*tumor protein 53*), which maintain correct cell functions. Mutations in the *APC* gene lead to the import of β -catenin to the nucleus and to the transcription of tumorigenic and invasive genes. In addition, *KRAS* and *PI3K* mutations lead to a constantly active MAP kinase, resulting in cell proliferation and survival, whereas mutations in the tumor suppressor *TP53*, encoding for the cell-cycle checkpoint p53, cause uncontrolled entry in the cell cycle (Pino and Chung 2010).
- (2) The second pathway is the microsatellite instability pathway (MSI). Microsatellites are polymorphic DNA loci containing repeated nucleotide sequences which have a higher mutation rate than other areas of the DNA (Brinkmann, Klitschar et al. 1998). Alterations occur in 15-20 % of sporadic colorectal cancers and cluster in genes responsible for the repair of DNA mismatches like *MLH1* and *MSH2*. The repair of these short DNA chains is reduced in tumors, resulting in an accumulation of alterations in those regions and thus in a defective DNA mismatch repair (MMR) (IARC Press 2014).
- (3) The third pathway is the CpG island methylator phenotype (CIMP) that is based on epigenetic instability. This pathway is characterized by hypermethylation of promoter CpG island sites which result in the transcriptional inactivation of a series of tumor suppressor genes like *APC* or the DNA mismatch repair gene *MLH1* (Ahuja, Mohan et al. 1997, Weisenberger, Siegmund et al. 2006). The CIMP status is defined by five markers including *CACNA1G*, *IGF2*, *NEUROG1*, *RUNX3* and *SOCS1*. A tumor is CIMP positive if at least three markers are methylated (Al-Sohaily, Biankin et al. 2012).

1.1.4. Classification of colorectal cancer

The classical adenoma-carcinoma sequence

Like many other types of cancer, mutations in specific genes are causal for the development of colorectal cancer. These alterations can occur in tumor suppressor genes, oncogenes, as well as in genes responsible for DNA repair. Due to the origin of these mutations, colorectal cancers are classified as sporadic and inherited.

Sporadic, non-hereditary CRC are mostly derived from point mutations and occur in 70 % of all CRCs. Most of the sporadic cancers follow a specific order of mutations, which are correlated with a specific morphological state, starting with adenoma development and culminating with carcinoma formation (Fearon and Vogelstein 1990, Marmol, Sanchez-de-Diego et al. 2017).

A scheme of the development of colorectal cancer starting from normal epithelium to adenoma and finally carcinoma by accumulation of genetic abnormalities is shown in Figure 1.

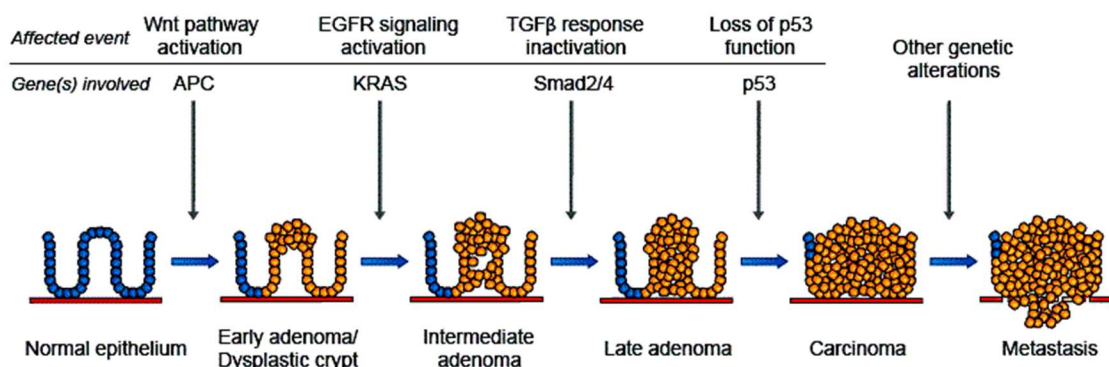


Figure 1: The Vogelstein adenoma to carcinoma sequence (modified by Davies). Scheme of the development of colorectal cancer starting from normal epithelium to adenoma and finally carcinoma by accumulation of genetic abnormalities ((Davies, Miller et al. 2005)/ copied from <http://syscol-project.eu/about-syscol/>).

The first mutation arises in a tumor suppressor gene termed *APC*, followed by mutations in *KRAS*, *TP53* and *DCC* (*Deleted in Colorectal Cancer*). The *APC* gene is located on chromosome 5q21-22 and encodes the APC protein. The latter is a negative regulator which controls β -catenin, a signaling molecule of the WNT-pathway (IARC Press 2014). Defects in the WNT-pathway lead to active c-Myc, which disturbs the balance between proliferation, apoptosis, and in the end result in a hyperproliferative epithelium (Fearon and Vogelstein 1990, Arends 2000).

The genotype/phenotype of a tumor differs, depending on where the alteration in the *APC* gene occurs. If the mutations are located in the first or the last third of the coding sequence (CDS), tumors are related to attenuated polyposis, alterations after codon 1444 to desmoid tumors while mutations in the central region show a severe phenotype (IARC Press 2014).

Additional alterations in *KRAS*, *TP53* and *DCC* trigger the formation of non-malignant adenomas, known as polyps. *KRAS* is a proto-oncogene which, due to mutations, gets activated and stimulates cell survival whereas mutations in the tumor suppressor gene *TP53* lead to its inactivation which results in a defective DNA repair and finally in the induction of growth arrest and apoptosis. These modifications lead to the imbalance between proliferation and apoptosis of epithelial cells, resulting in growth of polyps that in the end turn into carcinomas (Fearon and Vogelstein 1990, Arends 2000).

Another class of CRCs is the inherited form which accounts for 5 % of all CRCs. This form is caused by mutations which affect one allele of the mutated gene so that an additional point mutation in the second allele of the same gene leads to an accumulation of tumor cells and finally to a carcinoma.

Inherited cancers can also be classified into two groups: a polyposis and a non-polyposis group. The polyposis group includes familial adenomatous polyposis (FAP), characterized by the development of many potentially malignant polyps in the colon (Lynch and de la Chapelle 2003, Marmol, Sanchez-de-Diego et al. 2017). The second group is the hereditary non-polyposis colorectal cancer (HNPCC), also called Lynch syndrome, which is mainly caused by mutations in DNA repair mechanisms. These tumors often appear in the proximal colon and are due to microsatellite instability (MSI) (Green, Bradburn et al. 1998).

Consensus molecular subtypes (CMS)

There are often discrepancies in the classification of carcinomas which are due to differences in data processing and algorithms. To overcome these, Guinney et al. combined six independent classification systems into four molecular subtypes (CMS) with different characteristics (Figure 2).

CMS1 MSI immune	CMS2 Canonical	CMS3 Metabolic	CMS4 Mesenchymal
14%	37%	13%	23%
MSI, CIMP high, hypermutation	SCNA high	Mixed MSI status, SCNA low, CIMP low	SCNA high
<i>BRAF</i> mutations		<i>KRAS</i> mutations	
Immune infiltration and activation	WNT and MYC activation	Metabolic deregulation	Stromal infiltration, TGF- β activation, angiogenesis
Worse survival after relapse			Worse relapse-free and overall survival

Figure 2: Proposed taxonomy of colorectal cancer. CIMP: CpG island methylator phenotype; MSI: microsatellite instability; SCNA: somatic copy number alterations. Copied from (Guinney, Dienstmann et al. 2015).

Subtype CMS1 (MSI immune) accounts for about 14 % of colorectal cancers. These are microsatellite unstable, hypermutated, and have a strong immune activity. CMS2 (canonical) includes 37 % of colorectal carcinomas; which are epithelial and have a marked activation in the WNT and MYC signaling pathways. The metabolic subtype CMS3 includes carcinomas with an evident metabolic dysregulation and accounts for 13 % of colorectal cancers.

CMS4 (mesenchymal) comprises 24 % of cases and is characterized by a known activation of the transforming growth factor β (TGF- β), an invasion of the stroma and an increased angiogenesis. The remaining 13 %, which are not attributable to either CMS, are believed to be due to intratumoral heterogeneity or a transition phenotype (Guinney, Dienstmann et al. 2015). This classification of molecular subtypes is currently an appreciated reliable and most stable system for categorizing colorectal carcinomas.

1.1.5. Treatment

Classical: surgery, chemotherapy

The treatment of colorectal cancer mainly depends on the stage of the disease as well as the patient's state of health. The first choice of treatment in stage 0 or UICC stage I (localized disease) is surgery without any complementary therapy. However, most of CRCs (50-70 %) are diagnosed at more advanced stages, like stage II (cancer has spread beyond the colon into the submucosal tissue layers) or stage III (cancer has spread across the intestinal wall and into the surrounding lymph nodes). In these stages, adjuvant postoperative chemotherapy is used to destroy potentially existing micrometastases, thus increasing the recovery rate by reducing the disease recurrence.

Patients with metastatic disease (stage IV) can be classified into three different groups: unresectable metastatic disease, resectable disease, and initially unresectable disease. For the first group, palliative treatment based on chemotherapy is used to control tumor growth and improve the quality of life of these patients. Therapy of patients with resectable disease (i.e. low-tumor-burden) includes early resection of metastases combined with chemotherapy. However, the best sequence of surgery and chemotherapy has to be established. The last group, patients with initially unresectable disease first undergo chemotherapy to reduce tumor burden followed by surgery of metastases (Marin, Sanchez de Medina et al. 2012, Pox, Aretz et al. 2013).

For the adjuvant treatment of CRC, several chemotherapeutic drugs as well as targeted therapies are commonly used (Marin, Sanchez de Medina et al. 2012). In clinical praxis, standard treatments include 5-fluorouracil (5-FU), irinotecan, and oxaliplatin. 5-FU is a thymidylate synthase (TYS) inhibitor and has been used in the treatment of colorectal cancer since the 1990s (Marin, Romero et al. 2009). Interestingly, the combination of 5-FU with folinic acid (leucovorin, LV) improved the response on overall survival (OS) due to the fact that LV is stabilizing the 5-FU and TYS complex and thereby enhancing the anti-tumor effect of 5-FU (Gill, Loprinzi et al. 2004, Pox, Aretz et al. 2013, Andre, de Gramont et al. 2015).

Irinotecan, another TYS-inhibitor, is a camptothecin derivative which is used in second-line treatment for patients who do not respond to 5-FU-therapy (Rothenberg, Eckardt et al. 1996, Saltz, Cox et al. 2000). However, these drugs are mostly used in combination therapy, including irinotecan combined with leucovorin followed by 5-FU bolus and an infusion of 5-FU, called FOLFIRI (Marin, Sanchez de Medina et al. 2012).

Another chemotherapeutic drug, oxaliplatin, is often used in combination with other drugs. Oxaliplatin is a platin derivative which crosslinks metabolites with DNA resulting in the inhibition of DNA-synthesis (Graham, Mushin et al. 2004, Pox, Aretz et al. 2013). The most commonly used combination is oxaliplatin with LV and 5-FU, named FOLFOX.

Other approaches to treat CRC are targeted therapies with monoclonal antibodies (mABs) like bevacizumab (targeting the vascular endothelial growth factor; VEGF) or cetuximab (targeting the epidermal growth factor receptor; EGFR).

The EGFR is a glycoprotein, located on chromosome 7 with a size of 170 kD. It belongs to the transmembrane tyrosine kinase family and is typically activated by ligands such as TGF- α or EGF. Its activation leads to a homo- or heterodimerization and autophosphorylation of c-terminal residues resulting in activation of signaling pathways like the RAS/RAF/ERK-pathway or the PI3K-AKT-pathway and finally in survival and proliferation (Davies, Grosse et al. 1980, El Zouhairi, Charabaty et al. 2011, Hagan, Orr et al. 2013).

Since the EGFR is overexpressed in many epithelial tumors, two EGFR antagonists, cetuximab (Erbix™), and panitumumab (Vectibix™) have been approved by the Food and Drug Administration (FDA) in 2004 and 2006. Cetuximab is a chimeric immunoglobulin of the IgG1 isotype and targets the ligand binding domain of the EGF-receptor in different ways (Hagan, Orr et al. 2013).

In detail, cetuximab leads to a receptor downregulation and its reduced cell surface expression thus promotes receptor internalization and degradation. Additionally, effects on DNA transcription and repair are inhibited through blocking the nuclear import of the EGFR. Last but not least, the receptor dimerization is inhibited sterically (El Zouhairi, Charabaty et al. 2011). Furthermore, combinations of FOLFOX together with monoclonal antibodies are in use and reported to improve efficiency of colorectal cancer treatment (Preneen, Tejpar et al. 2010).

A new, upcoming therapy targets the immune system, e.g. the cell surface receptor programmed death (PD1/PDL1) pathway, also termed “immune checkpoints”. These receptors are often upregulated in tumors such as bladder cancer, non-small-cell lung cancer and melanomas which can be circumvented by using antibodies like pembrolizumab to block the system. This therapy has already been shown to be effective in 40 % of patients with MSI-H carcinomas in the UICC stage IV whereas it did not show any effect in MSS colorectal cancers (Le, Uram et al. 2015).

Prevention

Many approaches to avoid the development of colorectal cancer have been discussed. The most important approach is endoscopic screening which is lowering the risk of CRC by diagnosing CRC cases 2-3 years before showing symptoms (Cunningham, Atkin et al. 2010). However most of the chemopreventive drugs are controversial discussed.

For instance, calcium intake has been reported to reduce the risk of developing CRC by 10-15 % (Cho, Smith-Warner et al. 2004). This may be due to direct effects on epithelial cells or indirectly by binding bile acids and fatty acids in the colonic lumen. Some studies have shown that calcium intake reduces the risk of secondary adenomas by 15 % (Baron, Beach et al. 1999, Bonithon-Kopp, Kronborg et al. 2000) whereas others did not determine any significant protective effect (Wactawski-Wende, Kotchen et al. 2006).

Same is true for fiber-rich diets, which may decrease carcinogens in the colonic lumen and thereby reduce the risk of colorectal cancer development. However, this effect could not be confirmed in a meta-analysis by Park et al., 2005. Nevertheless, the American Institute for cancer research is recommending fiber-rich diets to “probably” prevent CRC.

Furthermore, vitamin D is linked to reduce the risk of colorectal cancer by 29 % (Garland, Garland et al. 1999, McCullough, Robertson et al. 2003). Other substances like cyclooxygenase (COX) inhibitors are also discussed to prevent colorectal cancer by about 40 %. These substances inhibit COX2 activity, which is often upregulated in CRC, and thereby the synthesis of prostaglandins which is associated with cancer development (Jaffe 1974, Bennett and Del Tacca 1975). In addition, the chronic use of non-steroidal anti-inflammatory drugs such as aspirin, have reduced the risk of developing colorectal cancer. Furthermore physical activity is suggested to be protective (Clapper, Chang et al. 2001).

Resistance

The most important difficulty of treating cancer, and colorectal cancer in particular, is the intrinsic and/or acquired resistance to chemotherapeutic drugs or targeted therapies. These resistances limit the effectiveness of current therapies and are believed to cause treatment failure in over 90 % of patients with metastatic disease (Cunningham, Humblet et al. 2004).

One example for an intrinsic resistance is the unresponsiveness of patients to EGFR-based therapy with cetuximab.

This is due to mutations in the *KRAS* gene, located on chromosome 12 and 13, encoding for the small GTPase downstream of EGFR (De Stefano and Carlomagno 2014). This is also supported by Lievre et al., who showed that *KRAS* mutations occur in 13 out of 30 tumors and that 68 % of

the nonresponders to cetuximab had that alteration whereas it wasn't detected in the responding group (Lievre, Bachet et al. 2006).

RAS proteins are small GTPases that are the most frequently mutated proteins in cancers and other diseases. Moreover, small GTPases are involved in the regulation of important cellular functions such as proliferation, differentiation, and apoptosis (Malumbres and Barbacid 2003).

In mammalian cells, three isoforms of RAS proteins are expressed: Kirsten RAS (KRAS4B, KRAS), Harvey RAS (HRAS) and neuroblastoma RAS (NRAS). These proteins can be present in an active (GTP-bound) or inactive (GDP-bound) state (Barbacid 1987).

All isoforms contain an almost identical G domain (residues 1-165) that binds guanosine nucleotides, whereas the C-terminal end (last 24-25 aa) is a variable region that differs in the isoforms and is necessary for the membrane anchoring. Thus, the specific subcellular locations of the isoforms are due to changes in their C-terminal domain.

The synthesis of RAS proteins occurs in the cytosol where they are found as hydrophilic proteins displaying different C-terminal sequences for several post-translational modifications e.g. farnesylation (CAAX), proteolysis (AAX), or cysteine methylation in the endoplasmic reticulum (Calvo, Agudo-Ibanez et al. 2010, Gelabert-Baldrich, Soriano-Castell et al. 2014).

Furthermore, active KRAS converts GTP to GDP, thus inactivating itself. The guanosine nucleotide exchange factor (GEF) catalyzes the release of the GDP molecule, facilitating the reactivation of KRAS through binding a new GTP molecule. Reactivated KRAS then binds to the serine/threonine kinase rapidly accelerated fibrosarcoma (RAF) (Bergstraesser, Hoeger et al.), which phosphorylates and thus activates the mitogen-activated kinase (MEK). Activated MEK then phosphorylates extracellular signal-regulated kinase (ERK), which subsequently activates transcription factors to increase transcription of genes that promote cell proliferation (Normanno, Tejpar et al. 2009, Lee and Kopetz 2015). Thus, mutations in the *KRAS* gene lead to stimulation in survival and proliferation.

Consequently, targets downstream of KRAS, like RAF or mTOR, may hold the promise to overcome therapy resistance.

There are many other molecular mechanisms of therapy resistance which are due to EGFR/ HER-2 oncogene amplification (Gnjatic, Wheeler et al. 2009, Bertotti, Papp et al. 2015), the reactivation of proangiogenic factors like the vascular endothelial growth factor (VEGF) (Kerbel, Yu et al. 2001) or mutations in the phosphatidylinositol 3-kinase (PIK3CA) (Samuels and Velculescu 2004).

1.2. Myotubularins

Myotubularins are a large family of 16 conserved proteins which dephosphorylate phosphatidylinositol(3)phosphate (PI(3)P), and PI(3,5)P₂ and thereby form PI and PI(5)P. They are involved in the control of cellular processes such as endocytic trafficking, autophagy, and cell proliferation.

The first described myotubularin was MTM1, followed by 15 other family members which are called myotubularin-related phosphatases (MTMR1-15). Seven of these phosphatases are inactive due to mutations within the catalytic motif. Nevertheless, some of these proteins are still involved in cellular functions and can cause diseases (Begley, Taylor et al. 2006).

Many myotubularins like MTMR1-6 and 12 are ubiquitously expressed in many tissues and cell types (Laporte, Blondeau et al. 1998, Nandurkar, Caldwell et al. 2001, Zhao, Qi et al. 2001), whereas some of them are tissue specific like MTMR5 in the testes or MTMR7, which is mainly expressed in the brain (Laporte, Blondeau et al. 1998, Firestein, Nagy et al. 2002).

1.2.1. Structure and substrate specificity

These lipid phosphatases consist of a PH-GRAM- (Pleckstrin-Homology-Glycosyltransferase), a RID (Rac-induced recruitment) domain, a dual specific tyrosine phosphatase C(X)5R-containing domain (PTP domain), a conserved SID- (Set Interaction Domain), and a coiled-coil-domain (Begley, Taylor et al. 2003, Laporte, Bedez et al. 2003, Begley, Taylor et al. 2006) (Figure 3).

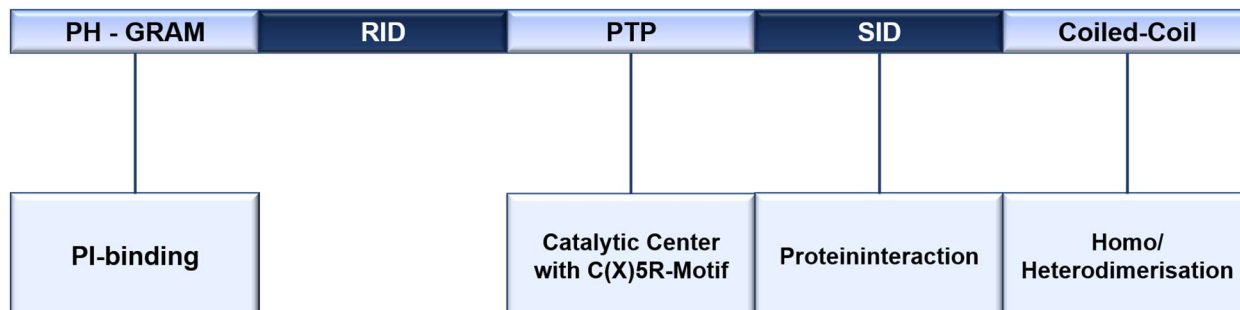


Figure 3: The schematic structure of the myotubularin protein family. PH-GRAM: Pleckstrin Homology Glucosyltransferase Rab-like GTPase Activator; RID: rac-induced recruitment domain; PTP: protein tyrosine phosphatase domain; SID: set interaction domain; "Coiled-coil" -Heterodimerization. Modified from (Hnia, Vaccari et al.)

The PH-GRAM domain mediates the interaction between enzyme and substrate through the binding of PI(5)P (Balla, Wymann et al. 2012), PI(3,5)P₂, PI(4)P and PI(3,4,5)P₃ (Berger, Schaffitzel et al. 2003), whereas the RID is a membrane targeting motif (Laporte, Blondeau et al. 2002). The PTP domain contains the substrate binding pocket with the C(X)5R active site motif (Yuvaniyama, Denu et al. 1996).

Because of their specificity for membrane embedded PI substrates, MTMs are unique among PTPs (Begley and Dixon 2005). This specificity underlies three structural characteristics: Firstly, the positive charge of the protein surface allows non-specific electrostatic interaction with negatively charged, PI-containing membranes, secondly, the dimensions of the substrate binding pocket are matched to those of the PIs, and thirdly, a selectivity towards lipophilic substrates is possible through a hydrophobic, the substrate binding pocket shielding helix (Begley and Dixon 2005).

In addition to the catalytic site, there are other MTM-typical domains that are important for the regulation of protein function: The above-mentioned RID, SID and coiled-coil domains mediate the central regulatory mechanism regarding enzymatic activity and subcellular localization. In particular, the coiled-coil heterodimerization domain mediates interaction with other myotubularins (Mochizuki and Majerus 2003, Balla, Wymann et al. 2012, Hnia, Vaccari et al. 2012), while the others either enhance them (SID) (Mochizuki and Majerus 2003) or are responsible for protein interactions with other protein classes, such as class III PI3K (Cao, Backer et al. 2008).

The myotubularins mainly use the 3-phosphorylated phosphoinositides as substrates by hydrolyzing PI(3)P and PI(3,5)P₂ at their 3-position (Taylor, Maehama et al. 2000, Zhao, Qi et al. 2001, Berger, Bonneick et al. 2002, Naughtin, Sheffield et al. 2010, Tooze and Yoshimori 2010, Velichkova, Juan et al. 2010) (Figure 4).

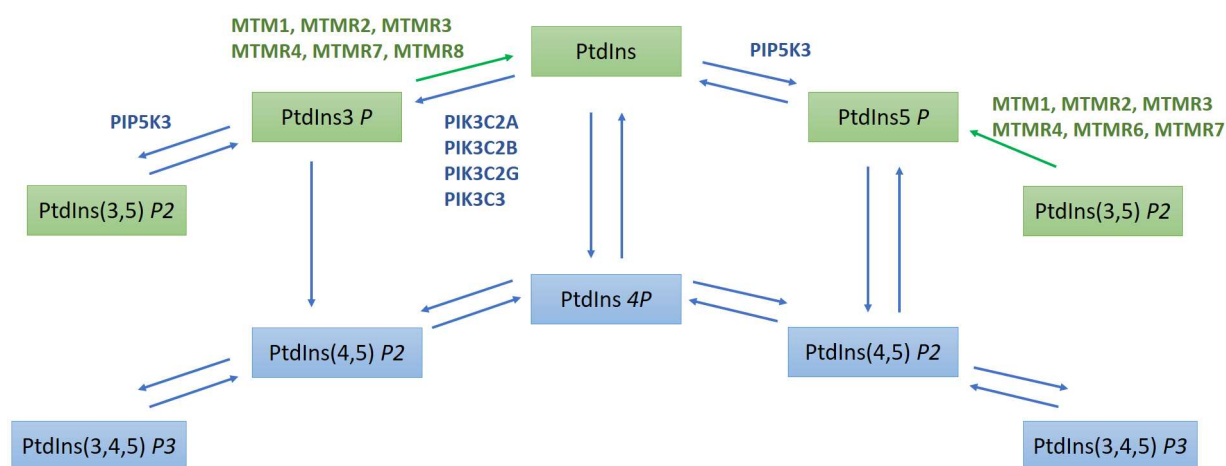


Figure 4: Substrate specificity of myotubularins. Seven different myotubularins are involved in PI metabolism. Metabolic reactions catalyzed by myotubularins are indicated in green. Adapted from (Hnia, Vaccari et al. 2012).

To understand the mechanism of action, the events of endosomal PI(3)P and PI(3,5)P₂ synthesis need to be explained. PI(3)P is produced on early and late endosomes by a type III PI3-kinase complex, consisting of a catalytic (hVsp34) and a regulatory (hVsp15) subunit (Gillooly, Morrow et al. 2000, Simonsen, Wurmser et al. 2001, Stein, Feng et al. 2003). Synthesis of PI(3)P starts with the activation of Rab5 and Rab7 GTPases on early and late endosomes (Christoforidis, Miaczynska et al. 1999, Feng, Press et al. 2001, Murray, Panaretou et al. 2002, Stein, Feng et al. 2003, Stein, Cao et al. 2005), followed by their binding and recruitment of the hVsp34/hVsp15 PI3-kinase complex and thereby activation of PI(3)P synthesis. On multivesicular endosomes PI(3)P is subsequently converted to PI(3,5)P₂ by the phosphoinositide kinase PIKfyve, leading to protein sorting into intraluminal vesicles (Rudge, Anderson et al. 2004, Nicot, Fares et al. 2006, Shisheva 2008). The synthesized products lead to the recruitment of myotubularins to membranes, where they degrade PI(3)P to PI.

The mechanism of activation/ inactivation of myotubularins was first described by Cao et al., showing that MTMR2 is interacting with the hVsp34/hVsp15 lipid kinase complex. They propose that membrane bound phosphatases begin to degrade PI(3)P until they become complexed again with hVsp34/hVsp15. This in turn leads to the steric occlusion of the phosphatase domain and the simultaneous displacement of the Rab GTPase, and thus causes the inactivation of the myotubularin (Cao, Backer et al. 2008).

Hence, myotubularins coordinate endosomal PI(3)P synthesis and degradation and thereby regulate endosomal transport.

1.2.2. Association with human disease

There are several human diseases which are due to mutations in either active or inactive myotubularins. The most prominent disorders are x-linked centronuclear myopathy (XLMTM) and Charcot-Marie-Tooth (CMT) (Laporte, Bedez et al. 2003, Robinson and Dixon 2006, Nicot and Laporte 2008).

The congenital disease XLMTM arises from mutations in *MTM1*; either loss of MTM function or the absence of MTM protein (Thomas, Williams et al. 1990, Liechti-Gallati, Muller et al. 1991). Disease occurrence varies from individual to individual and is due to the type of mutations. Generally, truncation or splice-site mutations are linked to severe forms, whereas missense mutations that occur outside of MTM functional domains, result in moderate or mild phenotypes (Nicot and Laporte 2008, Mruk and Cheng 2011). At the cellular level, the disease is most likely due to the improper regulation of PI(3)P and/ or PI(3,5)P₂, resulting in the disruption of vesicle

trafficking in the skeletal muscle of affected individuals (Mruk and Cheng 2011). XLMTM affects mainly males and is characterized by severe muscle weakness and often results in death from respiratory failure at an average age of 4 to 5 months (Laporte, Hu et al. 1996).

CMT is an inherited disorder, affecting motor and sensory neurons leading to progressive muscle weakness and atrophy in feet, legs, hands and arms. This disease is associated with mutations in the lipid phosphatases *MTMR2* and *MTMR13*, as well as with several other genes (Mruk and Cheng 2011). A mutation in the lipid phosphatase *MTMR2* leads to Charcot-Marie-Tooth disease type 4B1 whereas a mutation in its inactive binding partner *MTMR13* results in a similar clinical syndrome (Charcot-Marie-Tooth disease type 4B2) (Bolino, Muglia et al. 2000, Berger, Bonneick et al. 2002, Azzedine, Bolino et al. 2003, Senderek, Bergmann et al. 2003).

Notably, all genes involved in the development of CMT are encoding for proteins with functions in endocytosis and membrane trafficking which suggests that the pathogenesis of CMT is contributed by defects in these cellular processes (Mruk and Cheng 2011).

Furthermore, *MTMR9* gene is associated with obesity. This gene is expressed in the lateral hypothalamic area (LHA), paraventricular nucleus (PVN) and the arcuate nucleus (ARC) of the hypothalamus, and the center of food intake regulation (Yanagiya, Tanabe et al. 2007). In addition, it is located on segment 8p23-p22, which has been linked to obese phenotypes (Johnson, Luke et al. 2005).

MTMR7 gene is linked with the variant Creutzfeldt-Jakob disease, a type of brain disease within the transmissible spongiform encephalopathy (Lloyd, Mead et al. 2011, Sanchez-Juan, Bishop et al. 2012).

Finally, *MTMR3* is associated with an increased risk of gastric and colon carcinomas (Song, Kang et al. 2010).

1.2.3. Inactive myotubularins, protein complex formation and cellular functions

The myotubularins can be divided in active and inactive proteins and are localized to different cell compartments (Figure 5).

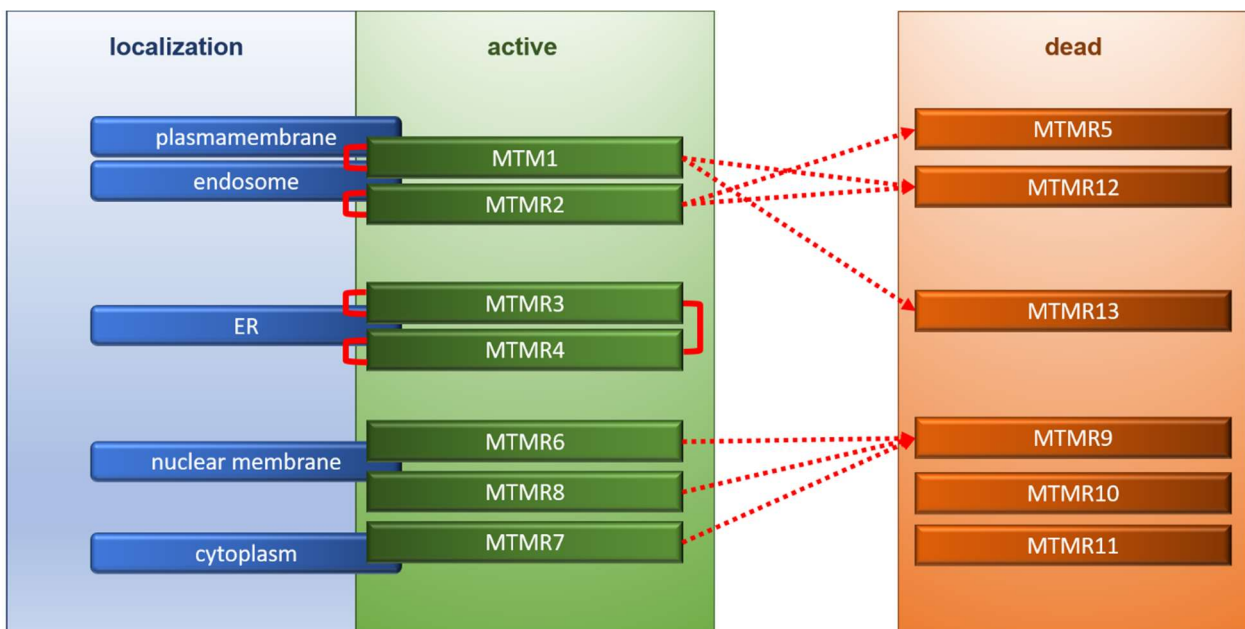


Figure 5: Localization and activity of myotubularins. 7 out of 16 myotubularins possess catalytic activity, dephosphorylating PI(3)P and PI(3,5)P₂ to PtdIns and PI(5)P. They can either homodimerize or heterodimerize into active-active (indicated by red brackets) or active-dead complexes (indicated by red arrows), which confers more precise regulation of myotubularin PI phosphatase activity. Adapted from (Hnia, Vaccari et al. 2012, Weidner 2016)

Inactive myotubularins are essential for the regulation and subcellular localization of active myotubularins (Berger, Schaffitzel et al. 2003, Kim, Vacratsis et al. 2003, Nandurkar, Layton et al. 2003, Berger, Berger et al. 2006). Inactive MTMR13, for example, forms a complex with active MTMR2 and thereby increases its activity towards PI(3)P and PI(3,5)P₂ by 10- and 25-fold. Furthermore, the subcellular distribution of the two proteins is overlapping under resting conditions while it diverges under hypo-osmotic stress situations. This fact suggests that inactive phosphatases do not only regulate the enzyme activity of the active ones but also their localization to subcellular compartments (Berger, Berger et al. 2006).

Other examples of interactions between myotubularins are the complex formation of MTM1 with MTMR12 as well as MTMR2 (Nandurkar, Layton et al. 2003, Cao, Laporte et al. 2007, Cao, Backer et al. 2008).

Inactive MTMR9 forms a complex with MTMR6, MTMR8 and MTMR7 while the last interaction requires the coiled-coil domain and leads to an increased MTMR7 phosphatase activity (Mochizuki and Majerus 2003, Lorenzo, Urbe et al. 2006).

Since myotubularins are using phosphoinositides as substrates, they play a role in the phosphoinositide signaling process. Because PI(3)P is localized to the plasma membrane and to early and late endosomes, myotubularins are regulators of endocytic trafficking like endocytosis, degradative pathways, recycling pathways, and autophagy (Gillooly, Morrow et al. 2000, Fares and Greenwald 2001, Gillooly, Raiborg et al. 2003, Xue, Fares et al. 2003, Tooze and Yoshimori 2010). One example for a recycling route is the sorting of the EGFR (Keohavong, DeMichele et al.) for degradation.

MTM1 and MTMR2 inhibit EGFR degradation (Tsujiita, Itoh et al. 2004, Berger, Tersar et al. 2011). In addition, PI(3)P are involved in autosomal initiation, a process in which portions of cellular contents are internalized into double membrane autophagosomes for degradation (Vergne, Roberts et al. 2009, Dowling, Low et al. 2010, Taguchi-Atarashi, Hamasaki et al. 2010).

Myotubularins have been initially identified as "survival" phosphatases and are said to positively regulate cell proliferation and/or inhibit apoptosis. For example, silencing of MTMR2 in cultured Schwann cells leads to decreased proliferation and enhanced caspase-dependent cell death (Chojnowski, Ravise et al. 2007).

1.2.4. MTMR7 and PPAR γ

The lipid phosphatase MTMR7 was first characterized by Majerus et al. to be specifically expressed in brain, neuronal cells, liver, kidney and the testis. MTMR7 has been localized to granules close to the nucleus and the cytosol assuming that it might be enriched in the Golgi apparatus or endosomes. It is found in a soluble form in the cytosol, where it uses free inositol-1,3-bisphosphate (Ins(1,3)P₂) as substrate (Mochizuki and Majerus 2003).

In 2016 our research group first described, the role of MTMR7 in colorectal cancer, where it inhibits the insulin-mediated activation of the AKT and ERK 1/2 signaling pathways, leading to a reduced proliferation in human colorectal cancer cells. MTMR7 protein was further downregulated in human colorectal cancer cells and many patients (Weidner, Söhn et al. 2016).

We identified the peroxisome proliferator-activated receptor gamma (PPAR γ) as a cytosolic binding partner of MTMR7 in a MALDI-MS screen (Söhn, Weidner et al., unpublished). PPAR γ belongs to the nuclear receptor superfamily of transcription factors. PPAR γ is involved in the regulation of several processes including, glucose and lipid metabolism (Polvani, Tarocchi et al. 2016), inflammation, differentiation, including tissue regeneration such as wound healing and cancer (Burgermeister and Seger 2007, Srivastava, Kollipara et al. 2014, Zurlo, Ziccardi et al. 2016).

PPAR γ is extensively expressed in brown and white adipose tissue, cells and organs of the immune system and the large intestine (Taheri, Salamian et al. 2015). It can be activated by its

natural ligands such as prostaglandin J2 derivatives or polyunsaturated fatty acids or by synthetic ones like rosiglitazone and pioglitazone, belonging to the thiazolidinedione and mostly used as anti-diabetic drugs and anti-cancer reagents (van Beekum, Fleskens et al. 2009, Peymani, Ghoochani et al. 2013). When activated, it forms a complex with the 9-cis retinoic X receptor (RXR), enters the nucleus and binds to the peroxisome proliferator response element (PPRE) (van Beekum, Fleskens et al. 2009). In the nucleus, PPAR γ initiates the transcription of genes but can also be inhibited. PPAR γ inhibition is due to constitutively active RAS, which leads to the permanent activation of MEK-1. This in turn leads to the export of PPAR γ from the nucleus to the cytosol (Burgermeister, Chuderland et al. 2007) and to the phosphorylation of ERK 1/2, which phosphorylates PPAR γ at serine 84/114 (in humans), resulting in inhibition of its transactivating potential on target gene promoters (Seger and Krebs 1995).

PPAR γ has a contradictory role on tumorigenicity. On the one hand a tumorigenic role has been described in several cancer types like bladder cancer, liposarcoma, mammary adenocarcinoma or hepatic tumors (Srivastava, Kollipara et al. 2014, Wu, Yang et al. 2016, Yousefnia, Momenzadeh et al. 2018). On the other hand, nuclear PPAR γ has been associated with good prognosis, higher survival rates and a less aggressive and metastatic phenotype in colorectal cancer patients (Ogino, Shima et al. 2009, Pancione, Forte et al. 2009). Thus, the MTMR7-PPAR γ -complex could be a druggable target for the treatment of *KRAS*-mutated CRC patients.

1.3. Aim of the thesis

The most important difficulty in treating colorectal cancer, is the intrinsic and/or acquired resistance to chemotherapeutic drugs or targeted therapies. This unresponsiveness to therapy with antibodies directed against the epidermal growth factor receptor (Karapetis, Khambata-Ford et al. 2008), is often due to mutations in the *KRAS* gene, leading to constitutive activation of the RAS signaling pathway and in turn to the proliferation and survival of the tumor cells. Thus, targets downstream of mutant RAS hold the promise to overcome therapy resistance in this patient group.

This thesis is focused on the lipid phosphatase MTMR7, which was first characterized by Majerus et al. to be specifically expressed in brain, neuronal cells, liver, kidney and the testis. MTMR7 has been localized to granules close to the nucleus and the cytosol, and is found in a soluble form in the cytosol, where it uses free inositol-1,3-bisphosphate (Ins(1,3)P₂) as substrate (Mochizuki and Majerus 2003). MTMR7 was found as a novel binding partner of the peroxisome proliferator activated-receptor gamma (PPAR γ) (Söhn, Weidner et al., unpublished). The expression of PPAR γ is correlated with a good prognosis in CRC patients and it is one of the candidates to inhibit RAS through the upregulation of Ras-inhibitory proteins like PTEN, DOK1 or Caveolin-1.

As already published, the lipid phosphatase MTMR7 inhibits the two major pathways RAF-MEK1/2-ERK1/2 and AKT/mTORC1/2 downstream of mutant *KRAS*, indicating an essential role in colorectal carcinoma (Weidner, Söhn et al. 2016). Thus, this thesis aimed to elucidate, if the MTMR7-PPAR γ -complex could be a druggable target for the treatment of *KRAS*-mutated CRC patients.

This should be achieved by (i) assessing whether the enzymatic activity of MTMR7 is modified by the activation of PPAR γ , using pharmacological ligands, (ii) determining if the PPAR γ -MTMR7 complex formation results in changes in the phosphorylation status of its lipid or protein substrates, (iii) investigating if these changes lead to a change in KRAS expression levels, (iv) examining, if the intrinsic unresponsiveness of *KRAS* mutant cells may be circumvented by the combination of PPAR γ -ligands (such as the antidiabetic drug rosiglitazone) with kinase inhibitors like RAF-inhibitors (sorafenib, vemurafenib) and mTOR-inhibitors (everolimus) downstream of mutant *KRAS*.

2. Material and Methods

2.1. Materials and Equipment

Table 1: General chemicals

Name	Company	Order number
4',6-diamidino-2-phenylindole	Roth GmbH	6335.1
1,4- Dithiothreitol (DTT)	Roth GmbH	6908.1
2-Mercaptoethanol	Sigma-Aldrich Chemie GmbH	M7522
2-Propanol	Merck KGaA	1096341000
Acetic acid ≥ 99,0 % (T)	Sigma-Aldrich Chemie GmbH	45740
Ammoniumperoxodisulfate	Roth GmbH	9592,3
Ampicillin > 99 %	Roth GmbH	K029.1
Antigen unmasking solution	Vector Laboratories	H-3300
Biozym LE Agarose	Biozym Scientific GmbH	840004
Boric Acid	Sigma-Aldrich Chemie GmbH	B6768
Bromphenol Blue	Sigma-Aldrich Chemie GmbH	B-5525
Complete Mini Protease inhibitor cocktail tablets	Roche Diagnostics GmbH	04693124062
Dithiothreitol (DTT)	Roth GmbH	1.114.740.004
Dual-Luciferase® Reporter Assay System	Promega Cooperation	E1910
DH5 alpha competent cells	Invitrogen GmbH	18265-017
Ethanol, absolute, ≥ 98 % (GC)	Sigma Aldrich	24194-5L R
Ethanol technical, 96 %	Roth GmbH	46139
Ethidium bromide (10mg/ml)	Sigma-Aldrich Chemie GmbH	15585-011
Eukitt	Sigma-Aldrich Chemie GmbH	03989
Fluorescent mounting medium	Dako North America	S302380-2
Formaldehyde 37 % ROTIPURAN	Roth GmbH	4979.2
Glycerol 99 %	Sigma-Aldrich Chemie GmbH	200-289-5
Glycine PUFFERAN ≥ 99 % p.a.	Roth GmbH	3908.3
Hemalum (Meyer)	Roth GmbH	T865.1
HEPES	Sigma-Aldrich Chemie GmbH	9105.3
Hydrochloric acid (1N)	Merck KGaA	1.090.571.000
Hydrochloric acid (37 %)	Sigma-Aldrich Chemie GmbH	435570
LB-Agar	Roth GmbH	X965.1
LB-Medium	Roth GmbH	X964.1
Magnesium chloride	Merck KGaA	5833 1000
Methanol ≥ 99,8 % (GC)	Sigma-Aldrich Chemie GmbH	32213
Milk powder	Sigma-Aldrich Chemie GmbH	T145.2
PBS Dulbecco	Merck KGaA	L182-50
Power SYBR Green PCR Master Mix	Applied Biosystems	4368577
Protein A/G Plus Agarose	Santa Cruz Biotechnology	sc-2003
Protein G Plus/Protein A-Agarose	Merck KGaA	IP05
Rotiphorese® Gel 30 (37,5 : 1)	Roth GmbH	3029.2
Roti®-Mark TRICOLOR	Roth GmbH	8271.1
Sodium Dodecyl Sulfate (SDS, ultra-pure ≥99.5 %)	Roth GmbH	2326.1
Sodium chloride	Sigma-Aldrich Chemie GmbH	31434-500G-R
Sodium orthovanadate (Na ₃ VO ₄)	Sigma-Aldrich Chemie GmbH	S6508
TEMED (N,N,N',N'-Tetramethylethane-1,2-diamin 99 %	Roth GmbH	2367.3
Top10 one shot competent cells	Invitrogen GmbH	C404010
TRIS PUFFERAN ≥ 99,9 % Ultra	Roth GmbH	5429.3

Triton® X-100	Sigma-Aldrich Chemie GmbH	1.122.980.101
Tween® 20	Roth GmbH	9127.1
Western Bright Sirius HRP substrate	Advansta Inc	K-12043-D10
X-Gal (5-bromo-4-chloro-indolyl- β -D-galactopyranoside)	Sigma-Aldrich Chemie GmbH	G5160
Xylol (mixture of isomers)	Roth	9713.1

Table 2: Cell culture reagents

Name	Company	Order number
Dimethyl sulfoxide, minimum 99,5 % GC	Sigma-Aldrich Chemie GmbH	D8418
Dulbecco's Modified Eagle Medium	Invitrogen GmbH	41966-052
Hyclone Fetal bovine serum	Invitrogen GmbH	SV 30 160.03
L-Glutamine	Invitrogen GmbH	25030-024
PBS phosphate buffered saline pH 7,4	Invitrogen GmbH	10010-056
Penicillin-Streptomycin	Invitrogen GmbH	15140-122
RPMI-1640	Invitrogen GmbH	21875-091
Thiazol Blue Tetrazolium Bromide (MTT)	Sigma-Aldrich Chemie GmbH	M 5655-1G
Trypan Blue stain (0.4 %)	Invitrogen GmbH	15250-061
Trypsin-EDTA (0.25 %), phenol red	Invitrogen GmbH	25200-056
TurboFect® in vitro transfection reagent	Fermentas GmbH	R0531

Table 3: Human cell lines

Name	Disease	Company
AGS	<i>Gastric Adenocarcinoma</i>	European Collection of Authenticated Cell Cultures (ECACC)
Caco2	Human colorectal adenocarcinoma	European Collection of Authenticated Cell Cultures (ECACC)
DLD1	Human colorectal adenocarcinoma	Deutschen Sammlung von Mikroorganismen und Zellkulturen GmbH (DSMZ)
HCT116	Human colorectal carcinoma	European Collection of Authenticated Cell Cultures (ECACC)
HT29	Human colorectal adenocarcinoma	European Collection of Authenticated Cell Cultures (ECACC)
HEK293T	Human embryonic kidney	Deutschen Sammlung von Mikroorganismen und Zellkulturen GmbH (DSMZ)
Lovo	Human colorectal adenocarcinoma	Deutschen Sammlung von Mikroorganismen und Zellkulturen GmbH (DSMZ)
PATU8902	pancreas adenocarcinoma	Deutschen Sammlung von Mikroorganismen und Zellkulturen GmbH (DSMZ)
SW480	Human colorectal adenocarcinoma	European Collection of Authenticated Cell Cultures (ECACC)

Table 4: Antibodies

Primary Antibodies		
Name	Company	Order number
MTMR7 (Full-length)	Abcam plc.	ab121222
cMTMR7	Abcam plc.	ab150458
MTMR7	MyBiosource	MBS#1497385
ERK1/2	Cell Signaling Technology	9101S

pERK1/2 (WB)	Cell Signaling Technology	9101
pERK1/2 (IHC)	Cell Signaling Technology	4370
HSP90	Santa Cruz Biotechnology	sc-7942
AKT2	Cell Signaling Technology	3063S
pAKT473	Cell Signaling Technology	4058
pAKT308	Cell Signaling Technology	2965S
PPAR γ	Cell Signaling Technology	2435
PPAR γ (H100)	Santa Cruz Biotechnology	Sc-7196
GFP	Roche Diagnostics GmbH	11814460001
HA	Roche Diagnostics GmbH	11867423001
Flag	Sigma-Aldrich Chemie GmbH	A2220
Flag	Cell Signaling Technology	2368S
Pan-RAS	Santa Cruz Biotechnology	Sc-166691
KRAS	Abcam plc.	172949
KI67	Novus Biologicals	NB600-1252
Lamin	Santa Cruz Biotechnology	Sc-20681
EGFR	Cell Signaling Technology	4267S
Rab5	Cell Signaling Technology	3547
Rab9	Thermo Fisher Scientific	MA3-067
Calnexin	Cell Signaling Technology	26798
Secondary Antibodies		
Alexa Fluor 488 Phalloidin	Thermo Fisher Scientific	A12379
Alexa Fluor 594 Phalloidin	Thermo Fisher Scientific	A12381
Alexa Fluor 488 donkey anti-rabbit	Thermo Fisher Scientific	A21206
Alexa Fluor 594 donkey anti-mouse	Thermo Fisher Scientific	A21203
Alexa Fluor 594 donkey anti-rabbit	Thermo Fisher Scientific	A21207
Anti-rabbit IgG, HRP-linked Antibody	Cell Signaling Technology	7074
Anti-mouse IgG, HRP-linked Antibody	GE Healthcare Europe GmbH	NA-931V

Table 5: Primer-sequences

mouse RT-qPCR primer		
Gene	Forward 5'-3'	Revers 3'-5'
<i>Aco</i>	caggaagagcaaggaagtgg	cctttctggctgatcccata
<i>B2m</i>	atgggaagccgaacatactg	cagtctcagtggggggtgaat
<i>Cyclind1</i>	gcgtagccctgacaccaatct	atctccttctgcacgcactt
<i>Hras</i>	atggcatcccctacattgaa	acagcacacattgcagctc
<i>Kras</i>	tgcaatgagggaccagtaca	ccaggaccataggcacatct
<i>Mtmr7</i>	ctgcagggaaaggctatgag	cagcctgagttctccagtcc
<i>Mtmr9</i>	cgaagcacttcggaaggtag	ttctcgtcttctcctgcacct
<i>Nras</i>	tgacttgccaacaaggacag	aaaaggcatcctccacacc
<i>p21</i>	cggtggaacttgacttctgt	cagggcagaggaagtactgg
<i>Tff3</i>	tctggctaattgctgttggtg	ctcctgcagaggtttgaagc
human RT-qPCR primer		
<i>ACO</i>	ctgtgaggcaccagtctgaa	gttcactcagggtcccctga
<i>B2M</i>	tgctgtctccatgtttgatgtatct	tctctgtccccacctctaagt
<i>CYCLIND1</i>	gatcaagtgtgaccggact	tcctccttctcctcctc
<i>HRAS</i>	ggaagcaggtgggtcattgat	atggcaaacacacacaggaa
<i>KCA3.1</i>	catcacattcctgaccatcg	acgtgcttctctgccttgtt
<i>KRAS</i>	tgtgtagttggagctgggtg	tgacctgctgtgtcgagaat
<i>N-MTMR7</i>	tgacggctacccatgtcata	aatgattagggaggcccatc

<i>C-MTMR7</i>	tctgtcagccaacagtgacc	cagtgagaaacacggctca
<i>Central-MTMR7</i>	tgcaaaaaatgctggaagtg	cactgcctttgcaatgaaga
<i>MTMR9</i>	ccaccacttgatcctgtcct	ttcaagcattcctccattcc
<i>NRAS</i>	ccaagaccagacagggtgtt	ccctgagtgccatcatcact
<i>P21</i>	gacaccactggagggtgact	caggccacatggtcttct
<i>TFF3</i>	ctccagctctgctgaggagt	gcttgaaacaccaaggcact

Table 6: Enzymes

Name	Company	Order number
BamHI restriction enzyme	Promega cooperation	R6021
EcoRI restriction enzyme	Promega cooperation	R6011
GoTaq® Green Master Mix	Promega cooperation	M 7121
HindIII restriction enzyme	Promega cooperation	R6041
JumpStart™ RedTaq Ready Mix™ PCR Reaction Mix	Sigma-Aldrich Chemie GmbH	P0982
NotI restriction enzyme	Promega cooperation	R6431
T4 Ligase 5 u/µl	New England Biolabs GmbH	15224017
RNase-free DNase Set	QIAGEN GmbH	79254

Table 7: Kits

Name	Company	Order number
BCA™ Protein Assay Kit	Thermo Fisher Scientific	23225
DAB Peroxidase Substrate Kit	Vector Laboratories	SK-4100
Duolink® in Situ PLA	Olink Bioscience	DUO92101
HighSpeed® Plasmid Midi Kit	QIAGEN GmbH	12643
QIAquick Gel Extraction Kit	QIAGEN GmbH	28704
PureYield™ Plasmid Mini Prep	Promega cooperation	A1222
PeqGold Total RNA Kit	Peqlab	12-6834-02
TOPO® TA Cloning® Kit	Invitrogen GmbH	450641
Vectastain® ABC kit peroxidase rabbit/mouse IgG	Vector Laboratories	PK-4000
Verso™ cDNA Kit	Thermo Fisher Scientific	AB-1453/B

Table 8: Stimulants

Name	Company	Order number
17-DMAG	Invivogen	ant-dgl-25
Amiloride	Sigma-Aldrich Chemie GmbH	A 7410
Cetuximab	Merck KGaA	UMM pharmacy
Chloroquine	Sigma-Aldrich Chemie GmbH	C6628
Everolimus	Cayman Chemical	11597
hEGF, lyophilized	Roche Diagnostics GmbH	000000011376454001
MG-132	Sigma-Aldrich Chemie GmbH	SML1135
Rosiglitazone	Cayman Chemical	71740
Sorafenib	Cayman Chemical	10009644

Table 9: Consumable material

Name	Company	Order number
Blue-Cap-Greiner 15 ml	Greiner bio-one	188 261
Blue-Cap-Greiner 50 ml	Greiner bio-one	227 261

Material and Methods

Cellstar cell culture flask 75 mm ³	Greiner bio-one	658 175
Cellstar cell culture flask 25 mm ³	Greiner bio-one	690 175
Cellstar cell culture dishes 10 cm	Greiner bio-one	664 160
Cellstar cell culture dishes 14,5 cm	Greiner bio-one	639 160
Cellstar cell culture dishes 6 cm	Greiner bio-one	628 160
Cellstar 6-well cell culture plate	Greiner bio-one	657 160
Cellstar 12-well cell culture plate	Greiner bio-one	665 180
Cellstar 24-well cell culture plate	Greiner bio-one	662 160
Cellstar 96-well cell culture plate	Greiner bio-one	655 180
Coverslips	Menzel GmbH & Co. KG	631-1580
10 µl pipette filter tips	Starlab	S1121-3810
200 µl pipette filter tips	Starlab	S1120-8810
1000 µl pipette filter tips	Starlab	S1126-7810
5 ml serological pipette	Greiner bio-one	606 180
10 ml serological pipette	Greiner bio-one	607 180
25 ml serological pipette	Greiner bio-one	760 180
50 ml serological pipette	Greiner bio-one	768 160
Kimwipes-Science	Roth	AA63.1
1.5 ml microcentrifuge tubes	Eppendorf AG	0030120086
2.0 ml microcentrifuge tubes	Eppendorf AG	0030120094
200 µl PCR tubes	Sarstedt AG & Co	72.737.002
Petri dish	BD Biosciences	351058
Superfrost® plus microscope Slides	Menzel GmbH & Co. KG	6310108

Table 10: Equipment

Machine	Company
Axiovert 40 CFL Microscope	Carl Zeiss MicroImaging
Centrifuge 3K12	Sigma
Centrifuge 5804R	Eppendorf AG
Centrifuge 5415D	Eppendorf AG
Disperser T10 basic Package	IKA®-Werke GmbH & Co. KG
Fusion Solo	PeqLab (VWR)
GelIX Imager	INTAS
GeneAmp® PCR System 9700	Thermo Fisher Scientific
HERAcell® 240 Incubator	Heraeus
Hera safe	Heraeus
Mastercycler personal	Eppendorf AG
Mini-PROTEAN® 3 Cell	Bio-Rad Laboratories GmbH
Mini-Sub® Cell GT	Bio-Rad Laboratories GmbH
Mini Trans-Blot® Electrophoretic Transfer Cell	Bio-Rad Laboratories GmbH
NanoDrop® Spectrophotometer ND-1000	PEQLAB Biotechnologie GmbH
Peqstar Light cycler	Peqlab
pH-Meter 766 calimatic	Knick
Pipettes	Eppendorf AG

Power Supply EV245	Consort
PowerPac Basic	Bio-Rad
Real Time machine 7900HT Sequence Detection System	Applied Biosystems
Shaker Certomat HK	B. Braun Biotech international
Table-cool centrifuge	Eppendorf AG
Tecan Infinite M200 microplate reader	TECAN Group Ltd.
Tube Rotator	
Vortexer Reax 2000	Heidolph
Water bath Certomat WR	B. Braun
Water system ELGA	Millipore

2.2. Software and Bioinformatics

Software	Manufacturer
Image J	Wayne Rasband
Prism 7	GraphPad
Office 2010	Microsoft

2.3. Cell culture

2.3.1. Growth conditions

Human embryonic kidney (HEK293T), DLD1, Lovo, and PATU8902 cell lines were from the German Collection of Microorganisms and Cell Cultures (DMSZ). HT29, Caco2, SW480 und HCT116 were from the European Collection of Authenticated Cell Cultures (ECACC). All cell lines, except DLD1, were cultured at 37 °C in a humidified atmosphere of 5 % CO₂ and 95 % air in high-glucose Dulbecco's Modified Eagle Medium (DMEM) supplemented with 10 % (v/v) fetal calf serum (FCS), 20 mM glutamine and penicillin / streptomycin (1000 units/ml; all from Invitrogen). For the DLD1 RPMI 1640 medium was used with the same supplements as for the other cell lines. Adherent cells were detached by using Trypsin-EDTA (0.25 %).

2.3.2. Transient transfection of human cell lines

Cells were seeded into 6-well plates and grown to 70 % confluency. The cells were then transiently transfected in DMEM medium with 2 µg DNA/well using TurboFect™ (Thermo Fisher) or 500 ng shRNA (Qiagen) according to the manufacturer's instructions. As a negative control, cells were transfected with either EV control or a control shRNA. Cells were transfected for 6 hours and the medium was changed thereafter.

2.3.3. Cell stimulation

MTT

The MTT assay is a colorimetric assay for assessing cell viability. Enzymes called NAD(P)H-dependent cellular oxidoreductase are supposed to reflect the number of viable cells present per well. These enzymes reduce 3-(4,5-dimethylthiazol-2-yl)-2,5-diphenyltetrazolium bromide (MTT, tetrazolium dye) to insoluble formazan (purple color). These assays can be used to study cell proliferation (cell growth under different conditions) or cytotoxicity, e.g. a loss of viable cells,

because of potential medical agents and toxic materials. In this thesis we only used proliferation assays, hereafter referred to as “viability-assays”.

Sorafenib/Everolimus

For viability assay cells were seeded into a 6-well plate transfected with an empty vector (EV) control, MTMR7 and MTMR9 (2 µg DNA/well) as described in 2.3.2. 24 h after seeding, cells were reseeded into 96-well plates (2000 cells/well). The next day, cells were treated with sorafenib (0, 0.1, 0.3, 0.6, 1, 3, 6, 10 µM)/ everolimus (0, 0.01, 0.1, 1, 6, 10, 30, 50 µM). Concentrations had to be adapted for HEK293T cells (sorafenib (0, 10, 30, 60, 100, 300, 600, 1000 nM)/everolimus (0, 0.1, 0.3, 0.6, 1, 3, 6, 10 nM)). Viability was measured for 7 days.

Knockdown

For viability assay cells were seeded into a 6-well plate, transfected with plasmids for control-shRNA-control or MTMR7-shRNA (1:1:1:1 mixture of four clones, 500 ng/well, Qiagen) as described in 2.3.2. 24 h after seeding, cells were reseeded into 96-well plates (2000 cells/well). Viability was measured for 7 days.

Peptide

For viability assay 2000 cells/well were seeded into a 96-well plate. The next day, cells were incubated with either a control peptide or a MTMR7 peptide (0, 0.01, 0.1, 0.5, 1, 10 µM). Important modifications were a myristic acid at the N-terminus for anchoring at the cell membrane and the amidation at the C-terminus. Viability was measured for 7 days.

MTMR7 peptide sequence:

LMAVKEETQQLLEEELEALEERLEKIQKVQL

2.4. Protein preparation and analyses

2.4.1. Total cell lysate

To prepare total cell lysates, cells were transfected as described before (2.3.2). After 48 hours (h) cells were washed once with ice-cold PBS and 500 µl SDS-lysis buffer (50 mM Tris-HCl, *pH* = 7.4, 1 % (*w/v*) SDS, 1 mM sodium orthovanadate (Na₃VO₄), 1 mM dithiothreitol (DTT), Protease Inhibitor Complete®) was added to the dish on ice. After scraping the cells, they were incubated on ice for 10 min, lysate was transferred to a 1.5 ml tube on ice and sonified with a stick sonicator. In the end, cells were centrifuged for 10 min at 4 °C (max. speed), and the supernatant was again transferred to a 1.5 ml tube and stored at -80 °C.

2.4.2. Total tissue lysate

To isolate proteins from tissue, approximately 3 mm³ of frozen tissue were cut off the block with a clean scalpel and put into a 2.0 ml tube with 5 x volumes of ice-cold tissue protein lysis buffer (20 mM HEPES, *pH* 7.4, 1 mM EDTA, 50 mM β-glycerophosphate, 10 % (*v/v*) Glycerol, 1 % (*v/v*) Triton X-100, 1 mM Na₃VO₄, 1 mM DTT, Protease Inhibitor Complete®). The tissue was then homogenized with a polytron homogenizer (Ultraturrax) for 10 sec. until no pieces remained. The lysates were incubated on ice for 1 h followed by centrifugation for 10 min at maximum speed in an Eppendorf centrifuge at 4 °C. Supernatant was collected and frozen at - 80 °C.

2.4.3. Subcellular fractionation of cells

For subcellular fractionation, the cells were lysed by hypotonic lysis (HL-buffer: 20 mM Tris-HCl, *pH* 7.4, 2 mM EDTA, 2 mM MgCl₂, 1 mM Na₃VO₄, 1 mM DTT, Protease Inhibitor Complete®). The nuclei were extracted in 150 µl of high salt buffer (HL buffer supplemented with 450 mM NaCl) on ice for 30 min with frequent vortexing for complete lysis. The remaining pellet containing all kinds of membranes/matrix components (endoplasmic reticulum, plasma membrane, nuclear matrix & membrane, chromatin) was subjected to extraction in 150 µl SDS lysis buffer (50 mM Tris HCl, *pH* 7.6, 2 % SDS (*w/v*)) for 5 min and sonication (10 sec, 35 %, Soniplus).

2.4.4. Coimmunoprecipitation

Coimmunoprecipitation (CoIP) is used to investigate protein-protein-interactions. For CoIP experiments, cells were seeded into a 10 cm dish and grown to 70 % confluence. On the next day, cells were transfected with 4 µg plasmid DNA for 48 h. Thereafter, cells were harvested by hypotonic lysis (10 mM Tris-HCl, *pH* 7.4, 2 mM EDTA, 2 mM MgCl₂, 1 mM Na₃VO₄, 1 mM DTT, Protease Inhibitor Complete®) and incubated on ice for 20 min. Cell lysates were then scraped, transferred to a 2.0 ml tube, pipetted up and down until foaming and centrifuged at 4 °C, maximum speed. Supernatant was transferred into a new 1.5 ml tube, 10 µl agarose beads were added for preclearing, and the samples were incubated for 1 h at 4 °C on a rotator. After the incubation, cells were centrifuged again for 10 min at 4 °C, at maximum speed. Lysates were then separated into three tubes: 1) without antibody (-) (AB), 2) with AB (+) 3) input. Antibodies were added to the (+) samples, and the samples were incubated on the rotator over night at 4 °C. The next day, 60 µl of agarose beads were added followed by incubation on the rotator for 2 h at 4 °C. Afterwards, cells were washed 3 times, eluted with 50 µl 100 mM Glycine (*pH* 2.2) for 2 min. Reaction was stopped by adding 10 µl 1.5 mM Tris-HCl, *pH* 8.8. After centrifugation for 1 min at maximum speed at 4 °C, the eluate was collected. Then, 20 µl SDS loading dye were added to the samples as well as the collected input. All samples were incubated at 99 °C for 10 min to perform Western blot analysis.

2.4.5. Ras pulldown activity assay

RAS pulldown assays were performed according to the manufacturer's protocol (Biocat). In detail, cells were seeded into a 10 cm dish and grown to 70 % confluence. On the next day, cells were transfected with 4 µg plasmid DNA for 48 hours. Cells were washed once with ice cold PBS and harvested by adding 1X assay/lysis Buffer (125 mM HEPES, *pH* 7.5, 750 mM NaCl, 5 % NP-40, 50 mM MgCl₂, 5 mM EDTA, 10 % Glycerol) provided by the kit. Plates were incubated on ice for 20 min, cells were scraped and put into a 1.5 ml tube. Lysates were cleared by centrifugation for 10 min (14.000 xg at 4 °C) and the supernatant was taken into a new 1.5 ml tube.

40 µl of resuspended RAF1 RBD Agarose beads were added to each tube followed by incubation at 4 °C for 1 h on a rotator. To pellet the beads, samples were centrifuged for 10 sec at 14.000 xg. The beads were washed 3 times with 0.5 ml of 1X Assay Buffer by centrifuging and aspirating each time. After the last washing step, the beads were pelleted, and the supernatant was carefully removed. The bead pellet was resuspended in 40 µl of 1 M Tris-HCL (*pH* 7.4) and 20 µl of SDS-PAGE loading dye (62.5 mM Tris-base, *pH* 10, 10 % (*w/v*) SDS, 5 % (*v/v*) β-mercaptoethanol, 50 % (*v/v*) glycerol, bromphenol blue). Samples were then boiled for 5 min at 99 °C and centrifuged for 10 sec at 14.000 xg.

2.4.6. Western Blot

Western blotting is an important technique used in cell and molecular biology to identify specific proteins extracted from cells or tissue. This is reached within three steps. First, the proteins are separated by size (SDS-gel electrophoresis), followed by the transfer to a solid support/membrane, and finally target proteins are detected using a primary and secondary antibody (Liu, Mahmood et al. 2014).

Sample preparation:

Proteins were isolated (see 2.4.1, 2.4.2), and the concentrations were measured with the BCA™ Protein Assay Kit (Thermo Fisher) according to the manufacturer's protocol. Samples were diluted in dH₂O to the same concentrations and boiled in 5 x SDS loading dye (62.5 mM Tris-base, pH 10, 10 % (w/v) SDS, 5 % (v/v) β-mercaptoethanol, 50 % (v/v) glycerol, bromphenol blue) for 10 min at 99 °C. After boiling, the samples were centrifuged and freshly loaded on a SDS-gel.

SDS-Gelelectrophoresis

To separate the protein samples by size, 30 ng protein were loaded onto either a 12.5 % or 10 % SDS-gel (Table 11).

Table 11: Components of SDS-Gels

Reagent	Separating gel		Stacking gel
	12.5 %	10 %	4 %
H ₂ O	2.59 ml	3.29 ml	1.53 ml
Acrylamide 30 %/0.8 %	3.5 ml	2.8 ml	333 µl
Tris-HCL 1.5 M pH 8,8 stock	2.1 ml	2.1 ml	
Tris-HCL 0.5 M pH 6,8 stock	-	-	625 µl
SDS 10 % stock	83 µl	83 µl	25 µl
APS 10 % stock	42 µl	42 µl	12.5 µl
Temed	2.8 µl	2.8 µl	2.5 µl

After loading, gels were run in a Mini-PROTEAN® 3 Cell system (Bio-Rad Laboratories) at 30 mA (constant) in running buffer (192 mM glycine, 25 mM TRIS-base, 0.1 % (w/v) SDS).

Transfer and detection

After the gel run, proteins were transferred to a nitrocellulose membrane (Whatman) using the Mini Trans-Blot® Electrophoretic Transfer Cell (Bio-Rad Laboratories) for 1 h at 100 V in transfer buffer (192 mM glycine, 25 mM Tris-base, 20 % (v/v) Methanol).

After the transfer, membranes were stained with Ponceau S and blocked in either 5 % (w/v) milk or BSA in T-PBS (Table 12) for 1 h under gentle agitation at room temperature (RT). The membrane was then incubated overnight with primary antibody (1:1000) at 4 °C in either 5 % (w/v) milk or BSA in T-PBS or just in T-PBS with gentle shaking. The next day, membranes were washed 3x15 min with T-PBS before adding horseradish peroxidase-labelled (HRP-labelled) secondary antibody (1:5000) in either 5 % (w/v) milk or BSA in T-PBS for one hour at RT. Membranes were washed again 3x15 min with T-PBS. Immunodetection was performed using

ECL Detection Reagent (Western Bright Sirius HRP substrate) according to the manufacturer's protocol. The membrane was placed into a darkroom (Fusion Solo, blot imager) for the respective exposure time, and pictures were taken with a digital camera.

Table 12: Antibody conditions.

Antibody	Blocking	1st antibody	2nd antibody
H-100 (55 kDa)	2 % BSA	1:1000, T-PBS	1:5000, T-PBS
Pan-RAS (21 kDa)	5 % milk	1:1000, T-PBS	1:5000, T-PBS
Lamin (70 kDa)	5 % milk	1:1000, T-PBS	1:5000, T-PBS
Tubulin (55 kDa)	5 % milk	1:1000, T-PBS	1:5000, T-PBS
EGFR (175 kDa)	5 % milk	1:1000, 5 % BSA	1:5000, 5 % milk
Flag rb	5 % milk	1:1000, 5 % milk	1:5000, 5 % milk
GFP	5 % milk	1:1000, 5 % milk	1:5000, 5 % milk
MTMR9 (63 kDa)	2 % BSA	1:1000, T-PBS	1:5000, T-PBS
MTMR7 (75 kDa)	5 % milk	1:1000, 5 % milk	1:5000, 5 % milk
p-ERK 1/2 (42/44 kDa)	5 % BSA	1:1000, 5 % BSA	1:5000, 5 % BSA
ERK 1/2 (42/44 kDa)	5 % milk	1:1000, T-PBS	1:5000, T-PBS
p-AKT Ser 473 (60 kDa)	5 % BSA	1:1000, 5 % BSA	1:5000, 5 % BSA
AKT 2 (60 kDa)	5 % milk	1:1000, 5 % milk	1:5000, 5 % milk

2.4.7. Luciferase reporter gene assay (SRE, PPRE)

Reporter gene systems like the serum response element (Lefebvre, Chen et al.) or the PPAR γ (PPRE) response element are used in cell biology to study gene expression as well as other cellular events coupled to gene expression, like receptor activity, intracellular signal transduction, protein folding and protein-protein interactions.

In the currently applied Luciferase Assay System, light is produced by converting the chemical energy of luciferin oxidation through an electron transition, forming the product molecule oxyluciferin. This reaction is catalyzed by firefly luciferase, a monomeric 61 kD protein, which oxidizes luciferin to oxyluciferin by using ATP•Mg²⁺ as a cosubstrate.

To perform PPRE (PPAR activity) assay, HEK293T, HCT116, and SW480 cells were seeded into a 6-well plate, transiently cotransfected with PPRE/EV and PPRE/MTMR7 plasmids for 24 h. Cells transfected with 3xPPRE-TK-luc (for PPAR γ activity) (from Fa. Hoffmann-La Roche AG) were stimulated with rosiglitazone (0, 1, 10, 100 μ M) over night. After aspirating the medium, 100 μ l of 1 x passive lysis buffer (Promega) was added. Cells were incubated for 10 min at RT on a shaker. Cells were transferred into 1.5 ml tubes and centrifuged for 10 min at 4 °C and maximum speed. Supernatant was transferred into a new tube, and the luciferase activity was measured by the Steady Glo luciferase assay system (Promega). To this end, 35 μ l of "Luciferase Assay Reagent" were mixed with 10 μ l of lysate. The light emission was measured using a Tecan reader (TECAN Group Ltd.). The data was normalized to the protein content of each sample.

2.5. Nucleic acid preparation and analysis

2.5.1. RNA extraction and purification of cells

Cells were seeded in 6-well plates and transfected or stimulated as required. After 48 h, medium was removed, and 350 μ l lysis buffer (provided by the kit) was added to each well. Cells were scraped and transferred to columns containing a silica membrane from the Total RNA Kit (PeqGold). RNA was extracted according to the manufacturer's protocol. By adding DNase I (Qiagen) for 20 min, free DNA was digested, and pure RNA was eluted in 35 μ l RNase-free water at RT.

2.5.2. RNA extraction and purification of tissue

To isolate RNA from tissue approx. 3 mm³ of frozen tissue were cut off the block with a clean scalpel and put into a 1.5 ml tube with 350 μ l lysis buffer (provided by the kit). The tissue was then homogenized with a polytron homogenizer (Ultraturrax) for 10 sec until no pieces remained. The lysates were transferred to a silica membrane from the Total RNA Kit (PeqGold). RNA was extracted according to the manufacturer's protocol. By adding DNase I (Qiagen) for 20 min, free DNA was digested, and pure RNA was eluted in 35 μ l RNase-free water at RT.

2.5.3. cDNA-synthesis

Reverse transcription, e.g. cDNA-synthesis was performed with 1 μ g of RNA using the VersoTM Kit (Thermo Fisher) according to manufacturer's protocol. After synthesis, H₂O was added to a final volume of 50 μ l.

2.5.4. qPCR

Quantitative real-time PCR was used for the analysis of gene expression. The reaction mix for one sample consisted of the following substances:

Reagent	Volume
DNA	2 μ l
Power SYBR-green Master Mix (Qiagen)	10 μ l
Forward Primer 10 μ M	1 μ l
Reverse Primer 10 μ M	1 μ l
dH ₂ O	6 μ l

The PCR was performed in a 96-well plate. Each well was filled with 2 μ l of cDNA and mixed with 18 μ l of master mix. After spinning the plate for 1 min at 1000 rpm, the PCR was performed on a Real Time Machine 7900HT Sequence Detection System (Applied Biosystems) using the following program:

Stage 1: 95 °C 10 min	1 cycle
Stage 2: 95 °C 0:15 min; 60 °C 1:00 min	40 cycles
Stage 3: 95 °C 0:15 min; 60 °C 0:15 min; 95 °C 0:15 min	1 cycle

During the PCR, the fluorescent dye SYBRgreen binds to the double stranded DNA which results in a fluorescence signal. Thus, an increase in the amount of DNA leads to an increase in fluorescence which can be measured for each cycle. After the PCR, the results were analyzed using the SDS 2.4 software (Applied Biosystems). To quantify the DNA amount, cycle thresholds (Ct-values) were exported to an Excel file. Afterwards, the mean value of the Ct was calculated for the same samples (duplicates), and the mean of the Ct value of the housekeeping gene ($\beta 2M$) was subtracted (ΔCt). Then, the “calibrator” was calculated by taking the mean value of all ΔCt values for one gene under different conditions (e.g. stimulation; different individuals like patients or mice). The calibrator was then subtracted from the ΔCt leading to the $\Delta \Delta Ct$ value. Finally, fold induction was calculated using the following term: $2^{-\Delta \Delta Ct}$.

Regular PCR

1 μg of RNA were transcribed into cDNA. For the PCR the GoTag@Green Master Mix (Promega) was used. The reaction mix for one sample consisted of the following substances:

Reagent	Volume
cDNA	2 μl
GoTag@Green Master Mix (Promega)	10 μl
Forward Primer 10 μM	1 μl
Reverse Primer 10 μM	1 μl
dH ₂ O	6 μl

2.5.5. Agarose gelelectrophoresis

PCR samples were analyzed on 1 % (*w/v*) agarose gels. Agarose (Biozym) was added to 1 x TAE buffer (40 mM Tris-base, 1 mM EDTA *pH* 8.0, 20 mM acetic acid), boiled for a few seconds and 0.25 $\mu g/ml$ ethidium bromide were added. The gel run was performed for 30 min at 100 V. For the detection of the DNA, a gel documentation device (Gel iX 20 Imager) and the software INTAS were used.

2.6. Immunohistochemical methods

2.6.1. Preparation of mouse tissue

For immunohistochemical staining mouse tissue had to be embedded in paraffin cassettes. Mouse tissue, e.g. Ileum, Colon and Cecum, was inserted in embedding cassettes and fixed overnight in 4 % (*w/v*) paraformaldehyde in PBS at 4 °C. Afterwards, tissue was dehydrated in an autotechnicon and embedded in paraffin. Blocks had to be transferred to -20 °C before being cut into 2-3 μm slices with a microtome (Leica RM 2145).

Tissue was also snap-frozen in liquid nitrogen using cryotubes (Sarstedt) and stored at -80 °C for later RNA or protein isolation. For analysis, frozen tissue was cut with a scalpel and RNA or protein was isolated as described in (2.4.1, 2.4.2).

2.6.2. Immunofluorescence staining of cells

Immunofluorescence is a technique which can be used on cells and tissue sections. It allows visualization of the distribution of your target protein within a cell. The technique uses specific antibodies which bind to their antigen present on your protein of interest. Secondary antibodies

coupled to fluorescent dyes are used to bind the Fc part of the primary antibody. After staining, samples can be viewed and analyzed with a fluorescence microscope.

For fluorescence staining, 300.000 cells were seeded on coverslips. The next day, cells were transfected with MTMR-GFP plasmid for 48 h. Cells were then fixed with 4 % formaldehyde for 20 min, washed with PBS (3x5 min), and blocked with 100 % of FCS for 30 min to avoid unspecific binding of the antibody. For intracellular staining, cells had to be permeabilized with 0.1 % Triton-X 100 (v/v) in PBS for another 10 min. Then, the first antibody was added and incubated at 4 °C overnight.

Coverslips were washed with PBS (3x5 min) and incubated with the secondary antibody (1:500) for one hour at RT in the dark. After another washing step, the coverslips were incubated with DAPI for 10 min at RT in the dark. Then, they were again washed with PBS and mounted onto glass-slides. After drying, stained cells could be visualized with a fluorescence microscope (Zeiss). (Antibody conditions are shown in Table 13).

Table 13: Conditions for immunofluorescent staining

Antibody	1 st Ab dilution	2 nd dilution	AB	Order number	Company
Flag	1:500	1:500		F7425	Sigma-Aldrich Chemie GmbH
cMTMR7	1:500	1:500		ab-150458	Abcam plc
pan-RAS	1:500	1:500		sc-166691	Santa Cruz Biotechnology
PPAR γ	1:500	1:500		2435	Cell Signaling Technology
RAB5	1:200	1:500		3547	Cell Signaling Technology
RAB9	1:500	1:500		MA3-067	Thermo Fisher Scientific

2.6.3. Immunofluorescence staining of tissue

For immunofluorescence staining, paraffin sections were deparaffinized in Xylol (mixture of isomers) and rehydrated in the following steps: 96 % EtOH (6 min), 80 % EtOH (6 min), 70 % EtOH (6 min) and dH₂O (2 min). Antigen retrieval was performed in unmasking solution (10 mmol/L citrate buffer, pH = 6.0; Vector Laboratories, Inc.). Sections were heated without boiling for 10 min in a microwave and afterwards cooled to RT for 30 min. After a washing step (3x5 min), slides were blocked with 100 % of FCS for 1 h to avoid unspecific binding of the antibody. Then, the first antibody diluted in 0.3 % Triton-X 100 (v/v) was added, and slides were incubated at 4 °C overnight.

Slides were washed with PBS (3x5 min) and incubated with the secondary antibody (1:350) for one hour at RT in the dark. After another washing step, the slides were incubated with DAPI for 10 min at RT in the dark. Then, they were again washed with PBS and mounted using mounting medium from DAKO. After drying, stained tissue sections could be visualized with a fluorescence microscope (Zeiss). (Antibody conditions are shown in Table 13).

2.6.4. Immunohistochemistry

Immunohistochemistry (IHC) is used to detect and localize proteins in cells of a tissue sections (Ramos-Vara et al, 2014). To understand the localization and the distribution of biomarkers and differentially expressed proteins, immunohistochemistry is often used in basic research. Furthermore, it's used in the diagnosis of abnormal cells in cancerous tissue. For immunohistochemical staining, paraffin sections were deparaffinized in Xylol (mixture of isomers) and rehydrated in the following steps: 96 % EtOH (6 min), 80 % EtOH (6 min), 70 % EtOH (6 min) and dH₂O (2 min). Antigen retrieval was performed in unmasking solution (10 mmol/L citrate

buffer, $pH = 6.0$; Vector Laboratories, Inc.). Sections were heated without boiling for 10 min in a microwave and afterwards cooled to RT for 30 min. Before quenching the endogenous peroxidase activity with 3 % (v/v) H_2O_2 in PBS, cells were washed in PBS (3x2 min). After quenching, slides were blocked with 5 % (v/v) normal goat serum in 1 % (w/v) BSA in PBS for 1 h at RT in a humidity chamber. Blocking solution was removed from the slides, primary antibody (1:100) was added, and the slides were incubated over night at 4 °C in a humidity chamber. Slides were washed 3x2 min in PBS and incubated with a biotinylated secondary rabbit (Vectastain® ABC Kit peroxidase rabbit IgG, Vectastain Laboratories, Inc.) antibody (1:500) in 1 % (w/v) BSA for 1 h at RT in a humidity chamber. After another washing step, slides were incubated in ABC-Mixture (Vector Laboratories, Inc.) for 30 min. Slides were washed additionally before adding DAB-mixture from the DAB peroxidase substrate Kit (Vectastain Laboratories, Inc.) for 1-5 min until the tissue turned slightly brown. Afterwards, slides were 3x1 min washed in dH_2O to stop the reaction and counterstained in “Mayer’s Hämalaum” (Merck) for a few seconds. Slides were washed for 10 min under tap water to get rid of the excessive color. Afterwards, slides were dehydrated using the following steps: 70 % EtOH (6 min), 80 % EtOH (6 min), 96 % EtOH (6 min) and Xylol (mixture of isomers) (6 min) and mounted with eukitt mounting medium using a glass coverslip. (Antibody conditions are shown in Table 14)

Table 14: conditions for immunohistochemical staining

Antibody	Antigen retrieval	Dilution	Order number	Company
KI67	Citrate/EDTA	1:100	NB600-1252	Novus Biologicals
KRAS	Citrate/EDTA	1:100	Ab-172949	Abcam plc
cMTMR7	Citrate/EDTA	1:100	ab-150458	Abcam plc

Immunohistochemical staining was either evaluated by scoring (0 = negative, 1 = weak positive, 2 = moderate positive and 3 = strong positive) or counting the cells (cells/ area). For the latter, positive cells per area were counted. In detail, at least of 5 images of normal tissues from *Apcmin/+ x Cav1-KO* mice (“adjacent normal”) were selected, area of crypts was measured (5 crypts), and the positive cells in each crypt were counted. For tumors of the *Apcmin/+ x Cav1-KO* mice, the area of the tumor was measured and the positive cells in this area were counted.

2.7. Proximity ligation assay

Proximity ligation assay (PLA, Duolink®) is a highly specific and sensitive technology to detect protein interactions and modifications.

Two antibodies of the proteins of interest were used to bind the antigens in the cell which were tested for their potential colocalization. The secondary oligonucleotide labeled antibodies, so called “PLA probes”, bind to the primary antibodies. If the PLA probes are in close proximity (< 40 nm) the DNA strands can interact, and the oligonucleotides are ligated and amplified in a rolling circle mechanism using oligonucleotides labeled with a fluorescent dye. These fluorescent oligonucleotides can be viewed in a fluorescent microscope as bright red fluorescent spots. PLA was performed according to the manufacturer’s protocol and all solutions were provided by the kit. For assay performance, HEK293T cells were grown on 18 mm² coverslips placed in a 6-well plate. Cells were then washed with PBS (3x5 min), fixed with 4 % formaldehyde for 20 min, washed again with PBS (3x5 min), and incubated with blocking solution (provided by the kit) for 30 min at 37 °C (dry incubator) in a humidity chamber to avoid unspecific binding of the antibody. Cells were then permeabilized with 0.1 % Triton-X 100 (v/v) in PBS for 10 min. Thereafter the primary antibody (1:250 in antibody diluent; provided by the kit) was added and incubated at 4 °C, overnight. Coverslips were washed in 1x Wash Buffer A (2x5 min) and incubated with the PLA

probe solution for 1 h at 37 °C in a humidity chamber. After another washing step in Wash Buffer A (2x5 min), coverslips were incubated with the Ligation-Ligase solution for 30 min at 37 °C. Afterwards, coverslips were washed twice in 1x Wash Buffer A for 2 min and then incubated with Amplification Polymerase solution for 100 min at 37 °C in the dark. After amplification, coverslips were washed once with Wash Buffer B for 10 min and stained with Phalloidin (1:500) in 1 x Wash Buffer B for 10 min. After an additional washing step with Wash Buffer B for 10 min, coverslips were washed in 0.01 x Wash Buffer B for 2 min, dried at RT in the dark and mounted on glass slides using Duolink in Situ Mounting Medium with DAPI.

2.8. Molecular cloning

For overexpression of huMTMR7 and huMTMR9 in cells, the human cDNA provided as commercial MGC clones from ThermoFisher Scientific for both proteins were inserted into the pTarget vector (Promega). The cDNAs were amplified by PCR with the following setup:

Reagent	Volume
cDNA	2 µl
GoTag®Green Master Mix (Promega)	10 µl
Forward Primer 10 µM	1 µl
Reverse Primer 10 µM	1 µl
dH ₂ O	6 µl

The PCR-program was as follows:

94 °C 5 min,
 (94 °C 30 sec; 55 °C 60 sec; 72 °C 120 sec) x 35 Cycles
 72 °C 120 sec

After the purification of the PCR-products on a 1 % agarose gel, bands with the size of 1,7 kb (MTMR9) and 2,0 kb (MTMR7) were cut with a clean scalpel under a UV-transilluminator, followed by DNA extraction using the QIAquick Gel Extraction Kit (Qiagen) according to the manufacturer`s protocol. Purified PCR products were used for TOPO TA Cloning® (Invitrogen) according to the manufacturer`s protocol. Reaction was setup as follows:

Reagent	Volume
Purified linear PCR product	0.5 µl - 4 µl
Salt Solution (provided by Kit)	1 µl
dH ₂ O (double distilled H ₂ O)	add to total volume of 5 µl
linear TOPO vector (provided by Kit)	1 µl
TOTAL volume	6 µl

The TOPO-reaction was incubated for 5 min at RT. Afterwards, 1 µl of the TOPO reaction was immediately transferred into competent OneShot® TOP10 *E.coli* and mixed gently. Bacteria then were incubated for 30 min on ice, followed by a heat shock for 45 sec at 42 °C and incubation for 2 min on ice. Then 500 µl SOC-Medium was added and the bacteria were incubated for 1 h at 37 °C gently shaking at 300 rpm. Afterwards, bacteria were plated on LB agar plates containing 100 µg/ml ampicillin and 40 mg/ml X-Gal (5-Brom-4-chlor-3-indoxyl-β -D-galactopyranoside, Sigma) and incubated overnight at 37 °C. The next day, positive white colonies (TOPO plasmid with correctly inserted PCR product) were picked and colony-PCR was performed. For the PCR, one colony was picked with a white pipette tip, transferred to another LB agar plate ("back up plate") followed by incubation of the tip in 100 µl LB medium for 1 h at 37 °C under gentle shaking

at 300 rpm. After incubation, 5 μ l of the bacteria suspension was used to perform the PCR reaction with the same setup as described before. The PCR products were again purified on a 1 % agarose gel. If a positive band was detected, clones from the “back up plate” were incubated overnight in 5 ml LB containing 100 μ g/ml ampicillin. The plasmid was purified using the PureYield™ Plasmid Mini Kit (Promega) according to the manufacturer’s protocol and sequenced by GATC Biotech AG. Clones with the correct MTMR7/MTMR9 sequence were then used for subcloning into the pTarget vector. The next step was the preparative restriction of the recipient vector by double digesting the DNA using the BamHI and NotI restriction enzymes (Promega) for pTarget and MTMR7/MTMR9_Topo. This reaction had the following setup:

Reagent	Volume
pTarget/Topo plasmid	2 μ g
BamHI / NotI	0.5 μ l
Buffer D	1 μ l
dH2O	total 10 μ l

The digested product was loaded on a 1 % (w/v) agarose gel. The insert and pTarget vector were cut and purified as described before. Then, insert and vector were subjected to ligation in a ratio 3 to 1.

Reagent	Volume	
T4 ligase	1 μ l	
T4 buffer	1 μ l	
insert	30 ng	} 8 μ l
vector	10 ng	

The reaction was incubated overnight at 11 °C in a PCR cycler, and then 1 μ l of the ligation mix was added to 50 μ l of OneShot® TOP10 *E. coli*. The reaction was performed as described before, followed by a colony-PCR on the next day. For the PCR, forward primer in pTarget vector and reverse primer in the insert were used. Positive clones were again picked for PureYield™ Plasmid Mini Preparation and sequenced by GATC company.

2.9. Patch-clamp

Patch-clamp experiments were performed in cooperation with Dr. Xiaobo Zhou, First Department of Medicine, Medical Faculty Mannheim, University of Heidelberg.

For patch-clamp measurements cells were seeded into 3.5 cm dishes (10.000 HCT116/ 20.000 SW480) and transfected with either MTMR7-GFP or an EV control for 48 hours. The patch-clamp measurements were performed and analyzed by X. Zhou according to the following protocol.

Standard patch-clamp recording techniques are used to measure currents in the whole-cell configuration.

Patch electrodes were pulled from borosilicate glass capillaries (MTW 150F; World Precision Instruments, Inc.) using a DMZ-Universal Puller (Zeitz-Instrumente Vertriebs GmbH). The electrodes were filled with pre-filtered pipette solution (126 mM KCl, 6 mM NaCl, 1.2 mM MgCl₂, 5 mM EGTA, 11 mM glucose, 1 mM MgATP, 0.1 mM Na₃GTP, and 10 mM HEPES adjusted to pH 7.2 with KOH). Currents were recorded at RT with an EPC-8 amplifier (HEKA Elektronik) connected via a 16 bit A/D interface to a pentium IBM clone computer. Before digitization to 5 kHz the signals are low-pass filtered (1 kHz). Data acquisition and analysis were performed using an ISO-3 multitasking patch-clamp program (MFK M. Friedrich). For whole cell recordings, the bath was superfused with physiological saline solution (PSS: 130 mM NaCl, 5.9 mM KCl, 2.4 mM

CaCl₂, 1.2 mM MgCl₂, 11 mM glucose, 10 mM HEPES, pH 7.4 with NaOH) and the pipette resistance ranged from 2-3 MΩ and the electrode offset potentials are always zero-adjusted before a Giga-seal is formed.

After obtaining a Giga-seal, the membrane under the pipette tip was disrupted by negative pressure so that the whole-cell configuration was established. Afterwards, the membrane capacitance and series resistance were compensated (60-80 %), and whole-cell currents were elicited by applying 300 ms step pulses to potentials ranging from -80 mV to +80 mV in 10 mV increments from a holding potential of -50 mV. Currents were recorded by ISO-3 and saved on the computer for data analysis. Measurements of the whole-cell currents took place at the end of each pulse and were normalized to cell capacitance to calculate the current density (pA/pF) which was then plotted versus the respective voltages, yielding the activation (I/V) curves of channels in the cell.

SK4 channel blocker, TRAM 34 or clotrimazole were applied to cells by a perfusion pipette. The blocker-sensitive currents were separated from I_m as SK4 channel currents (I_{SK4}).

2.10. Ubiquitin Immunoblotting and Proteasome Activity

These assays were performed in cooperation with Dr. Norbert Ponehies, Division of Experimental Surgery Center, Medical Faculty Mannheim, University of Heidelberg.

To measure the proteasome activity and the ubiquitin status of the cells, SW480 cells were seeded to 80 % of confluency into 15 cm dishes. The next day, cells were transfected with either MTMR7 or an EV control. After 24h, cells were lysed by addition of lysis buffer (3 mM KH₂PO₄/K₂HPO₄ pH 7.4). The lysates were immediately frozen in liquid nitrogen followed by three to five freeze and thaw cycles. Lysates were then centrifuged at 4 °C for 30 min at 40.000 g to clear the lysates from particulate and membranous material. The analysis was performed by N. Ponehies according the following protocols.

Ubiquitin Immunoblotting

The supernatants (30 µg per lane) were separated by SDS-PAGE and the expression of ubiquitin was evaluated by a rabbit anti-ubiquitin antiserum (1:500, (v/v); Sigma) using a horseradish peroxidase-labeled secondary anti-rabbit antibody (1:20.000, (v/v); Jackson ImmunoResearch). For quantification of free and conjugated ubiquitin, a standard was used in one of the lanes containing 100 ng ubiquitin. For the detection (SuperSignal West Femto Maximum Sensitivity Substrate; Pierce Biotechnology) was used. Analysis and quantification were accomplished by imaging software (Image-Master TotalLab 1.11; Amersham Biosource). A rabbit anti-mitogen-activated protein kinase (MAPK) p44/42 Ab (Cell Signaling Technology) served as a protein loading control.

Proteasome Activity

To determine the main hydrolytic activities (LLE—caspase-like, LVY— chymotrypsin, ARR— trypsin-like) fluorogenic substrates like carbobenzoxy-Leu-Leu-Glu-α-7-amido-4-methylcoumarin (Z-LLE-AMC), succinyl-Leu-Leu-Val-Tyr-AMC (Suc-LLVY-AMC), and carbobenzoxy-Ala-Arg-Arg-AMC (Z-ARR-AMC) were used (all from Calbiochem/Merck). Reactions were performed in microtiter plates using 50 µl/well volumes which contained 15 µg protein extract and assay buffer (50 mM Tris-HCl, 1 mM DTT, 5 mM ATP, 5 mM MgCl₂, pH 8.0). To differentiate peptidase- and proteasome-specific activities, inhibition by epoxomicin (10 µM) and Ada-(Ahx)₃-(Leu)₃-vinyl sulfone (10 µM) (Biomol International LP) was used. Fluorescence (excitation/ emission— 360 nm/465 nm) was detected at time intervals of 15 min for 1 h at 30 °C (Genios; Tecan) after adding substrates like Z-LLE-AMC (100 µM), Suc-LLVY-AMC (100 µM), and Z-ARR-AMC

(200 μ M). Proteolytic activity was calculated as pkat/mg total protein from the mean of three identical tests (Bergstraesser, Hoeger et al. 2012).

2.11. Data collection and Statistics

Imaging devices were used to collect optical densities (OD) of bands from Western blots (Fusion Solo, VWR). For Western blot, bands in gels were quantified with Image J (imagej.nih.gov/ij). For normalization, OD values of proteins of interest were divided by housekeeping proteins (HSP90, ERK 1/2). Each normalized value was then divided by the normalized value of the control (EV, untreated). Subsequently, the mean was calculated from at least three independent experiments (independent experiments = each experiment was performed with a different passage of the cells). Results for the real-time PCR were calculated as described in 2.5.4. Immunohistochemical staining was evaluated as mentioned in 0.

Statistical analysis was performed using GraphPad Prism (version 7.0). For pair-wise comparisons, p-values were calculated using Student's t-test or Mann Whitney test. For multiple comparisons, regular ANOVA or Kruskal-Wallis test were used (all unpaired and two-sided). For Western blot and PCR, quantitative results are expressed as means or -fold-change \pm S.E.

3. Results

3.1. Expression of MTMR7 in colorectal cancer cell lines and tissues

The endogenous expression of MTMR7 was investigated on protein as well as on mRNA levels in human CRC cell lines, a normal non-cancer cell line, and in mouse tissues by RT-PCR and Western blot.

3.1.1. mRNA expression in human CRC cell lines and mouse organs

To analyze the endogenous expression of MTMR7 and its inactive binding partner MTMR9, total RNA was extracted from CRC cell lines. RT-qPCR was performed with a primer set for *MTMR9* and three different primer sets for *MTMR7* (N-, C-terminal and the central region of the full-length *MTMR7* cDNA). The results are shown in Figure 6 and Figure 7.

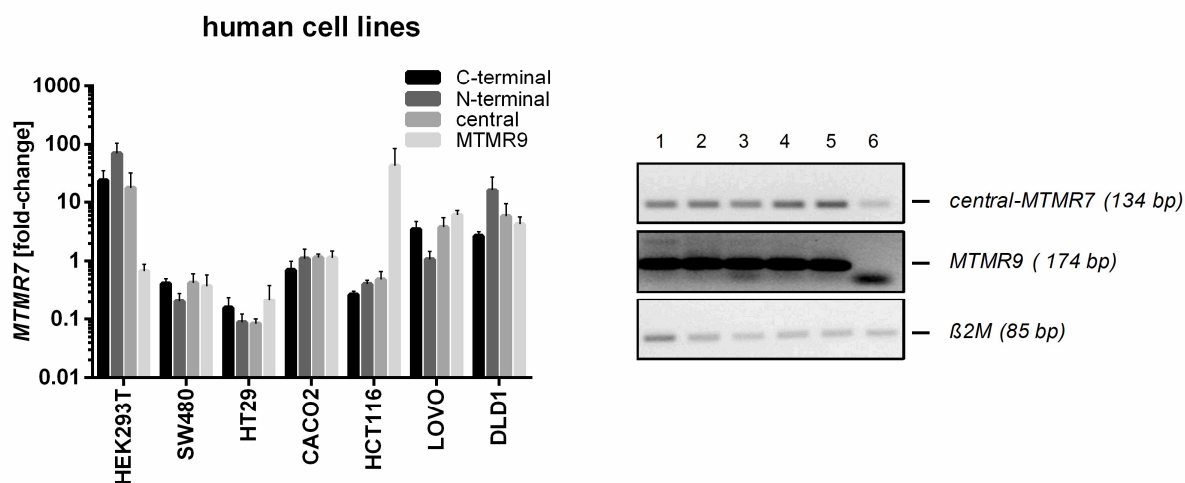


Figure 6: Expression of endogenous *MTMR7/MTMR9* in human CRC cell lines. Detection of *MTMR7/MTMR9* cDNA in total RNA extracted from human cell lines. Primers were designed for *MTMR9* and the N-terminal, central and C-terminal regions of *MTMR7*. Representative agarose gels of RT-PCR (35 x cycles) are shown together with the quantitative analyses. CT-values from RT-qPCRs on total RNA were normalized to beta2-microglobulin (*B2M*) and calculated as $-fold \pm S.E.$ ($n=3$ per cell line; Kruskal Wallis test). Legend: 1 = HEK293T, 2 = SW480, 3 = HT29, 4 = Caco2, 5 = HCT116, 6 = NTC = non-template control (water) control without specific bands. Expected sizes of amplification products: *MTMR7* = 134 bp, *MTMR9* = 174 bp and *B2M* = 85 bp.

MTMR7 showed a low expression in SW480 and HT29 cells, a medium expression in HCT116 and Caco2 cells, and a high expression in Lovo, DLD1 CRC cells, and in non-cancer HEK293T cells. *MTMR9* mRNA was highly expressed in HCT116, Lovo and DLD1 cells, moderately in Caco2 cells and low in SW480, HT29 and HEK293T cells (Figure 6).

To examine the endogenous expression of *MTMR7* and its inactive binding partner *MTMR9*, total RNA was extracted from frozen mouse organs. RT-qPCR was performed with primer sets for the central region of full-length *Mtmr7* cDNA and *Mtmr9*. The results are shown in Figure 7.

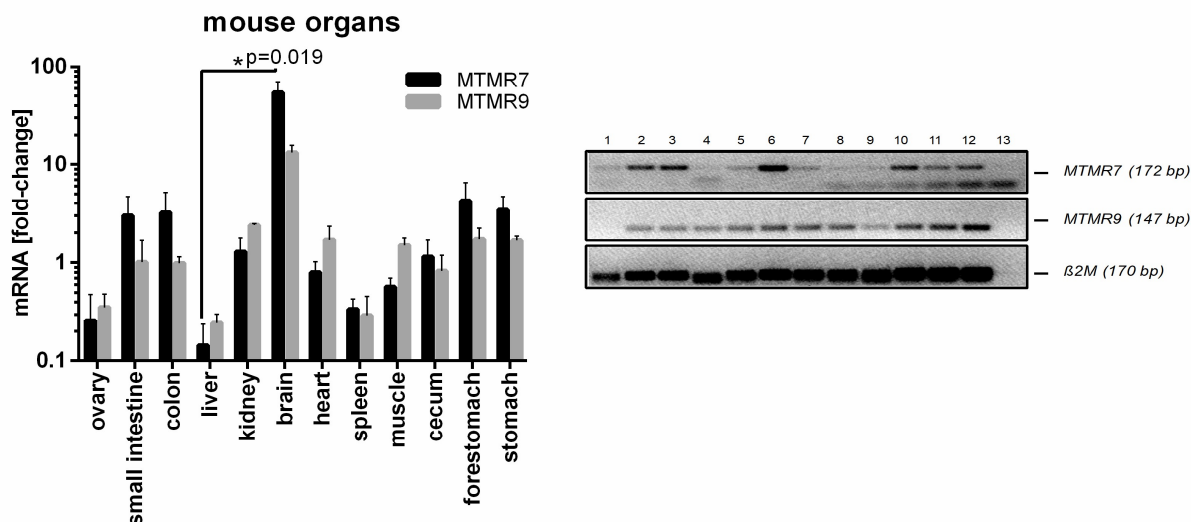


Figure 7: Expression of endogenous *Mtmr7/Mtmr9* mRNA in mouse tissues. Detection of *Mtmr7/Mtmr9* cDNA in total RNA extracted from frozen mouse tissues. Primers were designed for *Mtmr9* and the central region of *Mtmr7*. Representative agarose gels of RT-PCR (35 x cycles) are shown together with the quantitative analyses. CT-values from RT-qPCRs on total RNA were normalized to beta2-microglobulin (*B2m*) and calculated as -fold \pm S.E. (n=3 per organ; *p<0.05 liver vs. brain; Kruskal Wallis test). Legend: 1 = ovary, 2 = small intestine, 3 = colon, 4 = liver, 5 = kidney, 6 = brain, 7 = heart, 8 = spleen, 9 = muscle, 10 = cecum, 11 = forestomach, 12 = stomach, 13 = non-template control (water) control without specific bands. Expected sizes of amplification products: *Mtmr7* = 172 bp, *Mtmr9* = 147 bp and *B2m* = 170 bp.

Furthermore, RT-qPCR analysis revealed that *Mtmr7* and *Mtmr9* cDNA was abundantly expressed in different mouse organs. However, the amount between the organs differed. Both cDNAs were low expressed in ovary, liver and spleen, whereas there was a moderate expression in the colon, the small intestine, kidney, heart, muscle, cecum and stomach. Expression in brain tissue was very high as already shown by Majerus et al. in 2003 and served as control (Figure 7).

To conclude, *MTMR7/Mtmr7* and *MTMR9/Mtmr9* mRNA were expressed in 12 mouse gastrointestinal tissues, in human non-cancer cells (HEK293T) and in six human CRC cell lines (SW480, HT29, Caco2, HCT116, Lovo, DLD1).

3.1.2. Protein expression in human colorectal cancer cell lines and mouse organs

To investigate endogenous protein expression of MTMR7 (76 kD), protein was isolated from CRC cell lines, and Western blot was performed using an MTMR7 antibody, detecting the full-length MTMR7 protein. HEK293T cells transfected with a MTMR7 full-length plasmid (pT-MTMR7-FL) served as positive control compared to an empty vector (EV) control (Figure 8).

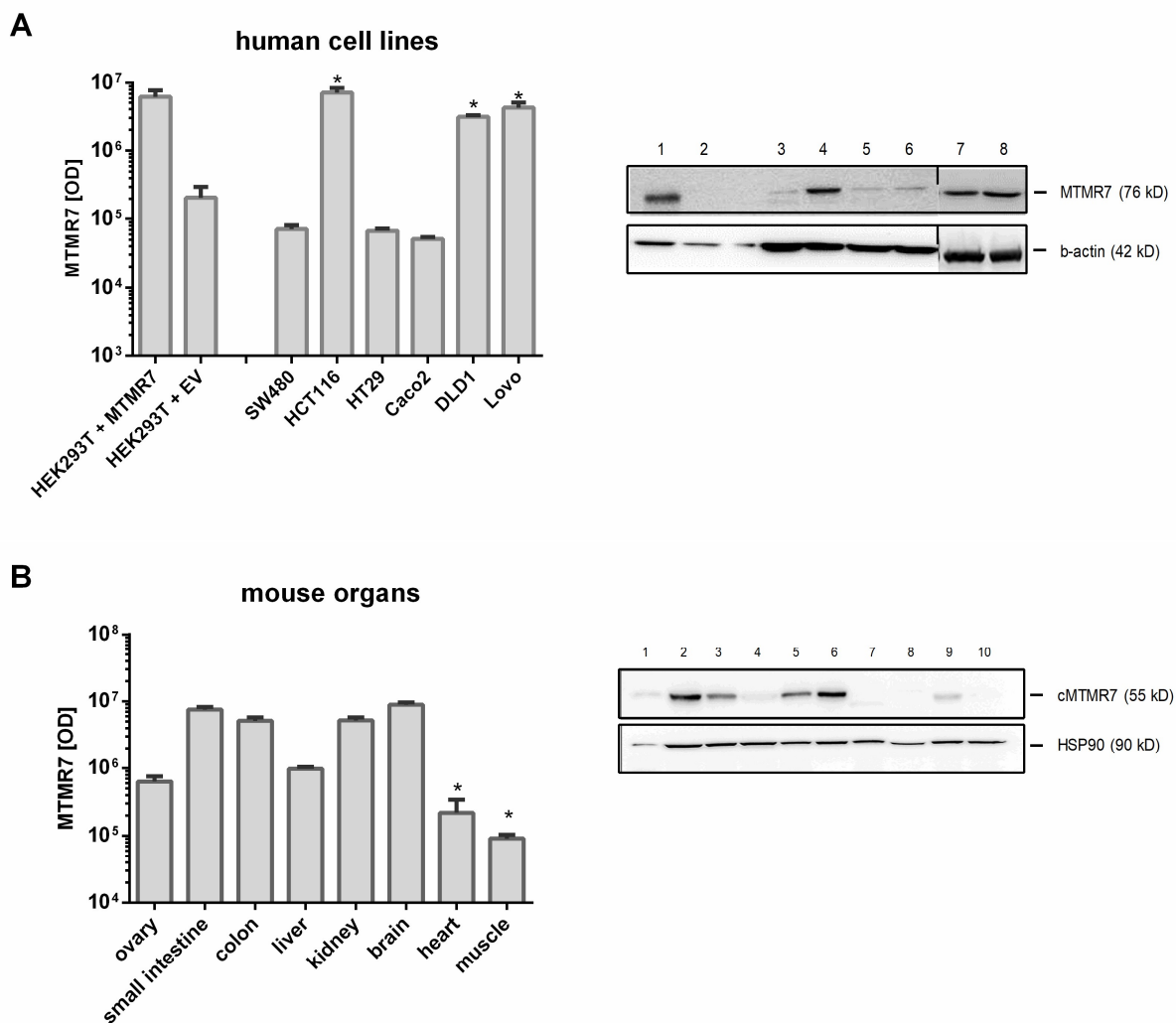


Figure 8: Expression of endogenous MTMR7 protein in human CRC cell lines and mouse tissues. A. Detection of MTMR7 (76 kD) protein in total cell lysates extracted from human cell lines using an MTMR7 Ab (ab121222) is shown together with the quantitative analyses. HEK293T cells were transfected with pT-MTMR7-FL and EV expression plasmids for 48 h. Transfected cells served as positive (HEK293T/MTMR7) and negative (HEK293T/EV) controls. OD values of bands in gels were normalized to beta-actin or HSP90 and calculated as means \pm S.E. (n=3 per cell line; *p<0.05 vs. EV; Kruskal Wallis test). Legend: 1 = HEK293T/MTMR7, 2 = HEK293T/EV, 3 = SW480, 4 = HCT116, 5 = HT29, 6 = Caco2, 7 = DLD1, 8 = Lovo. **B.** Detection of MTMR7 (55 kD) protein in total cell lysates extracted from a panel of mouse organs using the cMTMR7 Ab (ab150458) are shown together with the quantitative analyses. OD values of bands in gels were normalized to beta-actin or HSP90 and calculated as means \pm S.E. (n=3 per organ; *p<0.05 vs. brain; Kruskal Wallis test). Legend: 1 = ovary, 2 = small intestine, 3 = colon, 4 = liver, 5 = kidney, 6 = brain, 7 = heart, 8 = muscle, 9 = cecum, 10 = stomach.

The endogenous protein expression differed between the cell lines. The colorectal cancer cell lines SW480, Caco2, HT29, as well as the non-cancer cell line HEK293T showed a very low endogenous MTMR7 expression. In contrast, the CRC cell lines DLD1 and Lovo showed a moderate expression of endogenous MTMR7 and HCT116 a high expression of endogenous MTMR7 (Figure 8A).

Furthermore, proteins were isolated from a panel of mouse organs, and Western blot was performed using an antibody against the c-terminal region of MTMR7. Brain tissue served as a positive control. Western blot analysis revealed that the expression of MTMR7 varied between the different mouse organs. There was a low expression in the muscle, a moderate expression in ovaries, liver, cecum, heart and stomach, whereas it was highly expressed in the colon, the small intestine, the kidney and brain (Figure 8B).

3.2. Subcellular localization of MTMR7

The subcellular localization of the MTMR7 protein was investigated in immunofluorescence experiments. First, the localization of endogenous MTMR7 under different conditions was examined. HCT116 cells were starved overnight and treated with 50 ng/ml EGF, 20 % FCS, 1 μ M rosiglitazone (rosi), a pharmacological PPAR γ -agonist, or a physiological PPAR γ -agonist, 1 μ M linoleic acid for 1 hour before staining for the actin cytoskeleton using Phalloidin and the nuclei using DAPI and an antibody against MTMR7.

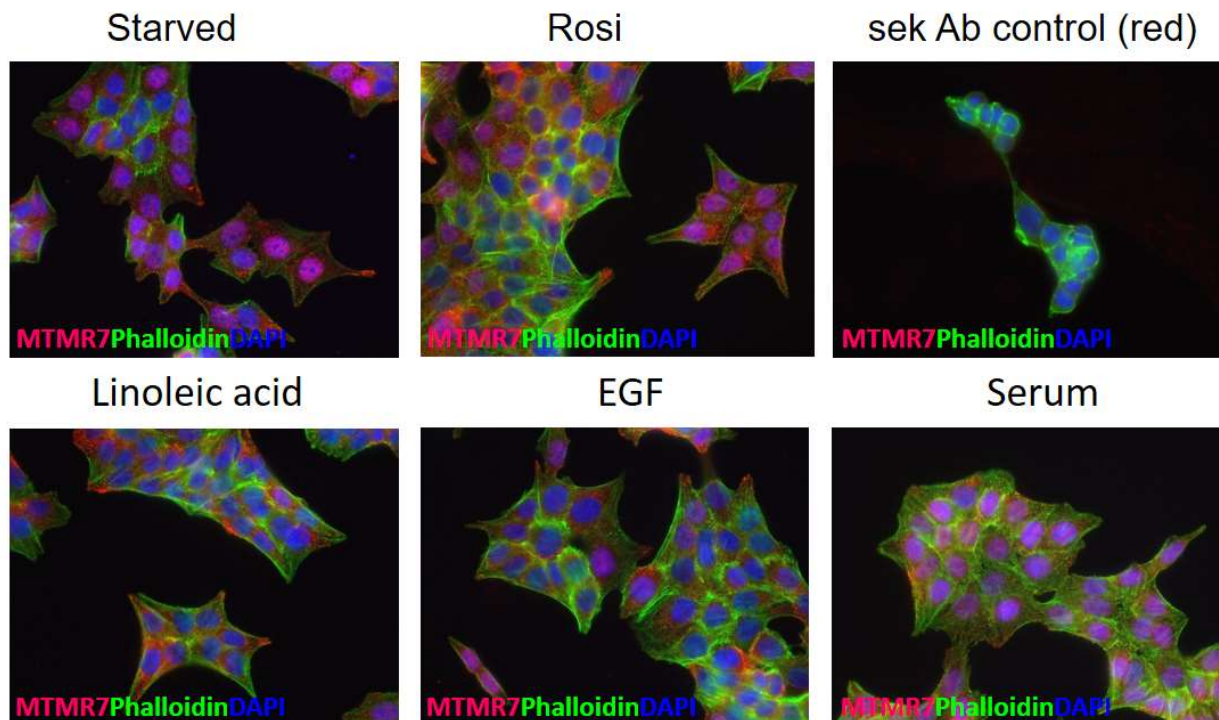


Figure 9 Subcellular localization of MTMR7. Starved HCT116 cells were treated with rosi (1 μ M), linoleic acid (1 μ M), EGF (50 ng/ml) and FCS (20 %) for 1 h before fixing and staining for immunofluorescence microscopy. MTMR7 was localized in sub-membranal spots and no difference between the treatment could be seen. Colors: red = MTMR7, green = phalloidin, blue = DAPI, Magnification 400x.

The results showed sub-membranal or cytoplasmic-nuclear spots in the starved cells and the EGF, FCS and rosi treated cells. The localization of MTMR7 was dependent on the number of cells on the slide. For single cells, nuclear localization was seen. However, cytoplasmic localization was observed, if the cells were grown confluent (Figure 9).

To further characterize the localization of MTMR7, double-color staining using specific markers for the cytoskeleton (phalloidin), the ER (calnexin) or for the early endosomes (RAB5) were used. The results did not show any colocalization of overexpressed pT-MTMR7-Flag with RAB5 or calnexin, but to some extent with phalloidin in the focal adhesions. Moreover, MTMR7 was recognized as small dots which may be colocalized with sub-membranal vesicles at the late endosomes or lysosomes. To further examine the localization of MTMR7, co-staining of late endosomal markers like RAB9 together with endogenous MTMR7 were performed. Here, a colocalization between RAB9 and MTMR7 was seen, so that MTMR7 may be located at vesicles that mark the late endosomal compartment (Figure 10).

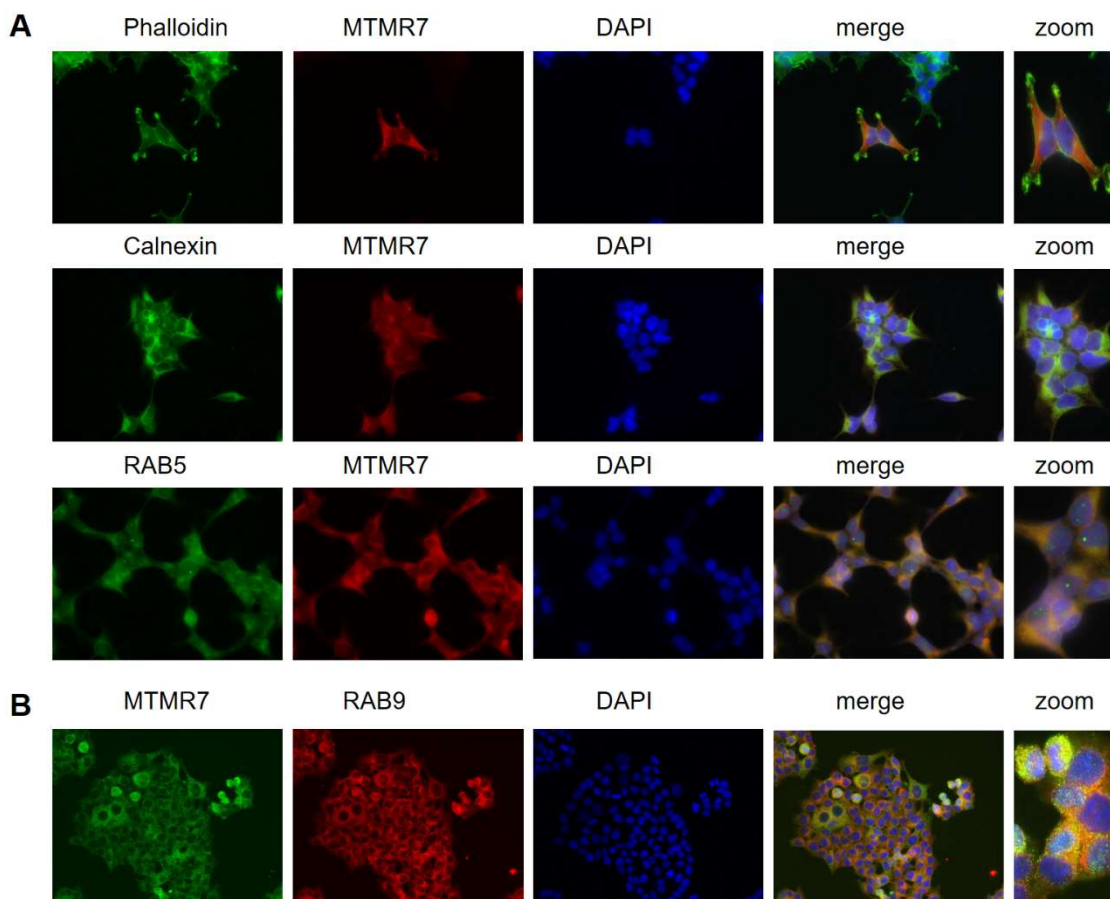


Figure 10: MTMR7 colocalizes with the late endosomal marker RAB9. Cycling cells were fixed and stained for immunofluorescence microscopy. **A.** HEK293T cells were transfected with pT-MTMR7-Flag and co-stained with antibodies for phalloidin, calnexin (ER marker) or RAB5 (early endosomal marker) together with an antibody against a FLAG-tag. No colocalization was seen for calnexin or RAB5 whereas MTMR7 partially colocalized with phalloidin in the focal adhesions. Colors: red = MTMR7, green = organelle Marker, blue = DAPI, Magnification 400x. **B.** Endogenous MTMR7 was co-stained with RAB9 (late endosomal marker) and a colocalization was seen. Colors: red = RAB9, green = MTMR7, blue = DAPI, Magnification 400x.

3.3. Interaction between PPAR γ and MTMR7

3.3.1. MTMR7 forms a complex with PPAR γ

Since MTMR7 was identified as a new binding partner of PPAR γ in the cytosol by a MALDI-MS proteomic interaction screen (Söhn, Weidner et al., unpublished), the interaction between the two proteins was further investigated using CoIP experiments on endogenous levels in HCT116 as well as with MTMR7-GFP transfected HEK293T cells. For both the endogenous and the overexpressed CoIPs, the IP was performed using polyclonal antisera against PPAR γ followed by detection of endogenous or overexpressed MTMR7 by Western blot (IB) using an antibody directed against MTMR7.

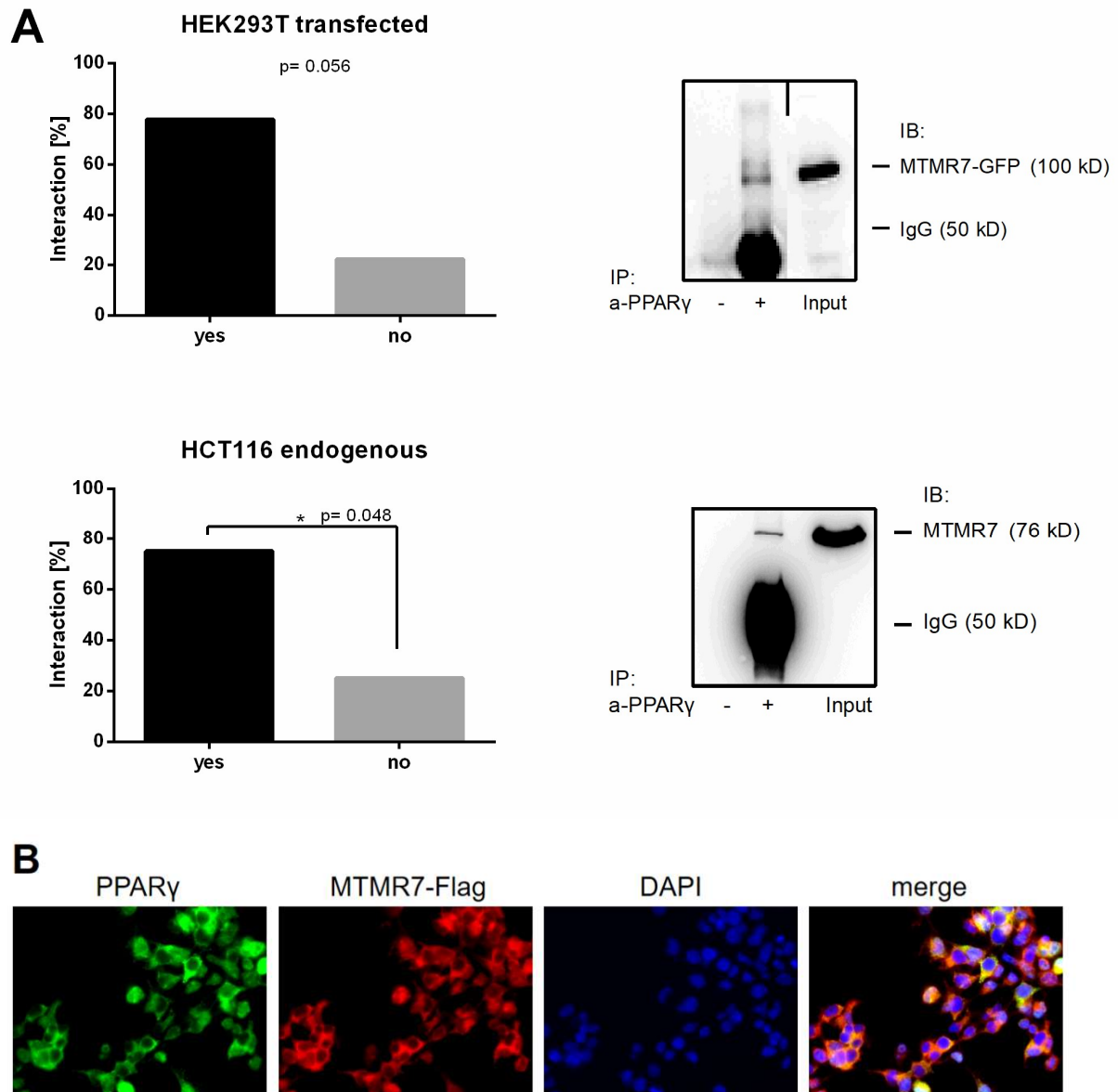


Figure 11: MTMR7 forms a complex with PPAR γ . **A.** CoIP of FL MTMR7 and PPAR γ from total cell lysates of endogenous HCT116 and transiently transfected HEK293T cells. Immunoprecipitation (“IP”) was performed using a PPAR γ or no Ab (bead control). Coprecipitated proteins were detected by Western blot (“IB”) using an antibody against MTMR7 (ab121222). Results are means \pm S.E; endogenous (n=8; * $p < 0.05$ complex vs. no complex; Unpaired t test) and overexpressed (n=9; $p = 0.0567$ complex vs. no complex; Mann Whitney test). **B.** pT-MTMR7-Flag transfected HEK293T cells were fixed and co-stained for endogenous PPAR γ (2435, CS) and overexpressed MTMR7-Flag. Colocalization of the two proteins was seen in the cytosol. Colors: red = MTMR7-Flag, green = PPAR γ , blue = DAPI, Magnification 400x.

Statistical analysis showed, that the MTMR7-PPAR γ -complex was detectable in 80 % of all performed CoIPs. However, the complex-formation was stronger on the endogenous level in HCT116 cells, whereas significance could not be reached in HEK293T cells after overexpression (Figure 11A).

In addition to CoIP experiments, immunofluorescence staining was performed in HEK293T cells. The cells were transfected with a pT-MTMR7-Flag plasmid for 48 hours and co-stained for endogenous PPAR γ and overexpressed MTMR7-Flag (Figure 11B). Fluorescent microscopy revealed cytosolic colocalization of the two proteins.

To verify the CoIP-results and immunofluorescence staining, proximity ligation assay (PLA) was performed. HEK293T cells were co-transfected with PPAR γ together with MTMR7-GFP plasmid or an EV control for 24 hours and PLA assay was performed using GFP- and PPAR γ -antibodies. This assay uses secondary oligonucleotide labeled antibodies (“PLA probes”). These probes bind to the primary antibodies and generate red spots, if the two proteins are near to each other. Interaction could be seen in the transfected cells compared to the untransfected cells (Figure 12).

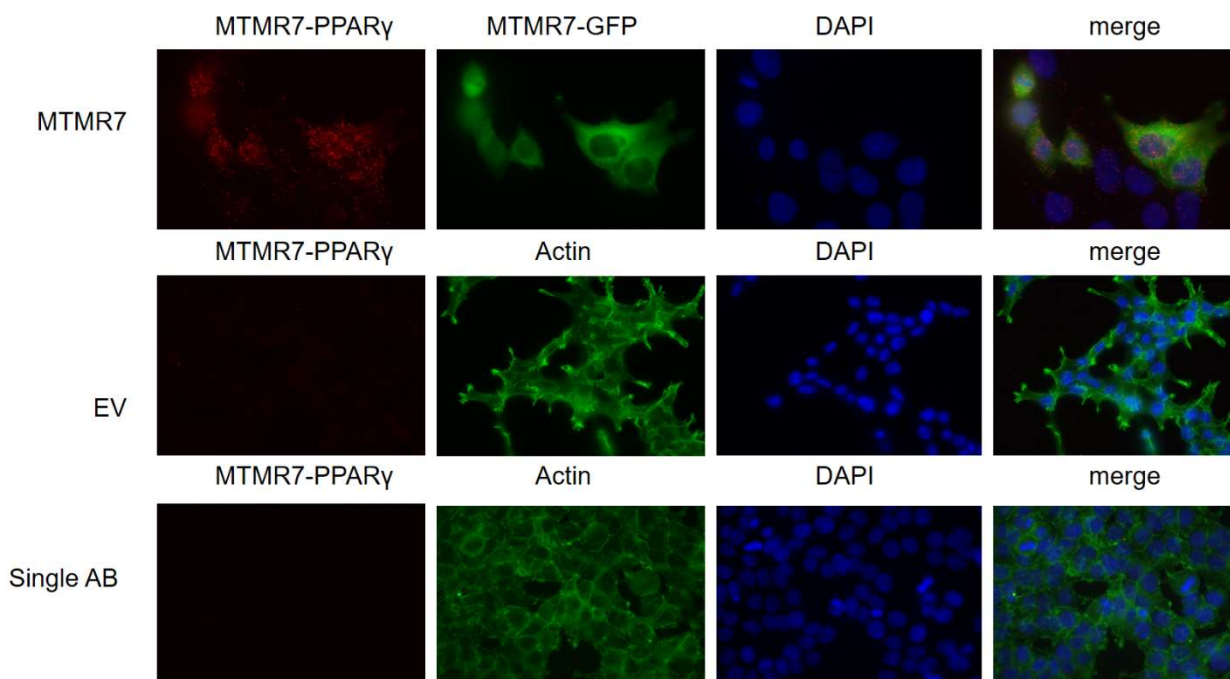


Figure 12: Proximity ligation assay (PLA). HEK293T cells were transiently transfected with PPAR γ together with MTMR7-GFP plasmid or an EV control for 24 h. Immunofluorescence staining was done with anti-GFP and PPAR γ (2435, CS) antibodies. Using a single Ab served as negative control. Colors: red dots = MTMR7–PPAR γ colocalization, green = actin/ MTMR7-GFP, blue = nuclei; magnification 400x.

3.3.2. MTMR7 reduces nuclear amount of phosphorylated PPAR γ protein

To further elucidate the MTMR7-PPAR γ interaction, effects of MTMR7 on nuclear PPAR γ were assessed. For this purpose, subcellular fractionation was performed to examine the localization of PPAR γ in different cell compartments upon MTMR7 overexpression. HEK293T cells were transfected either with MTMR7 or an EV control and stimulated with 1 μ M rosi or 20 % FCS for 1 hour. After cell lysis, Western blot was performed, looking for general PPAR γ and phosphorylated (“P”)-PPAR γ expression. β -tubulin and lamin served as loading controls (Figure 13).

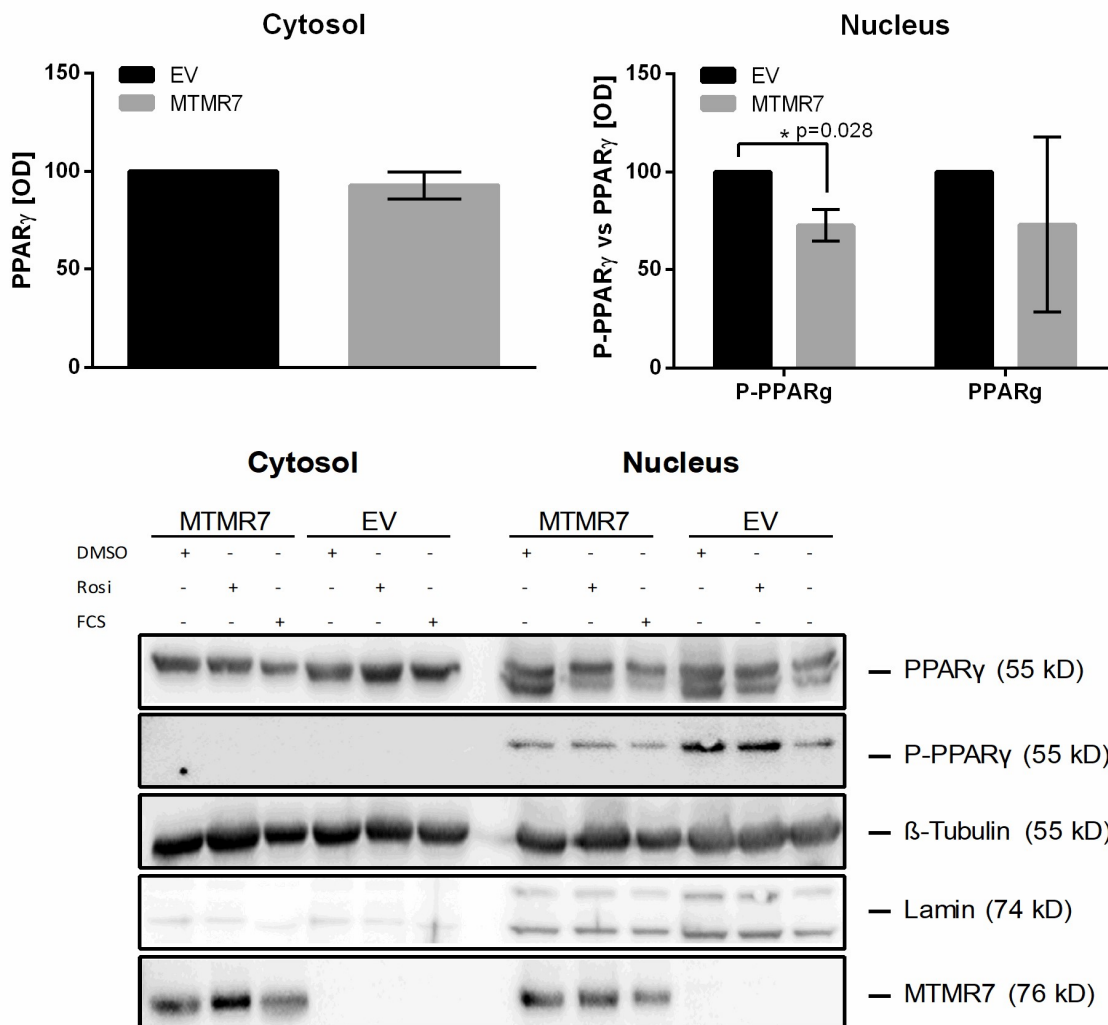


Figure 13: Decrease of nuclear P-PPAR_γ upon MTMR7 transfection. HEK293T cells were transiently transfected with MTMR7 or an EV control for 48 h. Cells were starved overnight and treated with rosi (1 μM) or FCS (20 %) for 1 h before subcellular fractionation. Detection of PPAR_γ/ P-PPAR_γ (55 kD) protein in cytosol and nucleus is shown together with quantitative analyses. Lamin and β-tubulin served as loading controls. OD values of bands in gels were normalized to Lamin or β-tubulin and calculated as means ± S.E. (n=4; *p<0.05 MTMR7 vs. EV; Mann Whitney test).

The results confirmed, that the amount of PPAR_γ did not change upon MTMR7 transfection in the cytosolic cell compartment. Furthermore, nuclear P-PPAR_γ was significantly downregulated by 30 % ± 8 % in MTMR7 transfected cells compared to an EV control in unstimulated cells. However, no changes were seen in cells stimulated with rosi or FCS. In addition, no influence of MTMR7 on PPAR_γ localization could be seen.

3.3.3. MTMR7 activates transcriptional response of PPAR_γ

To elucidate if MTMR7 promotes the transcriptional activity of PPAR_γ in the nucleus, luciferase reporter assays using a PPRE-LUC plasmid were performed. For this assay, cells were transiently co-transfected with PPRE (PPAR_γ-responsive-element)-driven luciferase reporter plasmid together with either MTMR7 or an EV control for 24 hours and then incubated with increasing concentrations (0, 0.1, 1, 10 μM) of rosi for additional 24 hours. Luciferase activity was measured in total cell lysates and normalized to protein content (Figure 14).

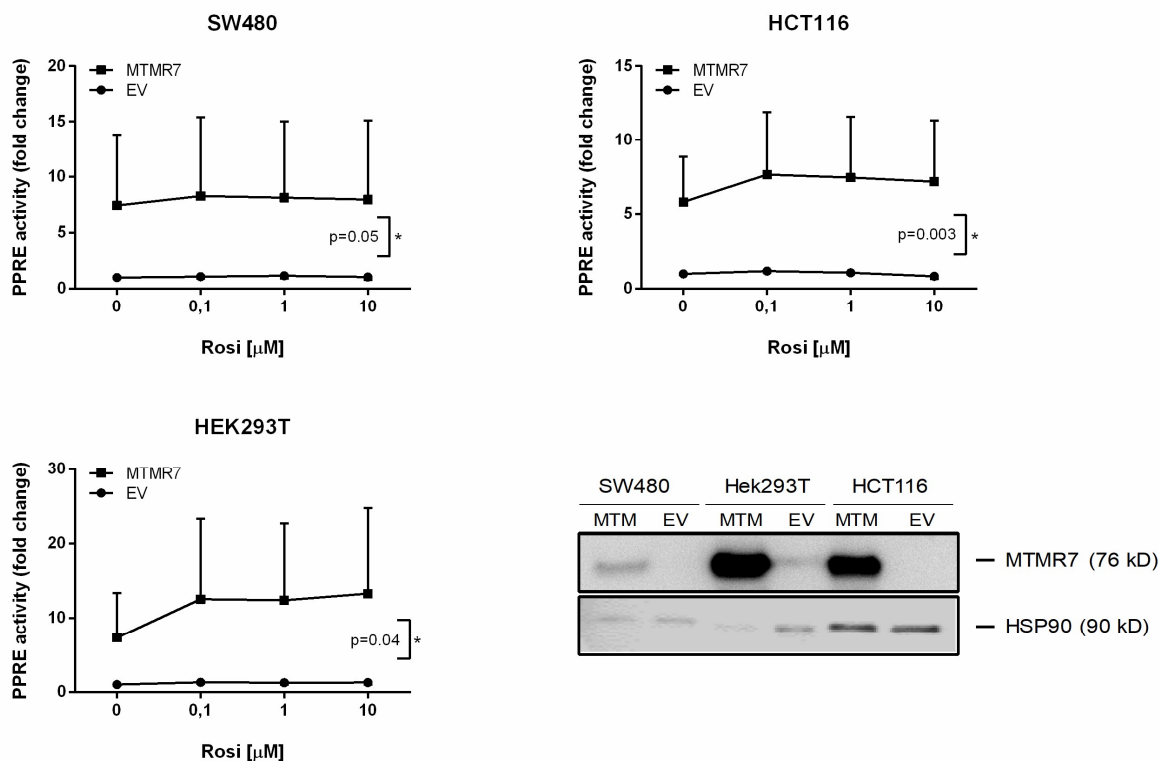


Figure 14: MTMR7 activates transcriptional response of PPAR γ . Cells were co-transfected with PPARE reporter plasmid and MTMR7 or an EV control for 24 h. After transfection, cells were treated with rosi (0-10 μ M) for 24 h. Luciferase activity in total cell lysates was normalized to protein content and calculated as -fold \pm S.E. (n=9; *p<0.05 MTMR7 vs. EV; Two-way ANOVA).

All three cell lines showed a significant increase of PPAR γ activation upon MTMR7 transfection. Transcriptional PPARE activity was significantly enhanced (9.5-fold) in SW480 cells transfected with MTMR7 compared to the EV transfected cells at 0.1 μ M rosi. In HCT116 cells, the activity was 8.5 times higher in the MTMR7 transfected cells compared to the controls at 0.1 μ M rosi. HEK293T showed a 14 times higher activity upon MTMR7 transfection and stimulation with 0.1 μ M rosi.

Taken together, the results confirmed that MTMR7 enhanced the transcriptional activity of PPAR γ in KRAS-mutated SW480 and HCT116 cells with high pan-RAS activity as well as in HEK293T non-cancer cells.

3.3.4. MTMR7 enhances PPAR γ target gene expression

To check the effect of transient MTMR7 overexpression on the nuclear PPAR γ response, RT-qPCR for quantification of cognate (or *bona fide*) PPAR γ -target genes like *phosphatase and tensin homolog (PTEN)*, *trefoil factor 3 (TFF3)*, *acyl-CoA oxidase (ACO)*, *phosphoenolpyruvate carboxykinase (PEPCK)* and *cluster of differentiation 3 (CD36)* was performed. HCT116 and HEK293T cells were transfected with either MTMR7 or an EV control and stimulated with 1 μ M rosi for 48 h before extraction of total RNA. RT-qPCR was conducted using primer for *PTEN*, *TFF3*, *ACO*, *PEPCK* and *CD36* (Table 5, material and methods). Results are shown in Figure 15.

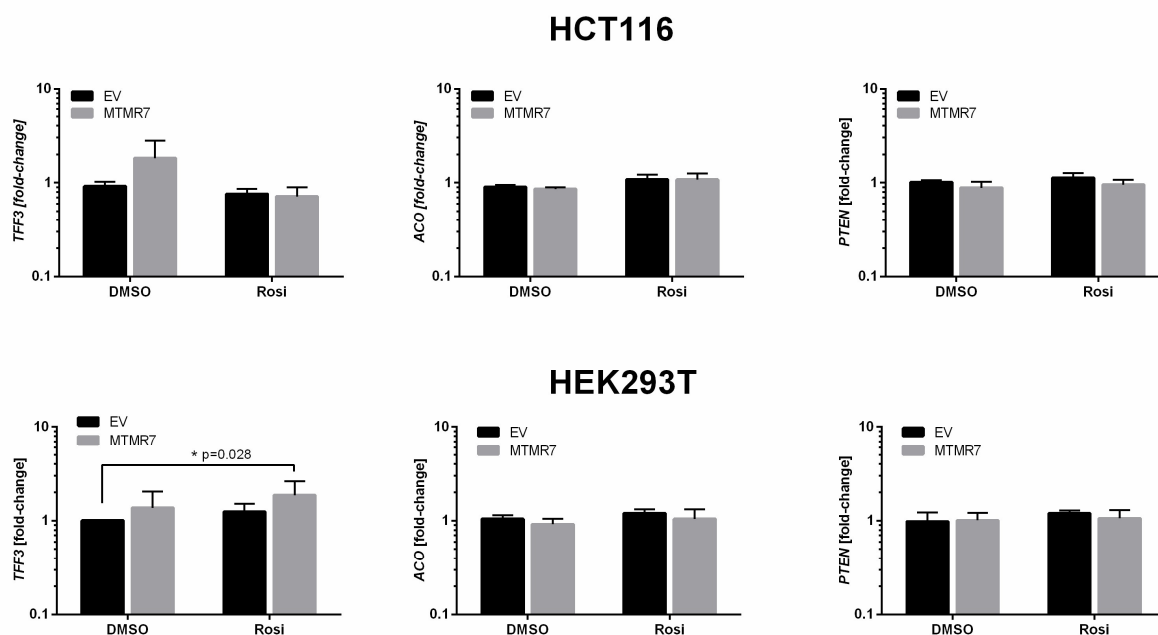


Figure 15: MTMR7 increases PPAR γ -target gene expression. Cells were transfected with MTMR7 plasmid or an EV control for 48 h. Cells were treated with rosi (1 μ M) or DMSO (vehicle control) for 24 h. CT-values from RT-qPCRs on total RNA were normalized to beta2-microglobulin (*B2M*) and calculated as -fold \pm S.E. (n=3 per cell line; *p<0.05 rosi vs. DMSO; Mann Whitney test).

RT-qPCR analysis on the cDNA pools showed that MTMR7 had no influence on *PTEN*, *ACO*, *PEPCK* and *CD36* but significantly increased *TFF3* mRNA expression levels by ~ 43 % in rosi stimulated HEK293T cells. For unstimulated HCT116 cells a trend in upregulation of *TFF3* mRNA upon MTMR7 transfection was seen but did not reach statistical significance. However, this trend could not be exceeded by stimulation with the PPAR γ ligand rosi.

Taken together, these results showed that MTMR7 does not influence PPAR γ localization but that it promotes transcriptional activity of PPAR γ in *KRAS*-mutated and HEK293T cells.

3.3.5. MTMR7 promotes membrane retention of EGFR and reduces nuclear EGFR

MTMR7 enhances the transcriptional activity of PPAR γ in *KRAS*-mutated SW480 cells with high pan-RAS activity. The next step was to find out if enhancement takes place by direct interaction between MTMR7 and PPAR γ or via inhibition of the negative regulatory pathway of PPAR γ , namely the EGFR-RAS-RAF-MEK1/2-ERK1/2 pathway.

To answer this, subcellular fractionation was performed, and cell fractions together with total cell lysates were analyzed by Western blot. SW480, HCT116 and HEK293T cells were transfected with either MTMR7 full-length plasmid or an EV control for 48 h. Before harvesting, cells were starved overnight and stimulated for 0, 15, 30, 60, 120 and 180 minutes with 20 % FCS to trigger GFR endocytosis, recycling, or degradation routes (Burgermeister, Höde et al. 2017). For subcellular fractionation, the cells were lysed by hypotonic lysis (cytosolic fraction). The nuclei were extracted in high salt buffer, and the remaining pellet containing membranes/matrix components (ER, plasma membrane, nuclear matrix & membrane, chromatin) was subjected to extraction in SDS lysis buffer and sonication. The samples were then analyzed by Western blot using an antibody against EGFR and pan-RAS to see whether those proteins are influenced by MTMR7 (Figure 16).

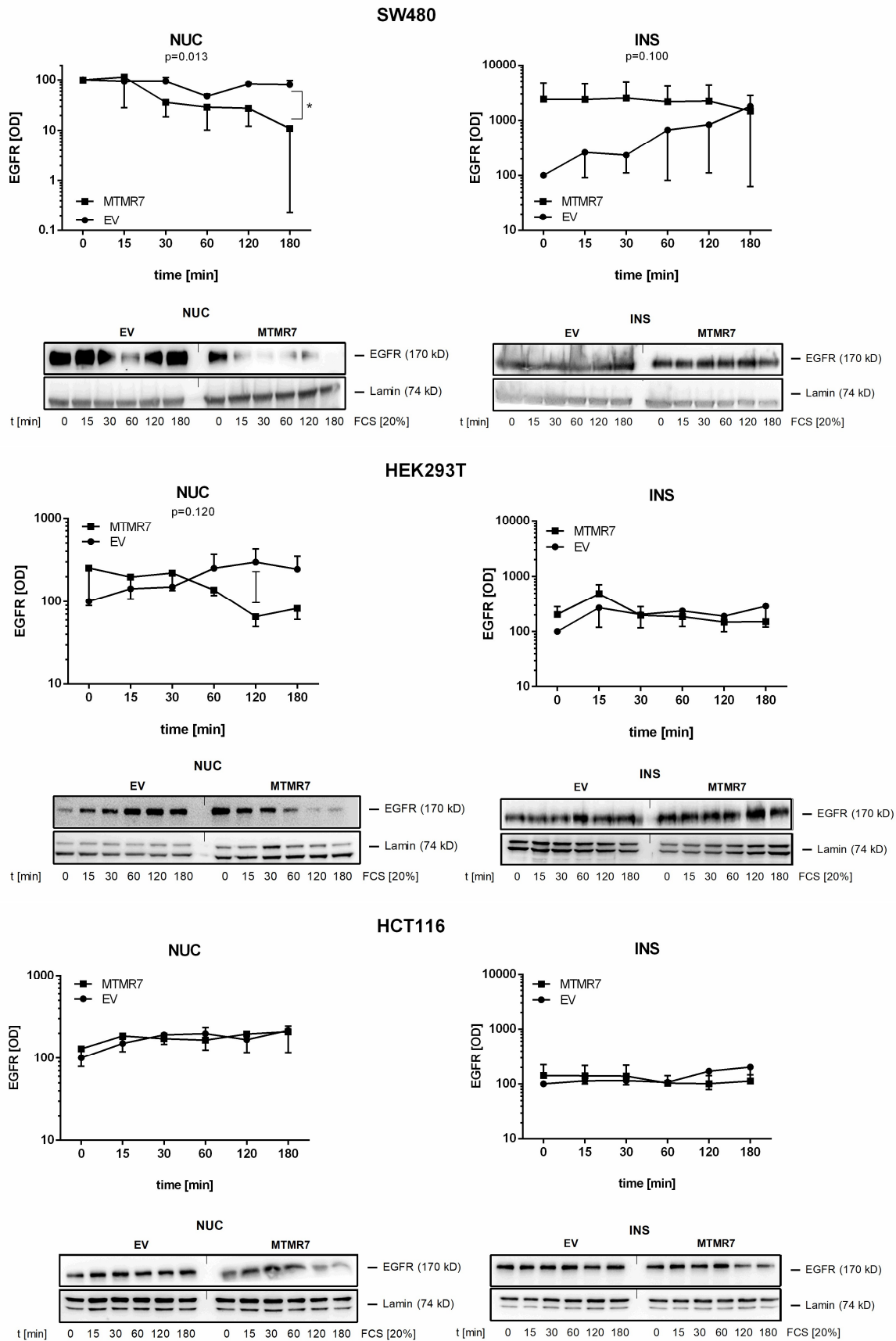


Figure 16: MTMR7 promotes membrane retention of EGFR and reduces nuclear EGFR in SW480 cells. Cells were transiently transfected with MTMR7 or an EV control for 48 h. After transfection, cells were starved overnight and treated with FCS (20 %) for 0-180 min before subcellular fractionation. Detection of EGFR (170 kD) protein in the insoluble and nuclear fraction is shown together with quantitative analysis. Lamin served as loading control. OD values of bands in gels were normalized to lamin and calculated as means \pm S.E. (n=3 per cell line; * $p<0.05$ MTMR7 vs. EV; Kruskal-Wallis test).

The results showed that MTMR7 promotes membrane retention of EGFR in SW480 cells. Thereby, nuclear EGFR expression (NUC), which has been associated with tumor progression and worse survival prognosis for several human cancers, was significantly reduced by $90 \pm 11 \%$ upon MTMR7 transfection and FCS stimulation for 180 minutes. A trend in the reduction (by $40 \pm 15 \%$) of nuclear EGFR was also seen in HEK293T cells after 120 minutes of stimulation, whereas the HCT116 cells were not responsive (Figure 16).

For all cell lines, a trend in decreasing pan-RAS protein upon MTMR7 transfection ($\sim 10 - 30 \%$) could be seen in the insoluble fraction (INS). Interestingly, the reduction was seen after about 30 minutes of stimulation in the colorectal cancer cell lines HCT116 and after 60 minutes in SW480, whereas HEK293T cells already responded after about 15 minutes of stimulation. In addition, no massive translocation to other compartments was observed (Figure 17).

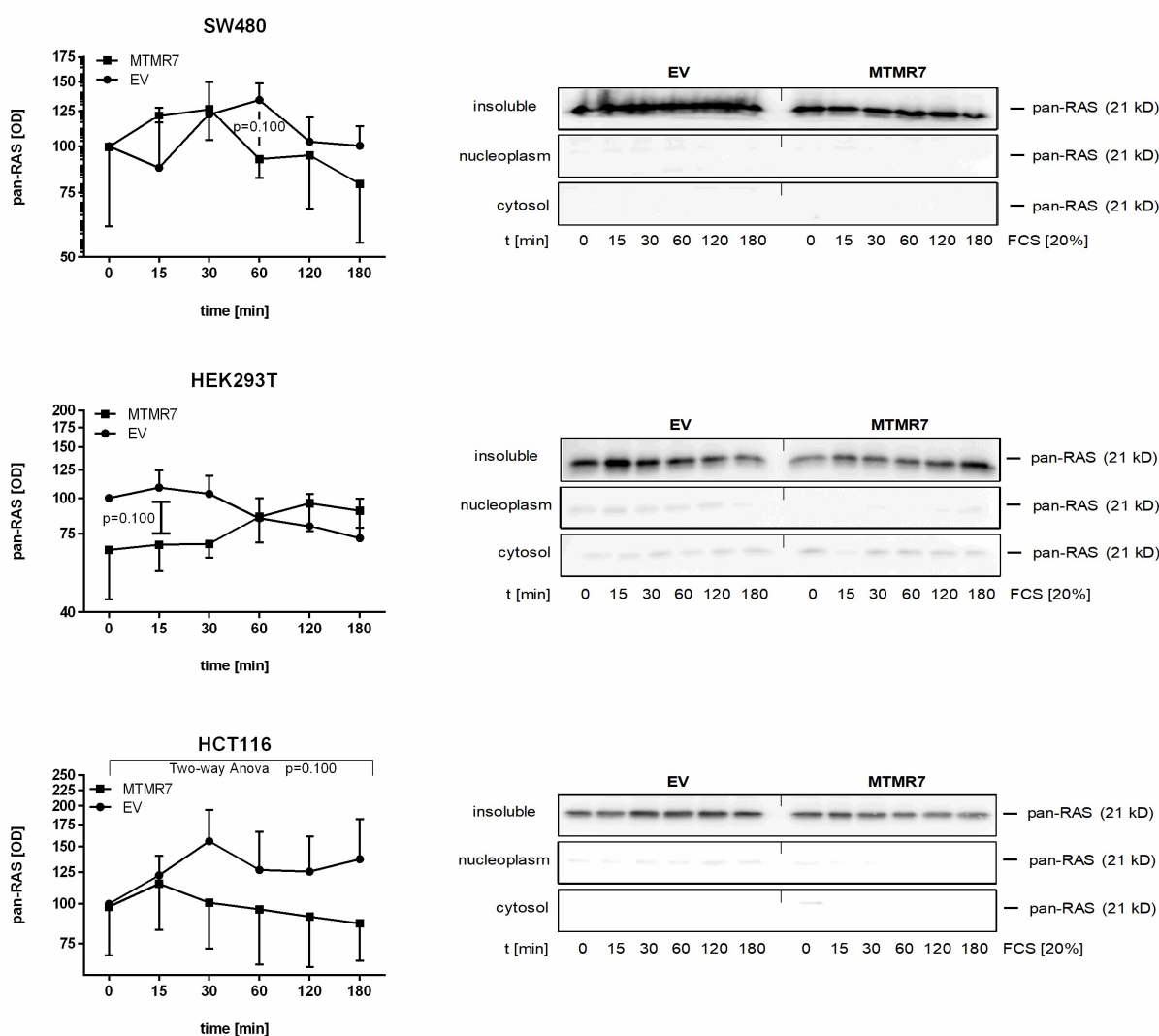


Figure 17: MTMR7 reduces pan-RAS protein levels. Cells were transiently transfected with MTMR7 or an EV control for 48 h. After transfection cells were starved overnight and treated with FCS (20 %) for 0-180 min before subcellular fractionation. Detection of pan-RAS (21 kD) protein is shown together with quantitative analyses. Results are means \pm S.E. (n=3; n.s.; Mann Whitney test (HEK293T, SW480) or Two-way Anova (HCT116)).

3.3.5.1. MTMR7 influences EGFR and pan-RAS protein expression

In addition to subcellular fractionation, the effect of MTMR7 on EGFR and pan-RAS expression was evaluated in total cell lysate samples. SW480 cells were transfected and treated as above, harvested after indicated time points, and total cell lysates were analyzed by Western blot using an antibody against EGFR and pan-RAS to evaluate if those proteins are influenced by MTMR7 (Figure 18).

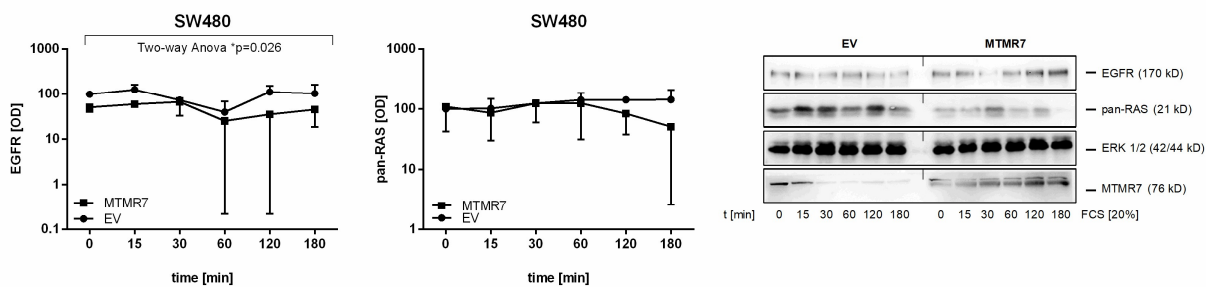


Figure 18: MTMR7 reduces pan-RAS protein levels. SW480 cells were transiently transfected with MTMR7 or an EV control for 48 h. After transfection cells were starved overnight and treated with FCS (20 %) for 0-180 min before lysis. Detection of pan-RAS (21 kD) protein is shown together with quantitative analyses. Results are means \pm S.E. (n=3; *p<0.05 MTMR7 vs. EV; Two-way ANOVA, Bonferroni n.s.).

A reduction of 75 ± 25 % of the EGFR, which did not reach significance, was detected after 60 minutes upon MTMR7 transfection in SW480 cells. The receptor expression was increased again after 120 minutes, suggesting a recycling or regeneration of the EGFR. As seen above, cells transfected with MTMR7 full-length plasmid showed a ~ 30 % lower pan-RAS expression than cells transfected with the EV control. However, this effect did not reach significance.

To conclude, MTMR7 promotes membrane retention of EGF-Receptor and reduces nuclear EGFR. Furthermore, an inhibitory effect of MTMR7 on total RAS-protein expression has been stated.

3.4. Down-regulation of KRAS by MTMR7

3.4.1. MTMR7 reduces the activity and total protein levels of pan-RAS in KRAS-mutated CRC cells

To further characterize the molecular mechanisms of RAS down-regulation by MTMR7, a pan-RAS pulldown assay provided by Cell Biolabs was performed to see if MTMR7 not only reduces the total protein level but also the GTPase activities of RAS proteins. Different CRC cell lines (SW480, HCT116, Lovo, DLD1), one pancreatic cancer cell line (PATU8902), and one gastric cancer cell line (AGS, data not shown), all KRAS-mutated, were transfected with MTMR7 full length plasmid and an EV control for 48 h. The cells were harvested, and RAS pulldown assay was performed according to the manufacturer's protocol. The samples were then analyzed by Western blot using an antibody against pan-RAS to detect the amounts of active pan-RAS proteins (Figure 19).

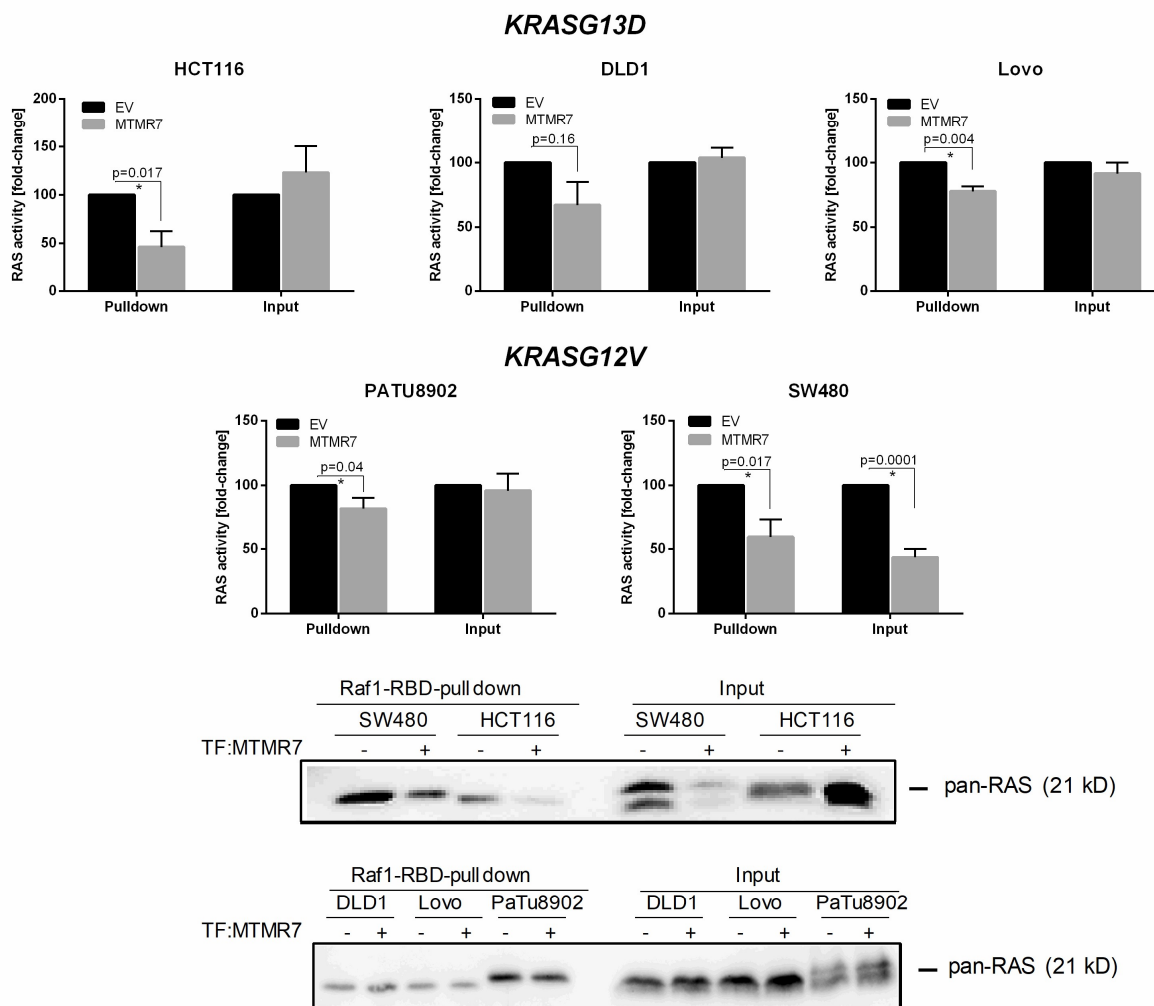


Figure 19: MTMR7 reduces the activity of pan-RAS in KRAS-mutated CRC cells. Cells were transfected with MTMR7 plasmid or an EV control for 48 h before performance of GST-pulldown assay. Detection of active pan-RAS (21 kD) protein is shown together with the quantitative analyses. Results are \pm S.E. ($n=3$ per cell line; $*p<0.05$ MTMR7 vs. EV; Unpaired t test (HCT116, Lovo, SW480) / One sample t test (DLD1, PATU8902)).

The quantitative analysis showed a significant downregulation of active as well as total pan-RAS protein by MTMR7 in SW480 cells (active: by $40 \pm 15\%$; total: by $55 \pm 7\%$). The significant decrease in mutant pan-RAS was also seen in HCT116 (by $55 \pm 27\%$), Lovo (by $23 \pm 4\%$) cells and a pancreatic cell line (by $18 \pm 8\%$). However, in contrast to the SW480 cells the effect on the total protein level was not seen in these cell lines. The colorectal cancer cell line DLD1 showed a trend in active RAS reduction (by $33 \pm 18\%$) which did not reach significance.

Results

Since MTMR7 was inhibiting active-mutant RAS, the effect on RAS was determined in total cell lysates of human colorectal cancer cell lines. HCT116, SW480 and KRAS wildtype HEK293T (as control) cells were transfected with either a MTMR7 plasmid or an EV control for 1-3 days and Western blot was performed using a pan-RAS antibody (Figure 20).

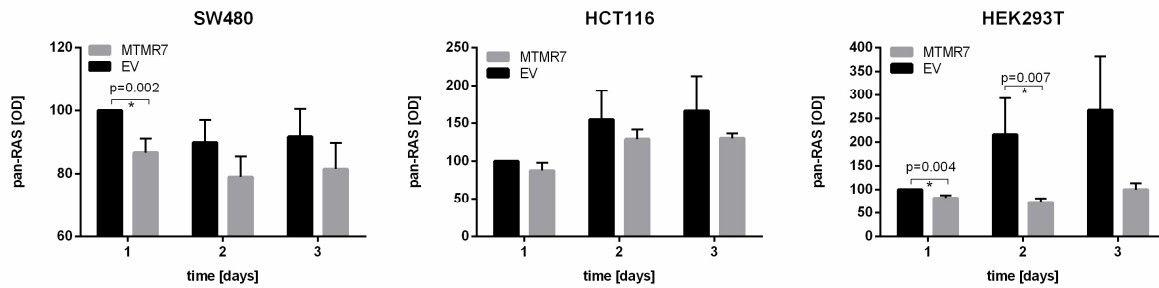


Figure 20: MTMR7 reduces total protein levels of pan-RAS. Cells were transfected with MTMR7 plasmid or an EV control for 1-3 days. Pan-RAS protein levels were reduced upon MTMR7 transfection. OD values of bands in gels were normalized to ERK 1/2 or HSP90 and calculated as means \pm S.E. ($n \leq 3$ per cell line; $p < 0.05$ MTMR7 vs. EV; Unpaired t test).

The statistical analysis confirmed a significant downregulation of RAS protein in SW480 by 14 ± 4 % after 1 day and in HEK293T cells after day 1 (by 18 ± 5 %) and 2 (by 144 ± 88 %). For HCT116 cells no trend in RAS inhibition could be seen.

The same experiment was done on mRNA level, but no effect was seen at all (Figure 44, 7.3).

3.4.2. RAS is not degraded by the proteasome

To further elucidate the mechanism of RAS inhibition by MTMR7, inhibitors of the proteasome (MG132) and lysosomal acidification (chloroquine) were used. To test for proteasomal degradation, SW480 cells were transfected with MTMR7 or an EV control. During transfection, cells were incubated in presence or absence of the proteasomal inhibitor MG132 ($3 \mu\text{M}$) for 8, 16, 24 and 32 hours. Cells were harvested after indicated time points and pan-RAS protein was detected by Western blotting.

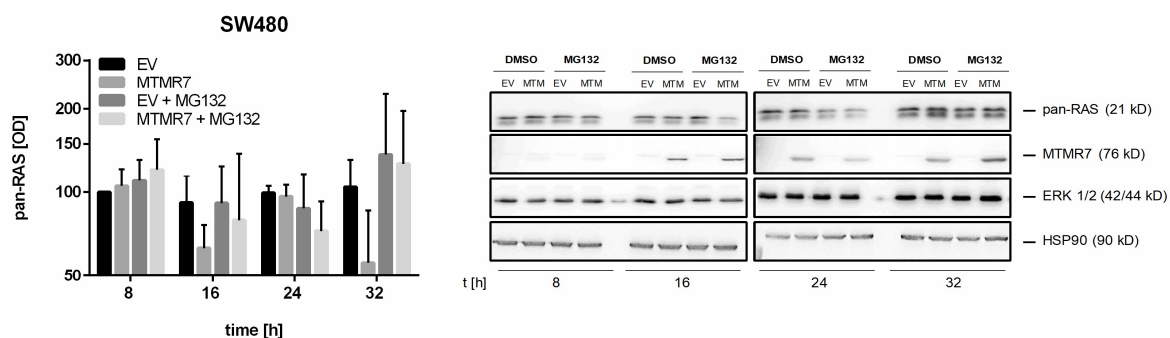


Figure 21: RAS is not degraded via the proteasome. SW480 cells were transfected with MTMR7 plasmid or an EV control. During transfection, cells were incubated in presence or absence of the proteasomal inhibitor MG132 ($3 \mu\text{M}$) for 8-32 h. Detection of pan-RAS (21 kD) protein in TCL is shown together with the quantitative analyses. OD values of bands in gels were normalized to ERK 1/2 and calculated as -fold \pm S.E. ($n=3$; n.s.; Two-way ANOVA).

The statistical analysis showed, that RAS down-regulation was seen in cells transfected with MTMR7 plasmid after 16 h. A regeneration of RAS protein was seen after 16 and 32 h in MTMR7-transfected cells treated with MG132. However, it did not reach significance (Figure 21).

To critically test these results with a more specific method, an ubiquitination and proteasome assay were performed in cooperation with Dr. Norbert Ponelies, Division of Experimental Surgery Center, Medical Faculty Mannheim, University of Heidelberg. To perform the assay, SW480 cells were transfected with MTMR7 or an EV control and harvested after 24 hours.

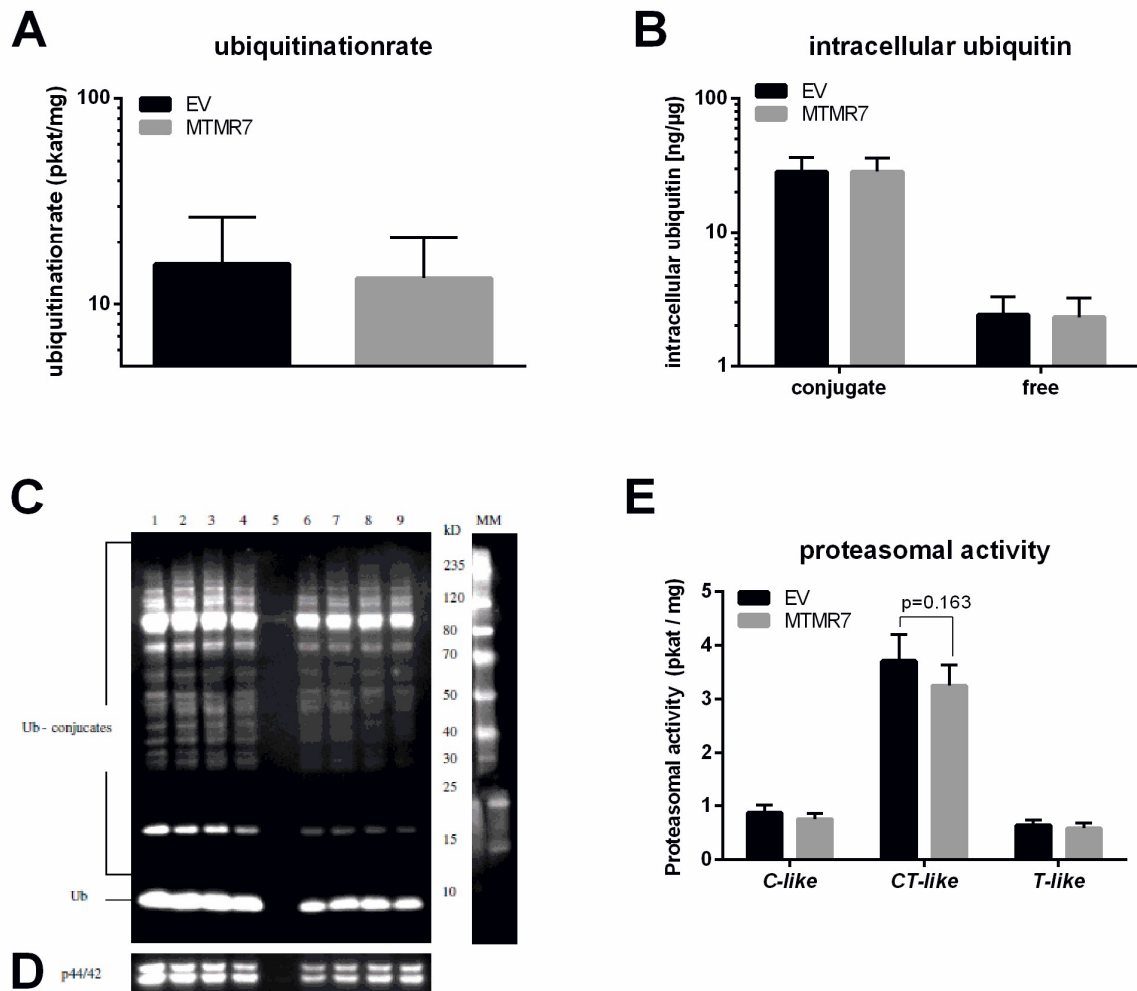


Figure 22: Detection of endogenous ubiquitin in cell lysates by immunoblotting. SW480 cells were transfected with MTMR7 plasmid or an EV control for 24 h before performance of ubiquitin/ proteasome assay. **A-C.** Detection of anti-ubiquitin in MTMR7-transfected (Lane 1,3,6,8)/ EV-transfected (Lane 2,4,7,9) cell lysates (30 µg/ lane) is shown together with the quantitative analyses; Lane MM –protein marker (Spectra Multicolor). No influence on the ubiquitinationrate and on the intracellular ubiquitin level upon MTMR7 transfection could be seen. **D.** The membrane was reprobed with an anti-MAPK 1/ 2 (p44/42) antibody as a protein loading control. **E.** Measurement of proteasomal activity in MTMR7-transfected cells compared to EV controls. Results are -fold ± S.E. (n=7; n.s.; Unpaired t test).

The experiment showed no influence on the ubiquitination rate and on the intracellular ubiquitin level upon MTMR7 transfection (Figure 22A, B).

Furthermore, proteasomal activity of the proteases' active sites that perform the proteolysis reactions was measured. Each of the three subunits has a slightly different proteolytic activity: β 1 cleaves the peptide chain of the unfolded protein to acidic amino acids (caspase-like activity, C-like), β 2 cleaves for basic amino acids (trypsin-like activity, T-like), and β 5 cleaves for hydrophobic amino acids (chymotrypsin-like activity, CT-like).

The results did not show any difference in the caspase- and trypsin-like protease activity. However, a tendency that the chymotrypsin-like proteasomal activity was decreased from 1.7-fold in EV transfected cells to 1.5-fold in MTMR7 transfected cells was seen (Figure 22E).

This confirmed previous findings which showed that MTMR7 has no influence on proteasomal degradation of pan-RAS (Figure 21).

Taken together, these results confirmed that RAS is not degraded via the proteasome.

3.4.3. RAS is not degraded by the lysosome

To elucidate if RAS protein might be degraded through lysosomal acidification, SW480 cells were transfected with MTMR7 and an EV control for 6 h. Directly after transfection, cells were cultivated in presence or absence of chloroquine (100 μ M) for 24, 48 and 72 hours. Similar experiment was done in a short-term time frame with transfection for 6 hours. After transfection, cells were cultivated for 48 hours and then starved overnight. After starvation, cells were pre-incubated with chloroquine (100 μ M) for 30 minutes and re-stimulated for 0, 60 and 180 minutes with 20 % FCS. Cells were harvested after the indicated time points and samples were analyzed by Western blot using an antibody against pan-RAS.

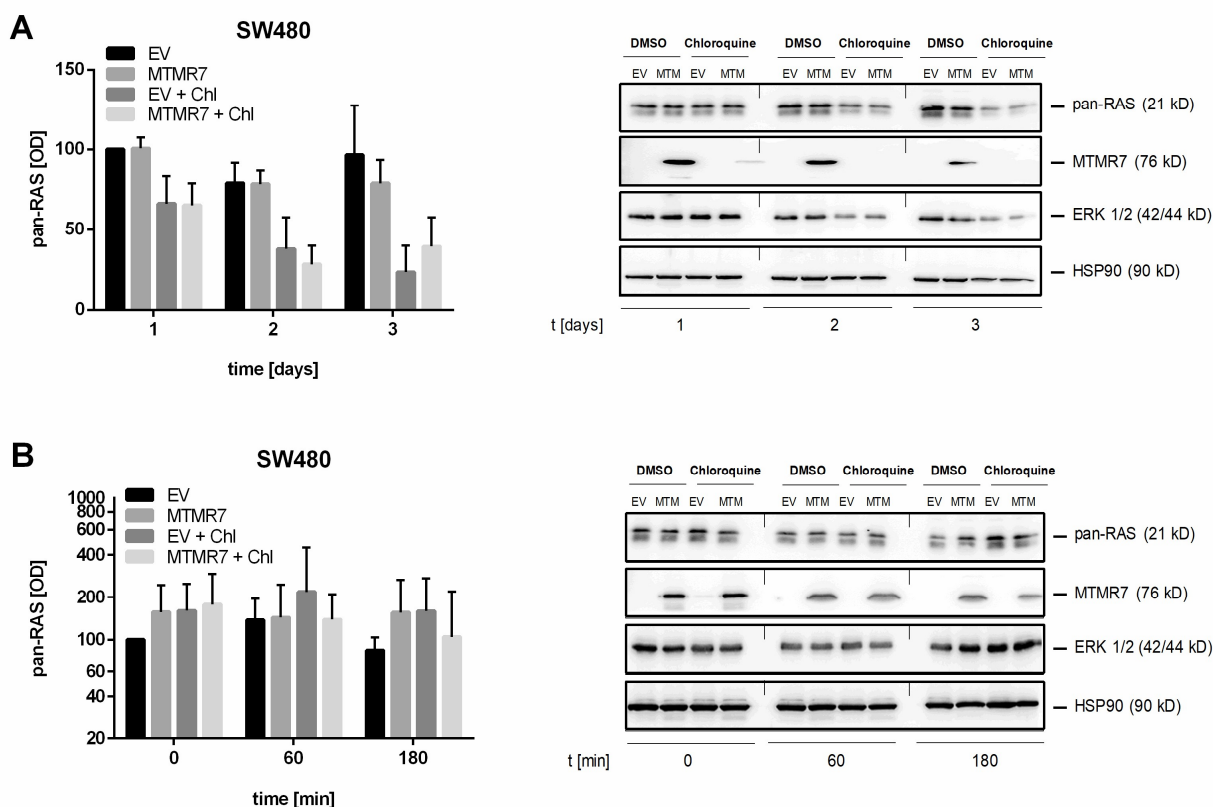


Figure 23: RAS is not degraded via the lysosome. **A.** SW480 cells were transfected with MTMR7 plasmid or an EV control for 6 h. After transfection, cells were treated with the lysosomal inhibitor chloroquine (100 μ M) for 1-3 days. Detection of pan-RAS (21 kD) protein in TCL is shown together with the quantitative analyses. OD values of bands in gels were normalized to ERK 1/2 and calculated as -fold \pm S.E. (n=3; n.s.; Two-way Anova). **B.** SW480 cells were transfected with MTMR7 plasmid or an EV control for 6 h. After transfection, cells were cultivated for 48 h and then starved overnight. After starvation, cells were preincubated with the lysosomal inhibitor chloroquine (100 μ M) for 30 min before re-stimulation with 20 % FCS for 0-180 min. Detection of pan-RAS (21 kD) protein in TCL is shown together with the quantitative analyses. OD values of bands in gels were normalized to ERK2 and calculated as -fold \pm S.E. (n=3; n.s.; Two-way Anova).

The results showed, that RAS inhibition could not be stopped by blocking the lysosomal degradation pathway in a long-term time frame. In contrast, the effect was enhanced upon

chloroquine treatment, meaning that RAS is not degraded via lysosomal acidification, but the reduction can be further promoted using a lysosomal inhibitor (Figure 23A). Notably, MTMR7 expression was also diminished in chloroquine treated cells, meaning that the used concentration might have been too high for the long-term treatment. In a short-term time frame, no loss of pan-RAS protein upon MTMR7 transfection or chloroquine treatment could be observed (Figure 23B).

3.4.4. Changes in membrane potential promote RAS down-regulation

3.4.4.1. KCl promotes RAS reduction and P-ERK 1/2 inhibition in colorectal cancer cell lines

Subcellular fractionation showed that MTMR7 prevents the recruitment of RAS proteins to membranes. As shown by Hancock et al, changes in the membrane potential promote detachment of RAS nanoclusters at the plasma membrane and internal membranes like endosomes (Zhou, Wong et al. 2015). Thus, modulators of ion channels (TRAM34, KCl) were used to study their effect on RAS. HEK293T, SW480 and HCT116 were transfected with either MTMR7 and an EV control for 6 h. Directly after transfection, cells were treated for a long-term time frame of 1-3 days with 100 mM KCl (SW480) or 50 mM KCl (HEK293T, HCT116).

A similar experiment was done in a short-term time frame with transfection for 6 hours. After transfection, cells were cultivated for 48 hours and then starved overnight. After starvation, cells were treated for a short-term time frame (0-30 minutes) with 100 mM KCl (SW480) or 50 mM KCl (HEK293T, HCT116). Cells were harvested after the indicated time points and samples were analyzed by Western blot using an antibody against pan-RAS and P-ERK 1/2.

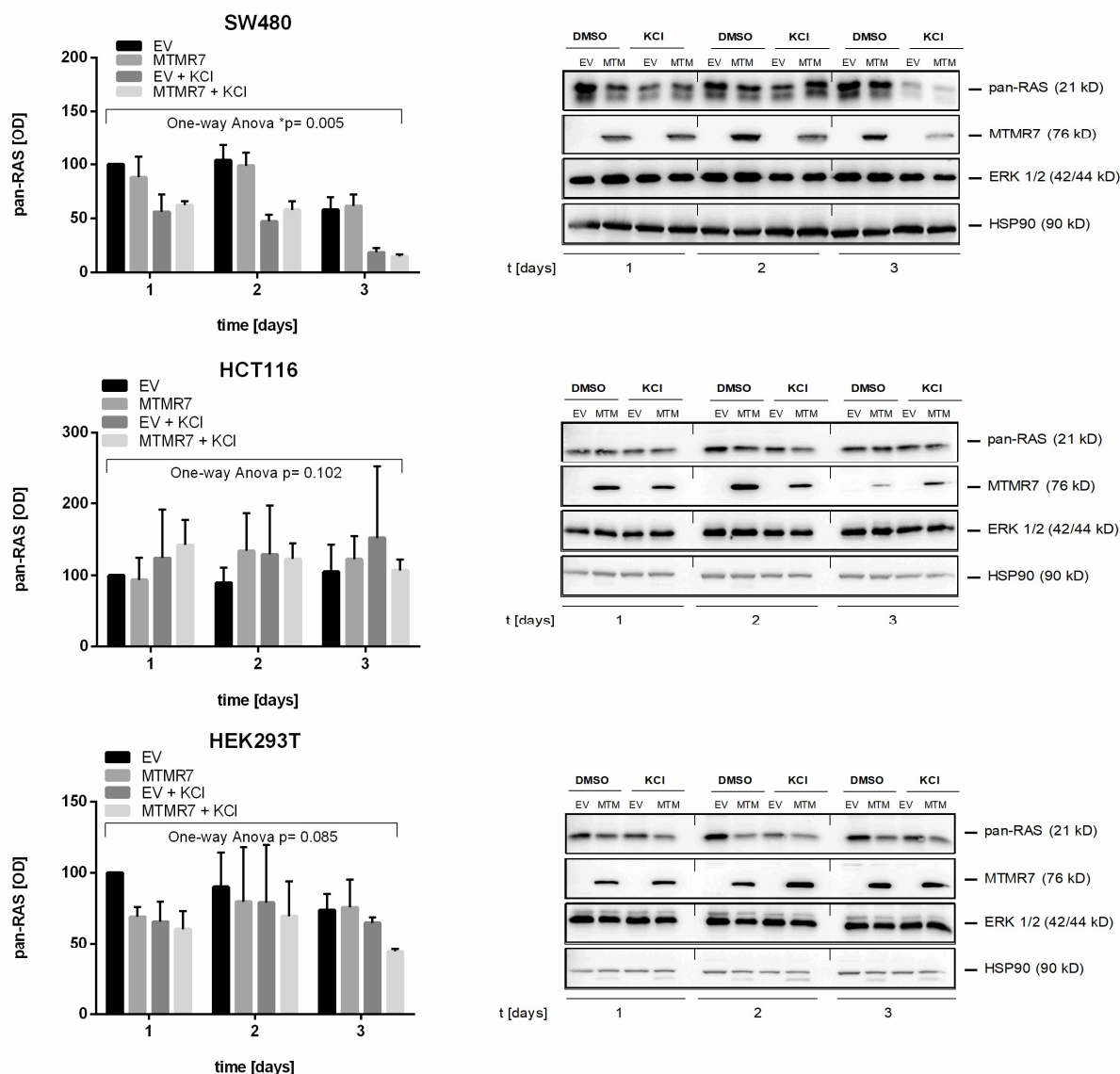


Figure 24: KCl promotes RAS down-regulation in colorectal cancer cell lines in a long-term time frame. Cells were transfected with MTMR7 plasmid or an EV control for 6 h. After transfection cells were directly treated with 100 mM KCl (SW480) or 50 mM KCl (HCT116/ HEK293T) for 1-3 days. Detection of pan-RAS (21 kD) protein in TCL is shown together with the quantitative analyses. OD values of bands in gels were normalized to HSP90 and calculated as -fold \pm S.E. (n=3 per cell line; *p<0.05 MTMR7 vs. EV; Kruskal-Wallis test; n.s. Dunn's multiple comparisons test).

The results of the long-term time frame experiment showed that RAS down-regulation was significantly promoted from 13 % reduction upon MTMR7 transfection to 40 % reduction upon MTMR7 transfection combined with increasing extracellular KCl concentrations in SW480 cells on day 3. The same trend was seen in HEK293T cells but not as strong as for the SW480 cells (Figure 24).

For the short-term stimulation with KCl the results confirmed a significant downregulation of pan-RAS protein by 37 ± 14 % in SW480 and by 14 ± 9 % in HEK293T cells, but not for the HCT116 cells. Furthermore, ERK 1/2 phosphorylation was significantly inhibited by increasing extracellular KCl concentrations in HEK293T (by 68 ± 20 %) and HCT116 (by 32 ± 3 %) cells after 30 minutes of stimulation. However, this inhibition could not be seen in SW480 cells (Figure 25).

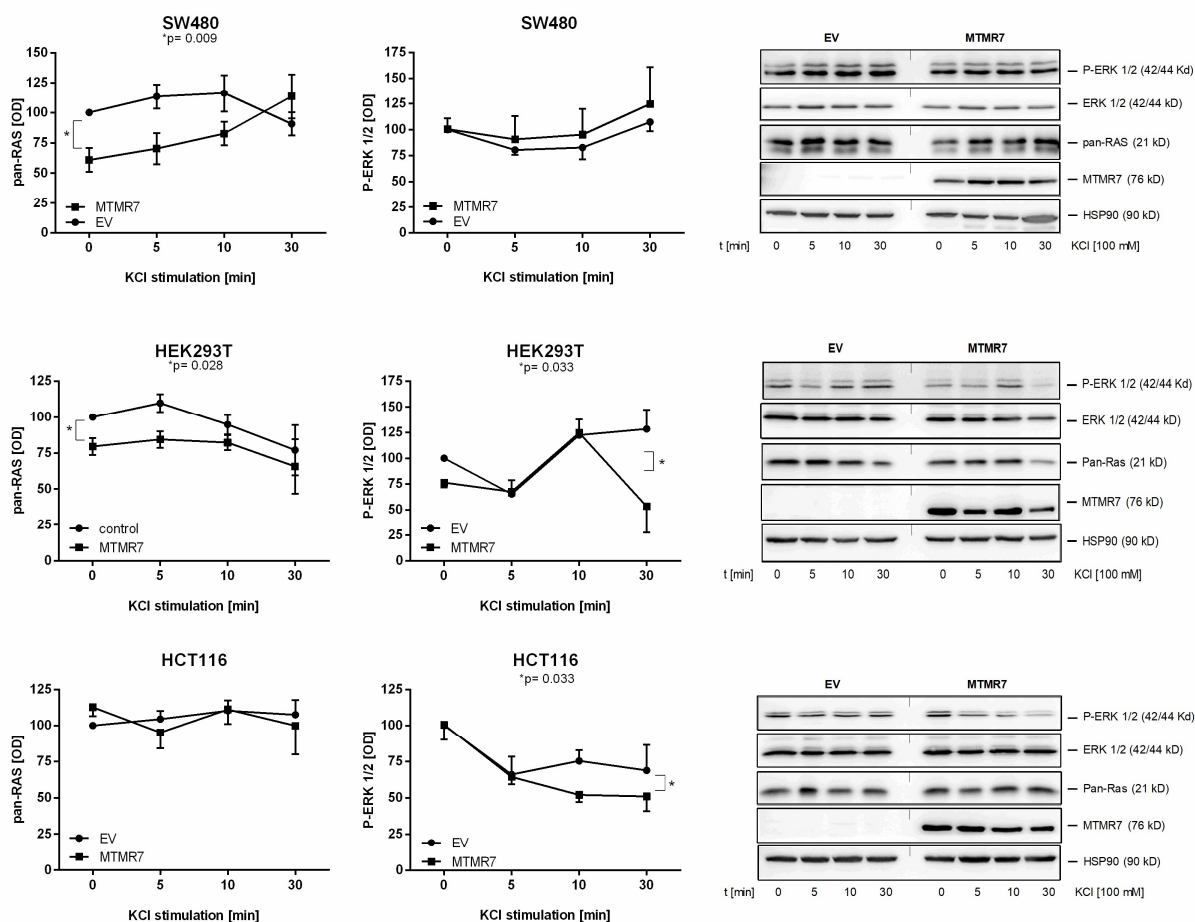


Figure 25: KCl promotes reduction of pan-RAS protein and P-ERK 1/2 inhibition in colorectal cancer cell lines in a short-term time frame. Cells were transfected with MTMR7 plasmid or an EV control for 6 h. After transfection cells were cultivated for 48 h and then starved overnight. After starvation cells were treated with 100 mM KCl (SW480) or 50 mM KCl (HCT116/ HEK293T) for 0, 5, 10 and 30 minutes. Detection of pan-RAS (21 kD) protein and P-ERK 1/2 in TCL is shown together with the quantitative analyses. OD values of bands in gels were normalized to HSP90 or ERK 1/2 and calculated as -fold \pm S.E. (n=3 per cell line; *p<0.05 MTMR7 vs. EV; Two-way ANOVA (SW480, HEK293T) or Kruskal-Wallis test (HCT116)).

Taken together, these results indicated that RAS down-regulation may be at least in part due to membrane depolarization, thus a biophysical mechanism.

Results

To further elucidate if pan-RAS protein is reduced by a biophysical mechanism, “patch-clamp” technologies were used. Experiments were performed on a sodium-dependent potassium channel (KCA3.1, SK4) in cooperation with Dr. Xiaobo Zhou, First Department of Medicine, Medical Faculty Mannheim, University of Heidelberg. This channel plays an important physiological role in the regulation of the membrane potential and calcium signaling in many cell types (Srivastava, Li et al. 2005). RT-PCR results showed that this channel was highly expressed in HCT116 and SW480 cells and weakly in Caco2 and HT29 cells (Figure 26).

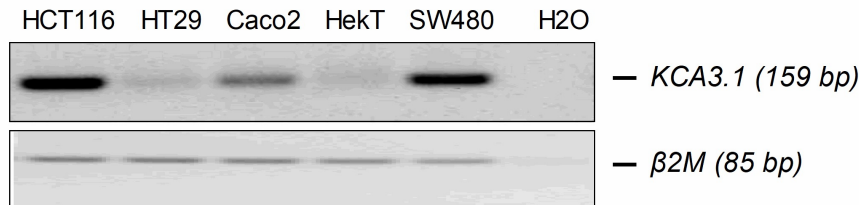


Figure 26: Expression of KCA3.1 channel in colorectal cancer cell lines. Detection of *KCA3.1* cDNA in total RNA extracted from human cell lines. Representative agarose gel of RT-PCR (35 x cycles) is shown. Expected sizes of amplification products: *KCA3.1* = 159 bp *B2M* = 85 bp (n=3 per cell line).

Furthermore, the KCA3.1 channel has been reported to be inhibited by MTMR6. Since MTMR6, MTMR7 and MTMR8 belong to the same subgroup of MTMs, the question was if MTMR7 can also influence that channel and thereby change the membrane potential (Srivastava, Li et al. 2005).

To examine this, SW480 and HCT116 cells were transfected with MTMR7-GFP or an GFP-tagged EV control for 48 hours. The GFP-tag was indispensable to distinguish between the transfected and untransfected cells. After incubation, “patch-clamp” measurements were performed by Dr. Xiaobo Zhou. Whole cell currents were evoked by pulses from -80 - 80 mV with a holding potential of -50 mV. Two KCA3.1 channel blockers, TRAM34 or clotrimazole, were applied to the cells by a perfusion pipette.

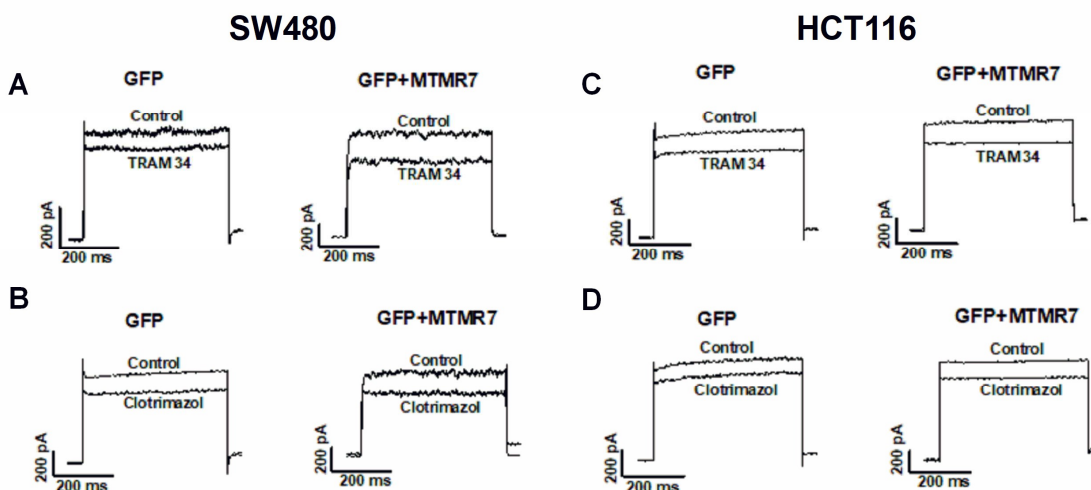


Figure 27: Overexpression of MTMR7 did not influence the KCA3.1 channel in SW480 and HCT116 cells. Whole cell currents (I_m) were evoked by pulses from -80 to +80 mV with the holding potential of -50 mV. KCA3.1 channel blocker, TRAM 34 (1 μ M) or clotrimazole (3 μ M) was applied to cells by a perfusion pipette. The blocker-sensitive currents were separated from I_m as KCA3.1 channel currents (SK4). **A.** Representative I_m traces in absence (control) and presence of 1 μ M TRAM 34 in SW480 cells expressed with GFP (left) or MTMR7-GFP (right). **B.** Representative I_m traces in absence (control) and presence of 3 μ M clotrimazole in SW480 cells expressed with GFP (left) or MTMR7-GFP (right). **C.** Representative I_m traces in absence (control) and presence of 1 μ M TRAM 34 in HCT116 cells expressed with GFP (left) or MTMR7-GFP (right). **D.** Representative I_m traces in absence (control) and presence of 3 μ M clotrimazole in HCT116 cells expressed with GFP (left) or MTMR7-GFP (right) (n = 10).

Figure 27, also kindly provided by Dr. Xiaobo Zhou, shows representative currents in presence or absence of 1 μ M TRAM34 (Figure 27A, C) and 3 μ M clotrimazole (Figure 27B, D) in cells transfected with EV-GFP (left) or MTMR7-GFP (right). These data showed that MTMR7 did not influence the KCA3.1 channel or the membrane currents.

To further prove if RAS is degraded by a biophysical mechanism, an epithelial sodium channel (ENaC) blocker called amiloride was used. It directly blocks the channel and thereby inhibits sodium reabsorption without depleting potassium, thus hyperpolarizes the plasma membrane. For this experiment, HEK293T cells were transfected with either MTMR7 and an EV control for 6 h. Directly after transfection, cells were treated with 0.1 mM amiloride for a long-term time frame of 1-3 days.

A similar experiment was done in a short-term time frame with transfection for 6 hours. After transfection, cells were cultivated for 48 hours and then starved overnight. After starvation, cells were treated with 0.1 mM amiloride for a short-term time frame (0-30 minutes).

Cells were harvested after the indicated time points and samples were analyzed by Western blot using an antibody against pan-RAS and P-ERK 1/2 (Figure 28).

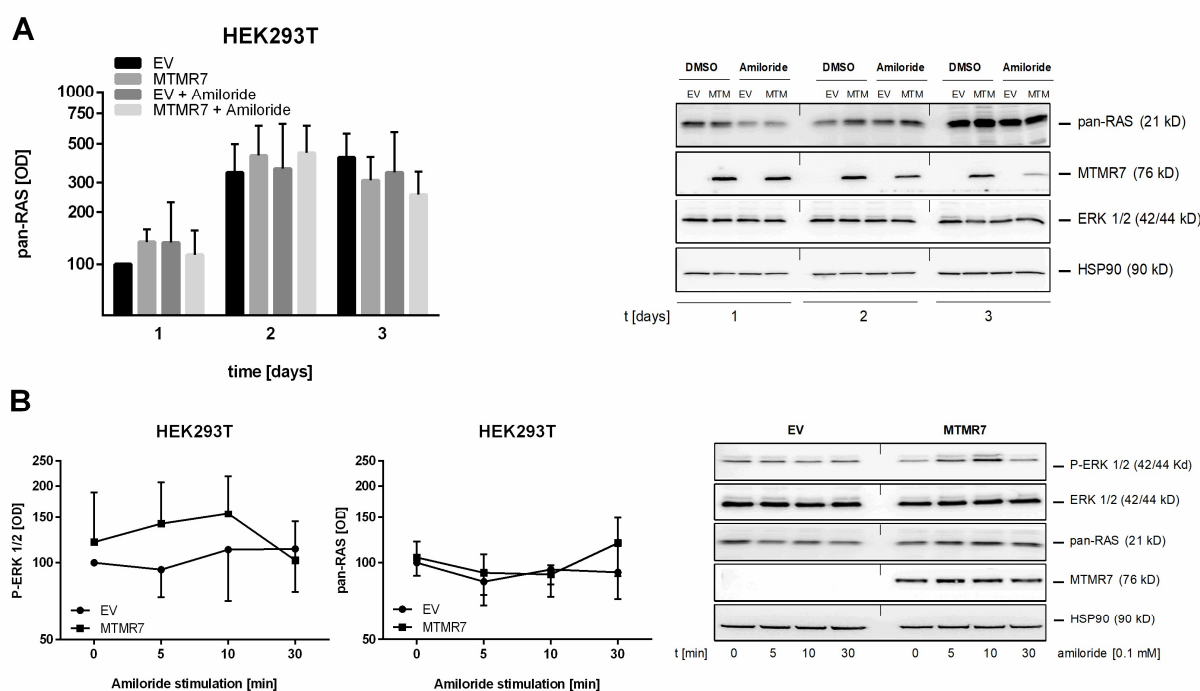


Figure 28: Amiloride prevents RAS down-regulation and P-ERK 1/2 inhibition in HEK293T. **A.** Cells were transfected with MTMR7 plasmid or an EV control for 6 h. After transfection cells were directly stimulated with 0.1 mM amiloride for 1-3 days. Detection of pan-RAS (21 kD) protein in TCL is shown together with the quantitative analyses. **B.** Cells were transfected with MTMR7 plasmid or an EV control for 6 h. After transfection cells were cultivated for 48 h and then starved overnight. After starvation cells were stimulated with 0.1 mM amiloride 0, 5, 10 and 30 minutes. Detection of pan-RAS (21 kD) protein and P-ERK 1/2 in TCL is shown together with the quantitative analyses. Neither RAS down-regulation nor P-ERK 1/2 inhibition was seen. OD values of bands in gels were normalized to HSP90 and calculated as -fold \pm S.E. (n=3; n.s.; Two-way ANOVA).

The results showed that MTMR7-mediated RAS reduction was prevented by treating the cells in a long- and short-term time frame. In addition, phosphorylation of ERK 1/2 was not inhibited. These data from two drugs affecting membrane polarisation indicate that MTMR7-mediated RAS down-regulation may be due to biophysical changes in membrane potential.

3.4.5. PPAR γ drug agonist does not promote MTMR7-mediated RAS down-regulation

Since MTMR7 inhibited RAS activity and forms a complex with PPAR γ which is druggable by PPAR γ agonist the effect on RAS reduction was determined by treating SW480, HCT116 and HEK293T cells with rosi. For this purpose, cells were transfected with MTMR7 full-length plasmid and an EV control for 6 h. After transfection, cells were stimulated with 10 μ M rosi for 1, 2, 3 days. Cells were harvested after indicated time points, and Western blot analysis was performed using an antibody against pan-RAS (Figure 29).

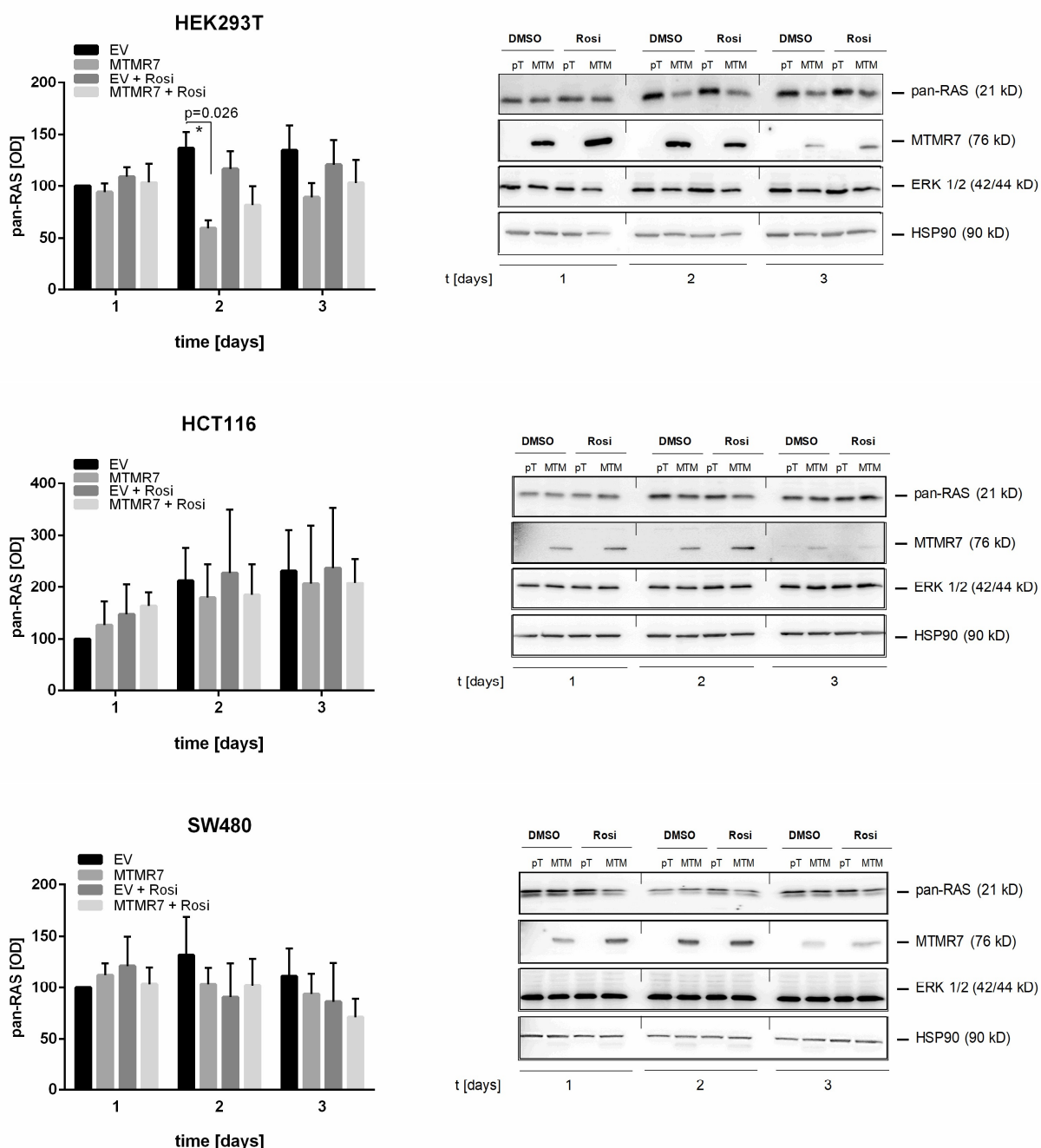


Figure 29: Rosiglitazone does not increase MTMR7 mediated RAS degradation in HEK293T cells. Cells were transfected with MTMR7 plasmid or an EV control for 6 h. After transfection cells were stimulated with 10 μ M rosi for 1, 2, 3 days. Detection of pan-RAS (21 kD) protein in TCL is shown together with the quantitative analyses. OD values of bands in gels were normalized to ERK 1/2 and calculated as -fold \pm S.E. (n=3 per cell line; *p<0.05 MTMR7 vs. EV; Two-way ANOVA).

The results confirmed that the reduction of RAS protein in HEK293T cells was significantly decreased by $40\% \pm 7.6\%$ upon MTMR7 transfection, no additional effect of rosi treatment was detected. However, reduction was neither seen for HCT116 nor for SW480 cells. Thus, treatment with PPAR γ ligand rosi did not further facilitate RAS down-regulation.

3.5. Effect of MTMR7 on therapy-resistance

3.5.1. Knockdown of MTMR7 promotes proliferation of human colorectal cancer cell lines

We have shown previously, that HCT116 and SW480 cells stably transfected with MTMR7 displayed a reduced proliferation rate within 5 days compared to cells transfected with an EV control (Weidner, Söhn et al. 2016).

To prove if these findings were due to MTMR7 overexpression, a knock-down of endogenous MTMR7 protein with MTMR7-shRNA plasmid in *KRAS*-mutant cells (HCT116, Lovo, SW480; DLD1) and in *KRAS*-WT cells (Caco2, HT29, HEK293T) was performed. Cell viability was measured using MTT assay. Cells transfected with a control shRNA plasmid served as control (Figure 30).

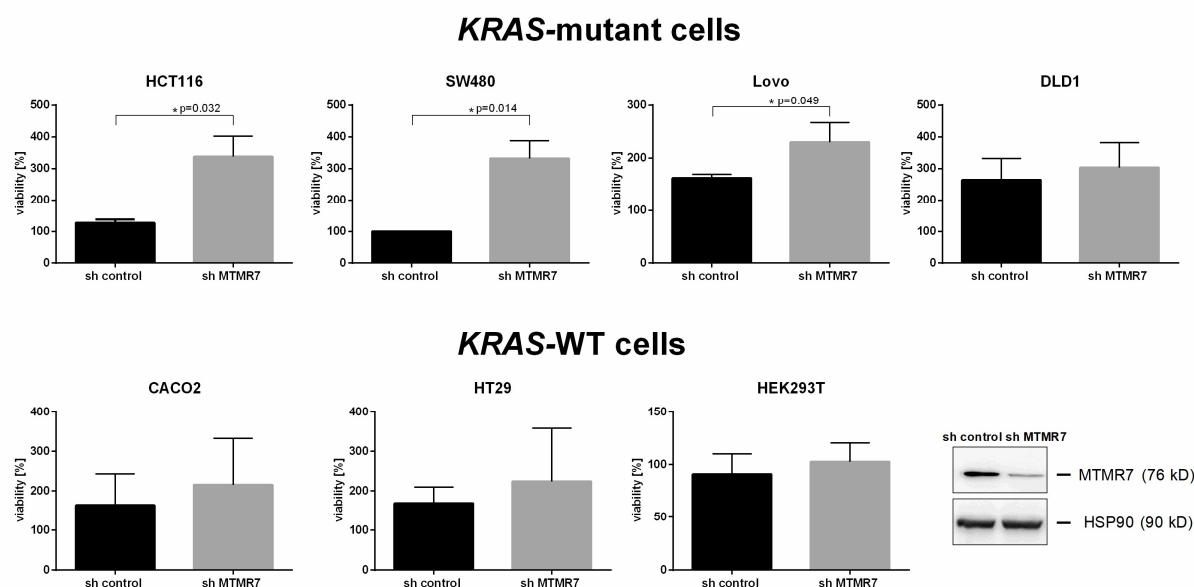


Figure 30: MTMR7 knockdown promotes cell growth. SW480, HCT116, Lovo, DLD1, Caco2, HT29 and HEK293T cells were transfected with either shRNA control or shRNA MTMR7 plasmid for 24 h. Viability was measured in MTT assay 2 days after transfection. OD values were calculated as -fold \pm S.E. (n=3 per cell line; *p<0.05 MTMR7-shRNA vs. control-shRNA; Unpaired t test) compared with day 0.

For *KRAS*-mutant HCT116 cells the results showed a significantly increasing cell viability upon transfection of MTMR7-shRNA compared with cells receiving control shRNA plasmid (sh MTMR7 $3.4 \pm 0.6\%$ vs. sh Control $1.3 \pm 0.1\%$). Similar results were found for Lovo (sh MTMR7 $2.3 \pm 0.4\%$ vs. sh Control $1.6 \pm 0.1\%$) and SW480 (sh MTMR7 $3.3 \pm 0.6\%$ vs. sh Control $1.1 \pm 0.01\%$) cells whereas *KRAS*-WT cells Caco2, HT29, HEK293T were less sensitive to MTMR7 knockdown (Figure 30). (Data already published in (Weidner, Söhn et al. 2016)).

3.5.2. MTMR7 sensitizes human *KRAS*-mutated CRC cells to mTOR-/RAF kinase-inhibitors

Since MTMR7 acts as a dual inhibitor of the RAS-RAF-MEK1/2-ERK1/2 and PI3K-AKT-mTOR-S6K signaling pathways, the idea was to assess whether this inhibiting effect can be mimicked by combining two approved drugs, a multi-kinase inhibitor (sorafenib), inhibiting the RAF-kinase and several tyrosine kinases of the VEGF signaling pathway, together with an mTOR-inhibitor (everolimus), to inhibit proliferation and survival of *KRAS*-mutated human CRC.

MTT viability assays with different concentrations of sorafenib and everolimus in presence and absence of MTMR7 were performed in SW480, HCT116 and HEK293T cells to figure out effective drug concentrations. MTMR9 was an additional control as it is an inactive binding partner of MTMR7. Results are shown in Figure 31.

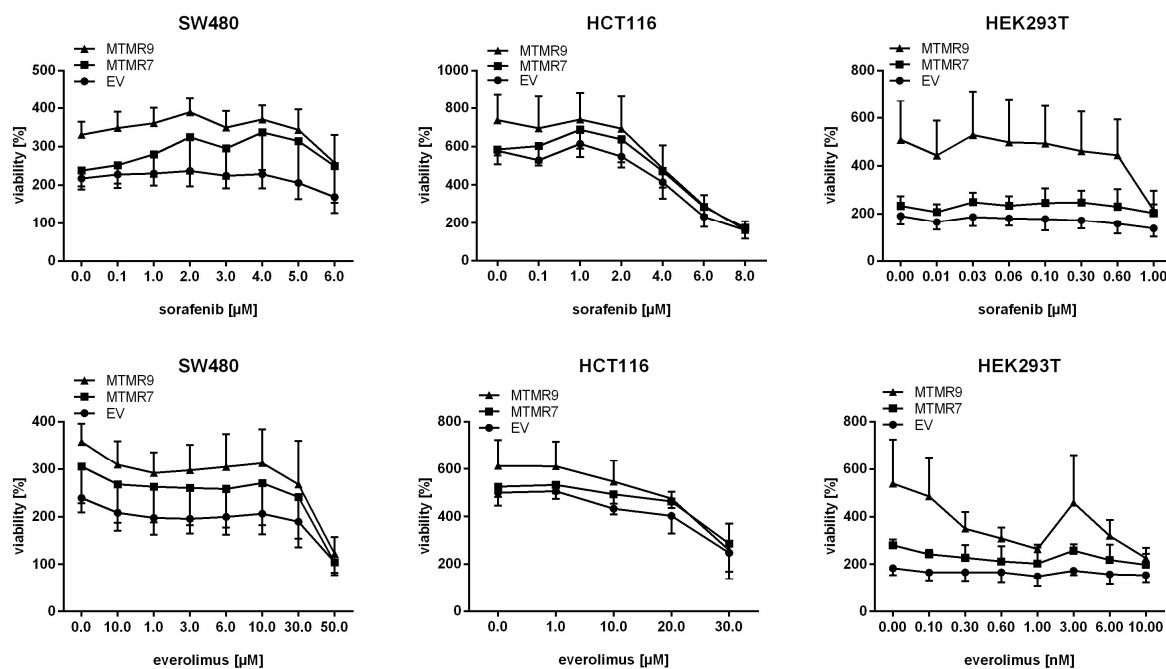


Figure 31: Effect of kinase inhibitors on colorectal cancer cell lines. SW480, HCT116 and HEK293T cells were transfected with either an EV control or MTMR7 plasmid for 24 h. The next day, cells were reseeded into 96-well plates (2000 cells/well). After additional 24h, cells were treated with either sorafenib (upper panel) or everolimus (lower panel) at different concentrations. Viability was measured in MTT assay after 96 h of treatment. OD values were calculated as -fold \pm S.E. (n=3 per cell line; n.s.; MTMR7 vs. EV; Two-way Anova) compared with day 0.

The results demonstrated, that low drug concentrations in the nanomolar range were needed for *KRAS*-WT cells e.g. HEK293T cells. In these cells, a synergistic effect of the drugs and MTMR7 transfection could not be seen. Nevertheless, HEK293T cells proliferated slower under drug treatment and thus showed no resistance against sorafenib or everolimus.

For the *KRAS*-mutated HCT116 and SW480 cells, very high concentrations (micromolar range) of the drugs were needed, and no synergistic effect of the drugs and MTMR7 was seen. Thus, the *KRAS*-mutated cells showed a resistance against both drugs.

To assess whether the resistance can be circumvented by combining these two kinase inhibitors, MTT assays were performed using a combination of sorafenib and everolimus (Figure 32).

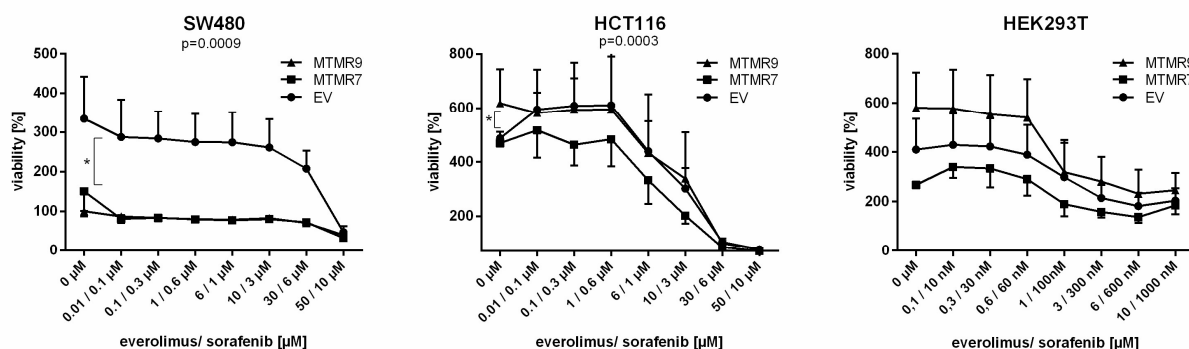


Figure 32: Combination therapy breaks resistance in colorectal cancer cell lines. SW480, HCT116 and HEK293T cells were transfected with either an EV control or MTMR7 plasmid for 24 h. The next day, cells were reseeded into 96-well plates (2000 cells/well). After additional 24h, cells were treated with a sorafenib/ everolimus combination. Viability was measured in MTT assay after 96 h of treatment. OD values were calculated as -fold \pm S.E. (n=2 per cell line; *p<0.05 MTMR7 vs. EV; Friedman test) compared with day 0.

The combination therapy showed that in presence of MTMR7 and the two drugs, proliferation of the cells was much slower as in the single therapy, whereas resistance remained in the absence of MTMR7. Proliferation was significantly inhibited in HCT116 and SW480 cells upon drug treatment and MTMR7 transfection (HCT116: MTMR7 3.5 ± 1.5 % vs. EV 4.5 ± 1.5 %; SW480: MTMR7 1.9 ± 1.0 % vs. EV 2.5 ± 0.4 % at a concentration of 10/ 3 μ M). The effect was also seen in HEK293T cells, but it was not as strong as in the two colorectal cancer cell lines.

To examine if the inhibiting effect of MTMR7 can be enhanced by additional treatment with PPAR γ ligand, cells were treated with the combination of the two kinase inhibitors +/- rosi. However, rosi did not further inhibit cell growth (data not shown).

In sum, MTMR7 inhibited proliferation of *KRAS*-mutated CRC cells with high pan-RAS activity (SW480) more efficiently than the kinase inhibitors alone, MTMR7 augmented the efficacy of the drugs, while the addition of rosi did not further influence growth inhibition.

3.5.3. Influence of MTMR7 on cetuximab treatment

To assess, whether the benefit of cetuximab treatment is dependent on the presence or absence of MTMR7 in cells, two *KRAS*-mutant CRC cell lines (HCT116, SW480) and one *KRAS*-WT cell line (HEK293T) were transfected with MTMR7 plasmid or an EV control for 24 hours and treated with cetuximab concentrations ranging from 0 to 1000 μ g/ml in a long-term time frame of 6 days (Figure 33).

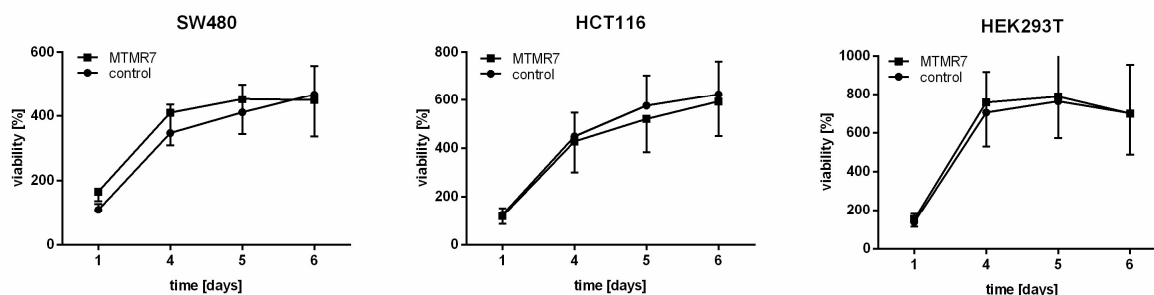


Figure 33: Benefit of cetuximab treatment is not dependent on the presence of MTMR7. SW480, HCT116 and HEK293T cells were transfected with either an EV control or MTMR7 plasmid for 24 h. The next day, cells were reseeded into 96-well plates (2000 cells/well). After additional 24h, cells were treated with 1000 µg/ml cetuximab. Viability was measured in MTT assay 1-6 days. OD values were calculated as -fold ± S.E. (n=3 per cell line; n.s. Two-way Anova) compared with day 0.

The results showed that, MTMR7 did not promote cetuximab treatment in any cell line. However, a different effect could be seen in the three cell lines. The SW480 and HCT116 cells were resistant to cetuximab treatment at all, even in the highest used concentration.

For the HEK293T cells no differences could be seen upon MTMR7 transfection and cetuximab treatment. However, these cells are not *KRAS* mutated and should respond at least to cetuximab treatment alone (without MTMR7 transfection). This indicates that the antibody was not functioning properly, which might be due to the use of antibody remnants of the clinic.

3.5.4. MTMR7 peptide inhibits proliferation of human *KRAS*-mutated CRC cell lines

Since MTMR7 is lost in many colorectal cancer patients, the idea was to resupply it to patients. To this end, Dr. Elke Burgermeister designed a docking site peptide which mainly consists of the coiled-coil domain of MTMR7. This domain is an amphipathic leucine-rich helix which is responsible for the binding of MTMR9 which in turn enhances the MTMR7 phosphatase activity. A scrambled peptide served as control.

To assess, whether the MTMR7 peptide can imitate signaling inhibition by MTMR7 overexpression, a series of 7 human cancer cell lines (SW480, HCT116, DLD1, Lovo, HEK293T, AGS, PATU8902) were grown for 7 days in presence of either 0.5 µM MTMR7-peptide or scrambled peptide, and cell viability was measured each day by MTT assay (Figure 34).

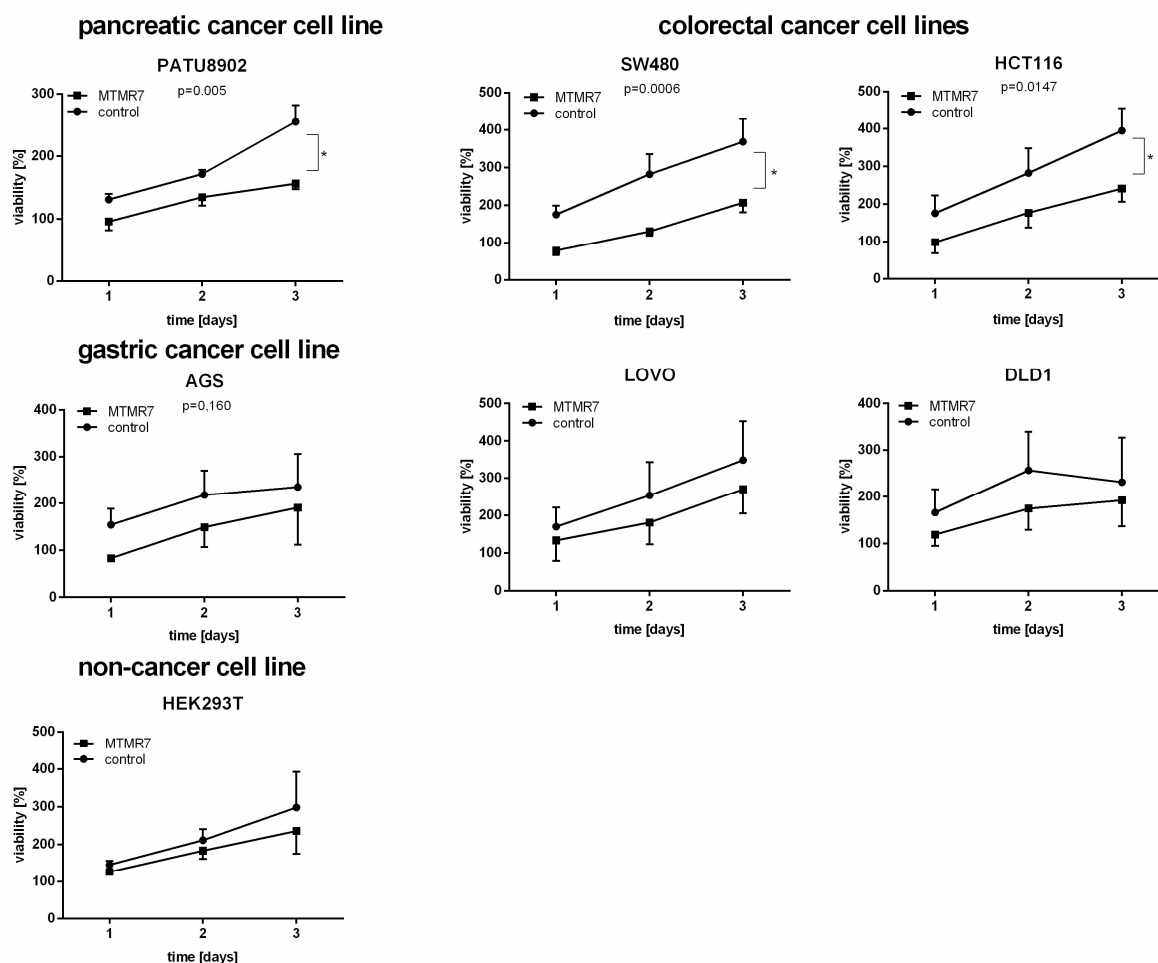


Figure 34: MTMR7 peptide inhibits cell growth. SW480, HCT116, Lovo, DLD1, PATU8902, AGS and HEK293T cells were treated with either 0.5 μ M MTMR7-peptide or control-peptide. Viability was measured in MTT assay after 1-3 days. OD values were calculated as $-\text{fold} \pm \text{S.E.}$ ($n=3$ per cell line; * $p<0.05$ MTMR7-peptide vs. control-peptide; Two-way ANOVA) compared with day 0.

The results revealed that MTMR7 peptide significantly inhibited cell growth already after 1 - 2 days in SW480 (MTMR7 peptide 1.3 ± 0.1 % vs. control peptide 2.8 ± 0.5 %), HCT116 (MTMR7 peptide 1.7 ± 0.4 % vs. control peptide 2.8 ± 0.7 %) and PATU8902 (MTMR7 peptide 1.6 ± 0.1 % vs. control peptide 2.6 ± 0.3 %) cells. Furthermore, a trend for reduced proliferation was seen in AGS cells whereas the response in Lovo, DLD1 and HEK293T cells was not as effective.

3.5.4.1. Effect of MTMR7 peptide on RAS-ERK 1/2 signaling

To study the effect of MTMR7-peptide on AKT-mTOR and ERK 1/2 signaling pathways downstream of KRAS, SW480, HCT116, and HEK293T cells were incubated with either MTMR7-peptide or a control-peptide. After 24 hours, cells were starved for 16 h and stimulated with EGF (50 ng/ml) for 0-30 minutes, and samples were analyzed by Western blot using an antibody against pan-RAS, P-AKT and P-ERK 1/2 (Figure 35).

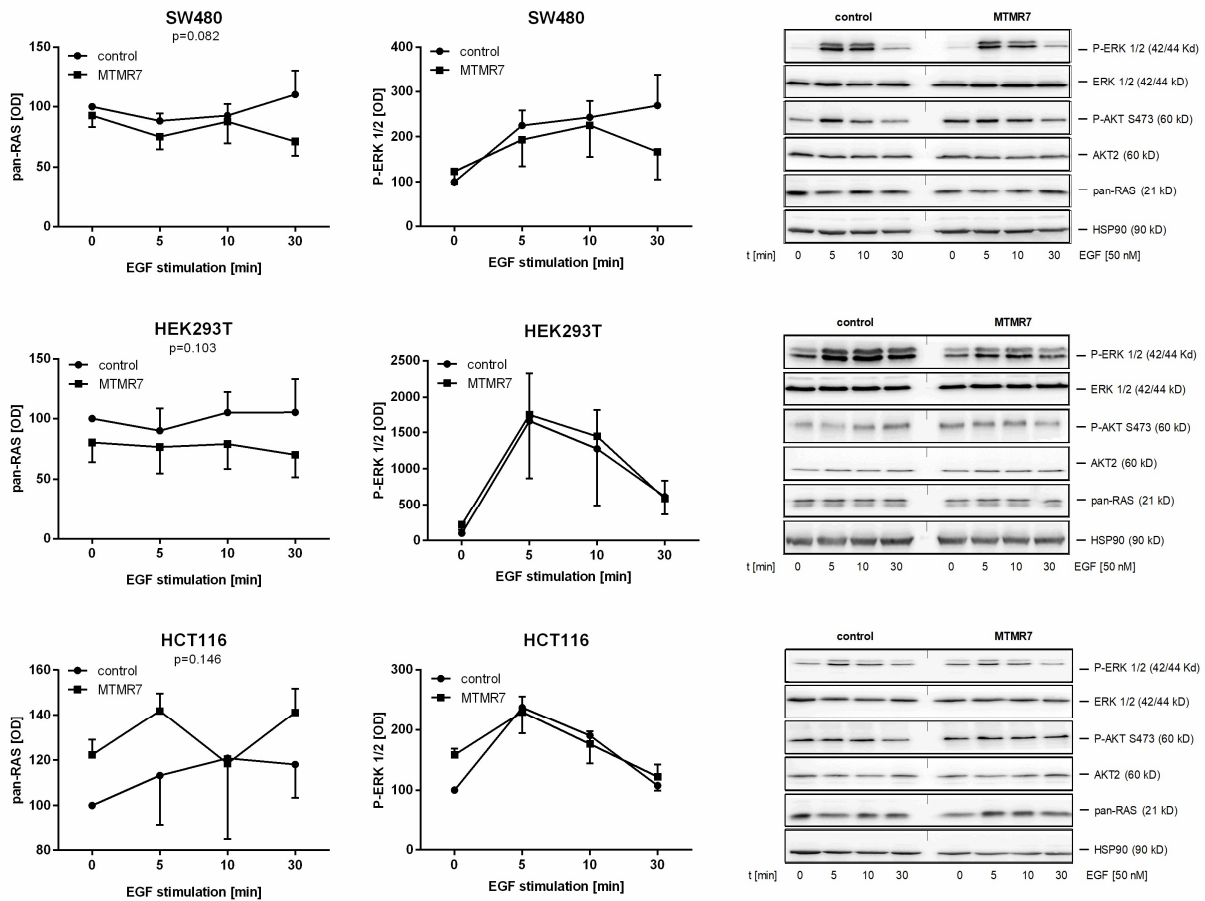


Figure 35: MTMR7 peptide promotes RAS down-regulation. SW480, HCT116 and HEK293T cells were incubated with MTMR7-peptide or a control-peptide. After 24 h cells were starved for 16 h and stimulated with 50 ng/ml EGF for 0-30 min. Detection of pan-RAS (21 kD) and P-ERK 1/2 protein in TCL is shown together with the quantitative analyses. MTMR7-peptide promoted RAS down-regulation in all cell lines but did not influence P-ERK 1/2 expression. OD values of bands in gels were normalized to ERK 1/2 and calculated as -fold \pm S.E. (n=3; n.s.; Two-way Anova).

A tendency for down-regulation of pan-RAS protein levels by about 30 % after 30 minutes of stimulation was seen in SW480 and HEK293T cells. However, this effect could not be seen more downstream in ERK 1/2 phosphorylation. Here, all cell lines showed a significant change in P-ERK 1/2 expression over time, but not between MTMR7-/control-peptide treatment. Furthermore, P-AKT expression was not influenced by MTMR7-peptide (data not shown).

3.5.4.2. MTMR7-peptide reduces serum response element activation

Furthermore, functionality of the MTMR7-peptide was determined by measuring the transcriptional activation of the serum response element (SRE) (Lefebvre, Chen et al.) using luciferase reporter assays as a readout. SW480, HCT116 and HEK293T cells were incubated with either MTMR7-peptide or a control-peptide. After 24 and 48 hours, luciferase activity of SRE was measured (Figure 36).

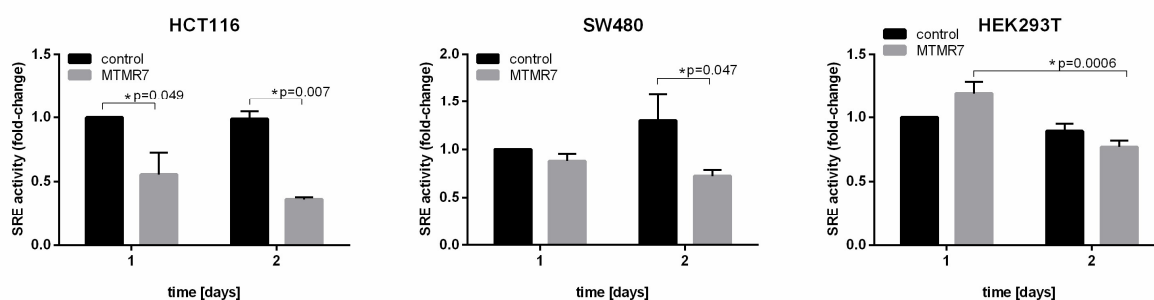


Figure 36: MTMR7 peptide inhibits SRE-reporter gene activity. SW480, HCT116 and HEK293T cells were treated with either 1 μ M MTMR7-peptide or control-peptide for 24/48 h. Luciferase activity in total lysates was normalized to protein content and calculated as -fold \pm S.E. (n=3; *p<0.05 MTMR7-peptide vs. control peptide; Two-way ANOVA) compared with day 0.

All three cell lines showed a significant decrease of SRE activation upon MTMR7-peptide treatment after 48 hours, indicating that the peptide is active and inhibits RAS-ERK 1/2 signaling.

SRE activity was significantly decreased by 35 % in HCT116 cells treated with the MTMR7 peptide compared to the control-peptide.

In SW480 cells, the activity was inhibited by 20 % in the peptide treated cells compared with the untreated controls.

HEK293T cells did not show a difference between the MTMR7-peptide and the control-peptide treatment. However, a significant decrease in SRE activity by 35 % upon MTMR7-peptide treatment was seen on the second day, compared with the first day.

The effect was stronger in HCT116 cells, carrying the weaker *KRAS* G13D mutation, than in SW480 cells with the *KRAS* G12V mutation.

3.6. In vivo analysis of *KRAS* signaling in *Apcmin/+ x Cav1-KO* mice

3.6.1. Therapy of *Apcmin/+ x Cav1-KO* mice with an HSP90 inhibitor

CoIP experiments showed, that MTMR7 is not only forming a complex with PPAR γ and MTMR9, but also with the Heat-shock protein 90 (Hsp90) (Figure 43, 7.1). In addition, MTMR7 lowered HSP90 protein levels significantly in rosi treated cells (Weidner 2016).

Hsp90 is a molecular chaperone which is involved in maturation, stabilization and nuclear translocation of a large (> 200 proteins) set of substrate proteins, known as client-proteins. These clients include many oncogenes, hormone receptors (e.g. PPAR γ) and kinases (Prince 2011). Thus, the idea was to target these clients with an Hsp90 inhibitor and to determine if Hsp90 is also involved in the stabilization of MTMR7 using an *Apcmin/+ x Cav1-KO* mouse model. Mice (at an age of 6 months) were randomized into treatment and control groups (n=3) and treated with 17-DMAG, a water-soluble derivative of geldanamycin, via i.p. injection ((12,5 mg/kg); 4 x times per week) for 4 weeks. At 7 months of age, mice were sacrificed, and drug response was analyzed. The HE-staining and macroscopic analysis revealed a diminished lesion size of about 50 % in the treated mice compared to the untreated ones. Furthermore, microscopic analysis showed a lower tumor amount in the colon of the treated *Apcmin/+ x Cav1-KO* mice compared to the untreated *Apcmin/+ x Cav1-KO* mice (Figure 37).

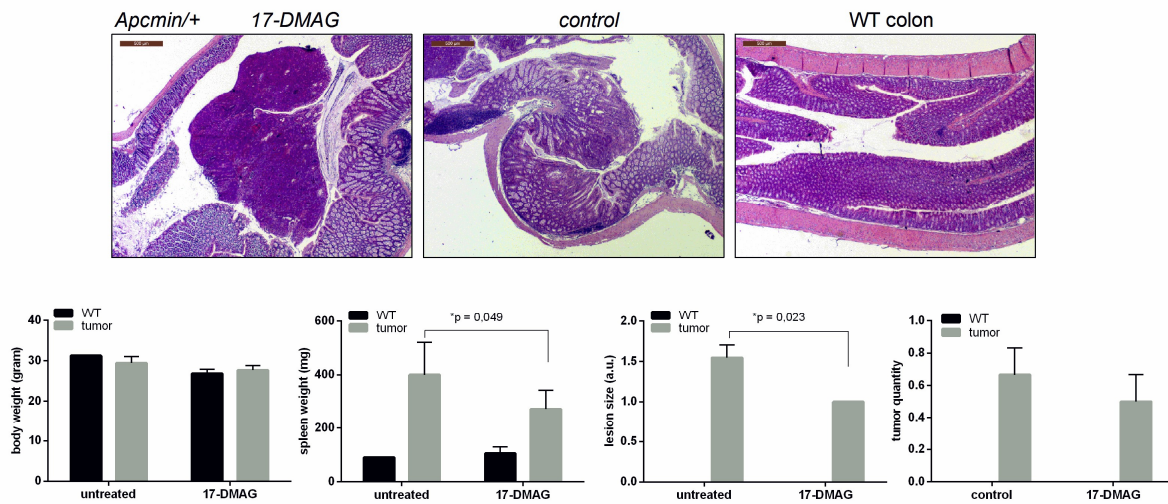


Figure 37: HE-staining of *Apcmin/+* x *Cav1-KO* mice treated with an Hsp90 inhibitor. *Apcmin/+* x *Cav1-KO* mice were treated with the Hsp90 inhibitor 17-DMAG (i.p., 12,5 mg/kg, 4 x per week, n=3 per group) for 4 weeks. Representative HE (adenomas) images are shown. Macroscopic analysis of tumor therapy (lesions size: 0=none; 1= small white adenoma (< 5 mm); 2= large “red” vascularized colorectal adenoma/tumor (> 5 mm) (*p<0.05; Kruskal-Wallis test or ANOVA).

3.6.2. Therapy influence on PPAR γ -target gene expression

Due to quantitative reasons, tissue of the ileum (100 % penetrance of lesions) was used to investigate the expression of PPAR γ target genes such as *Tff3*, *p21* and *CyclinD1*, using RT-qPCR (Figure 38).

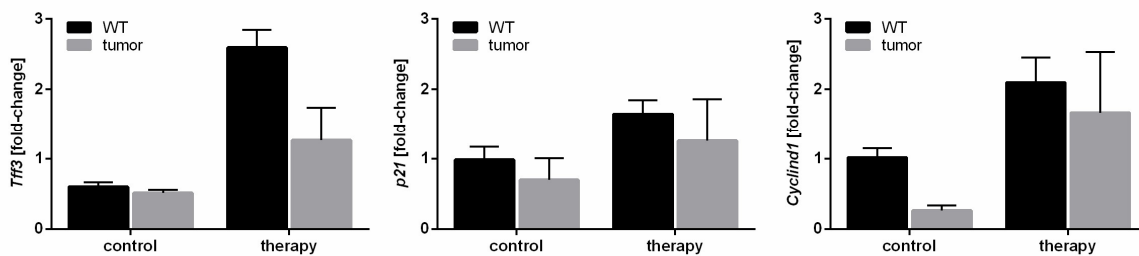


Figure 38: Influence of 17-DMAG therapy on PPAR γ target gene expression. Gene expression was measured in total RNA extracted from frozen mouse tissues. CT-values from RT-qPCRs on total RNA were normalized to beta2-microglobulin (*B2m*) and calculated as -fold \pm S.E. (n=3 per organ; n.s.).

RT-qPCR showed an upregulation of *Tff3* in the treated mice compared to the untreated mice (WT and *Apcmin/+* x *Cav1-KO* mice).

Same was true for the cell cycle inhibitors (CDKIs), *CyclinD1*, and *P21*, indicating that the Hsp90 inhibitor promotes senescence in these mice.

In contrast, no changes were found in the samples of colon tissue (data not shown).

Furthermore, immunohistochemical staining of KRAS and KI67 (Figure 39) was performed.

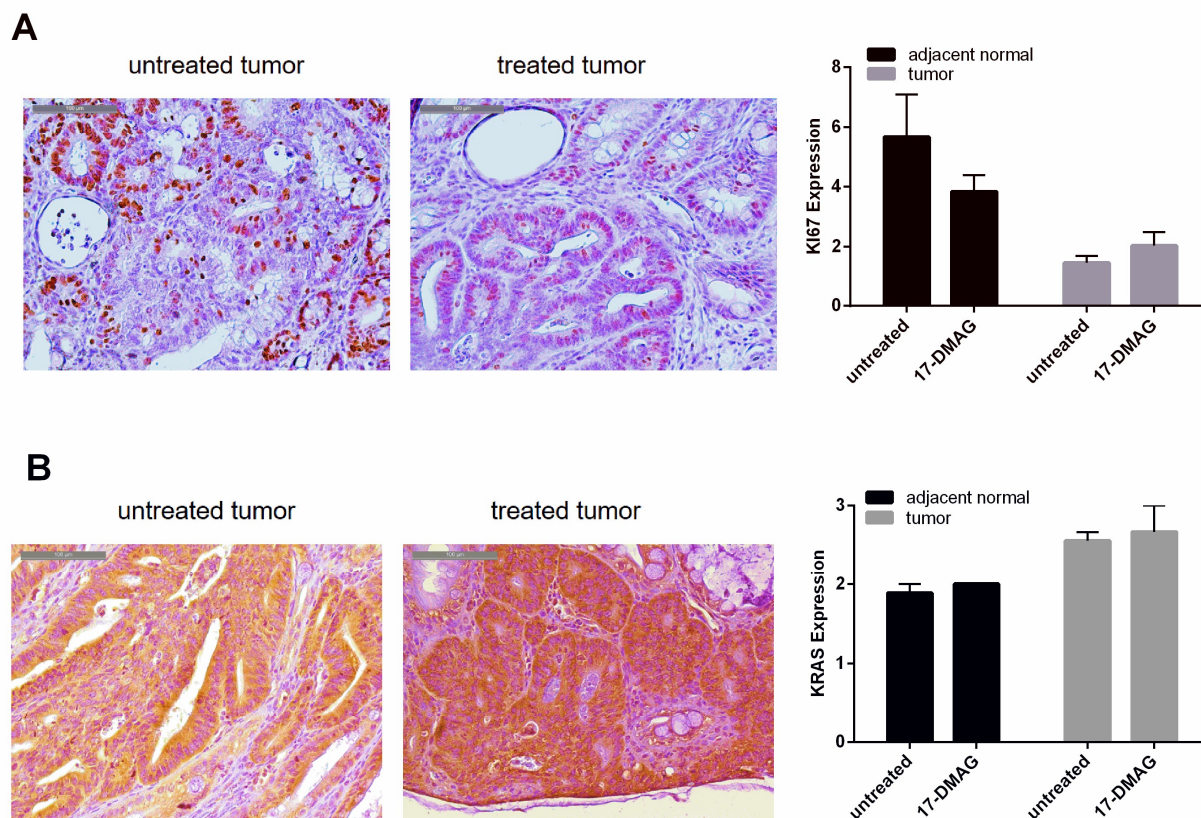


Figure 39: KI67 and KRAS staining in 17-DMAG treated *Apcmin/+ x Cav1-KO* mice. **A.** Representative images are shown together with statistical analysis after counting of positive cells (see 2.6.4). Magnification 200x. Results were calculated as -fold \pm S.E. (untreated n=6; treated n=6; n.s.; Two-way Anova). **B.** Representative images are shown together with statistical analysis after scoring (see 2.6.4). Magnification 200x. Results were calculated as -fold \pm S.E. (untreated n=6; treated n=6; n.s.; Two-way Anova).

Immunohistochemical staining demonstrated that the expression of KI67 is not significantly changed under therapy. Notably, adjacent normal tissue had a higher proliferation rate than the adenoma tissue, indicative of a possible senescence in these lesions which did not progress to adenocarcinoma (Figure 39A).

For KRAS no difference could be seen between the adjacent normal tissue and tumor tissue. In addition, 17-DMAG treatment had no impact on KRAS expression in the *Apcmin/+ x Cav1-KO* mice (Figure 39B).

3.6.2.1. 17-DMAG therapy decreases P-ERK 1/2 levels in *Apcmin/+ x Cav1-KO* mice

In addition to immunohistochemical staining of KRAS and KI67, P-ERK 1/2 and pan-RAS levels were examined. Proteins were extracted from frozen tissue samples of the colon, and Western blots were performed using antibodies against P-ERK 1/2, pan-RAS and p-AKT proteins. The antibodies for AKT-2 and ERK 1/2 served as controls (Figure 40).

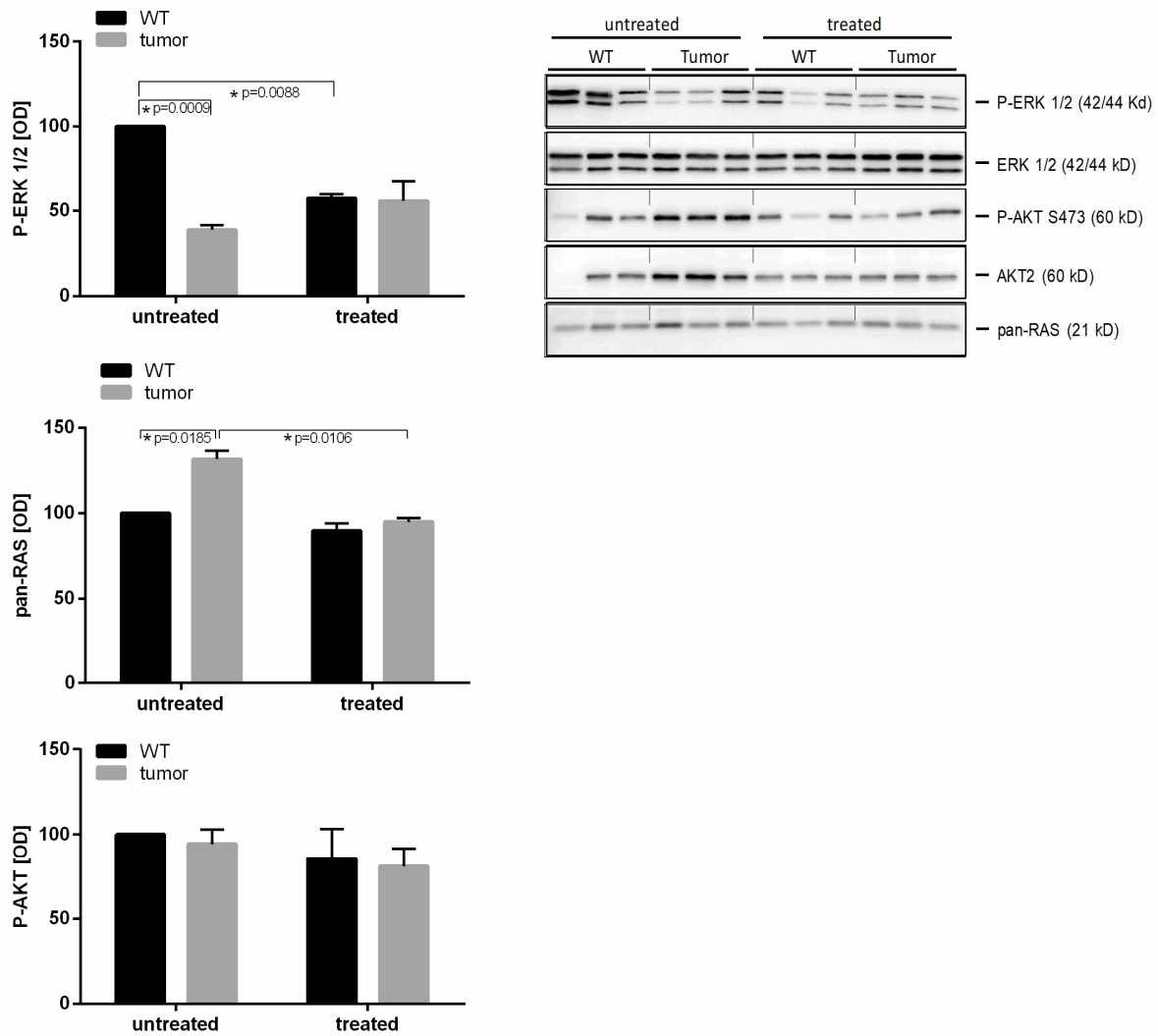


Figure 40: Western blot analysis of *Apcmin/+ x Cav1-KO* mice treated with a Hsp90 inhibitor. *Apcmin/+ x Cav1-KO* mice were treated with the Hsp90 inhibitor 17-DMAG (i.p., 12,5 mg/kg, 4 x per week, n=3 per group) for 4 weeks. Detection of P-ERK 1/2 (42/44 kD), pan-RAS (21 kD), P-AKT protein in TCL is shown together with the quantitative analyses. 17-DMAG treatment reduced pan-RAS protein levels and influenced P-ERK 1/2 expression. OD values of bands in gels were normalized to ERK 1/2 or AKT2 and calculated as -fold \pm S.E. (n=3; *p<0.05 treated vs. untreated; Two-way ANOVA).

Western blot experiments demonstrated a significant decrease in P-ERK 1/2 expression in tissue of untreated WT compared with untreated *Apcmin/+ x Cav1-KO* mice.

For pan-RAS expression, an expected significant increase of 30 % \pm 5 % was seen in the untreated *Apcmin/+ x Cav1-KO* mice compared with the untreated WT mice. In addition, a downregulation by 35 % of pan-RAS protein was seen in the treated *Apcmin/+ x Cav1-KO* mice compared with the untreated *Apcmin/+ x Cav1-KO* mice. In contrast, no changes between untreated WT mice compared with treated WT mice was detected.

Examination of P-AKT expression revealed no changes, neither between the untreated nor between the treated WT and *Apcmin/+ x Cav1-KO* mice.

Taken together, these *in vivo* data suggest that Hsp90 may be important for stabilizing PPAR γ /MTMR7 complex. However, this experiment needs to be repeated with a minimum of n = 5-10 per group due to the limited case number.

3.6.3. Therapy of *Apcmin/+ x Cav1-KO* mice with rosiglitazone

To establish the effect of rosi treatment on the expression level of KRAS, immunohistochemical staining was performed. Paraffin blocks of a *Apcmin/+ x Cav1-KO* mice therapy with rosi (provided by Teresa Friedrich (Friedrich, Richter et al. 2013)) were used. The *Apcmin/+ x Cav1-KO* mice received a chow diet supplemented with 0.02 % (w/w) rosi (~25 mg/kg*day) for 4 months and were sacrificed at 7 months of age (Figure 41).

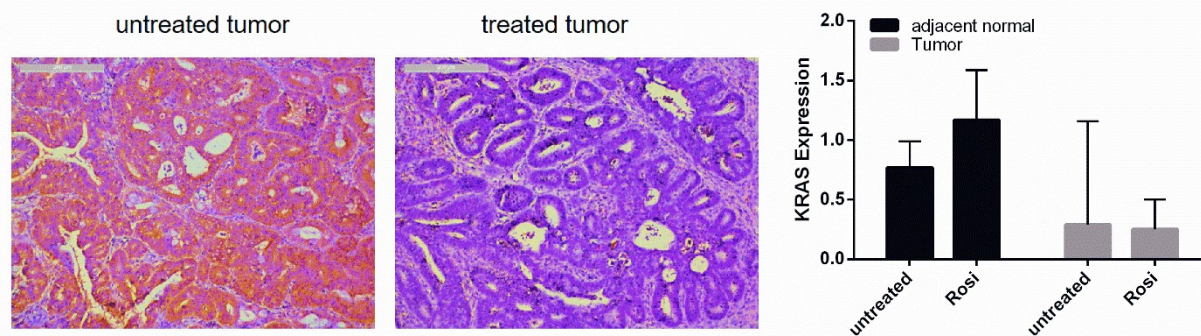


Figure 41: Loss of KRAS staining in rosiglitazone-treated *Apcmin/+ x Cav1-KO* mice. Representative pictures are shown together with statistical analysis after scoring (see 2.6.4). Magnification 100x Results were calculated as -fold \pm S.E. (untreated n=6; treated n=5; n.s.; Two-way ANOVA).

Immunohistochemical staining revealed a reduction of KRAS staining in tumor tissue compared with adjacent normal tissue in the untreated and the treated *Apcmin/+ x Cav1-KO* mice. Although, no difference between the treated and the untreated *Apcmin/+ x Cav1-KO* mice was detected. Generally, KRAS level was lower in APC mutant mice irrespective of treatment compared to WT mice (data not shown).

Due to low case numbers, this experiment is a preliminary impression of rosi impact on KRAS expression in *Apcmin/+ x Cav1-KO* mice.

4. Discussion

The major aim of the thesis was to characterize the role and function of the lipid phosphatase MTMR7 in colorectal cancer *in vivo* and *in vitro*. MTMR7 was found as a novel binding partner of PPAR γ (Söhn, Weidner et al., unpublished). Since mutations in RAS genes (*KRAS*, *NRAS*) cause intrinsic unresponsiveness of colorectal cancer (CRC) patients to therapy with antibodies directed against the epidermal growth factor receptor (Karapetis, Khambata-Ford et al. 2008), targets downstream of mutant RAS hold the promise to overcome therapy resistance in this patient group. The already published inhibiting effect of the phosphatase MTMR7 on the two major pathways RAF-MEK1/2-ERK1/2 and AKT/mTORC1/2 downstream of mutant *KRAS* indicated that the lipid phosphatase MTMR7 plays an essential role in colorectal carcinoma (Weidner, Söhn et al. 2016). Thus, this thesis aimed to elucidate, if the MTMR7-PPAR γ -complex could be a druggable target for the treatment of *KRAS*-mutated CRC patients.

With respect to tissue expression, this work completed the expression analysis in murine tissue performed in the initial description by Majerus et al. 2003. As reported, expression of MTMR7 is found in neuronal tissue, liver, and kidney tissues on the mRNA level. A further agreement can be found in the quantitative evaluation of the mRNA content, in which the high expression in brain tissue was confirmed. In addition to the earlier MTMR7 expression analyses, MTMR7 mRNA could also be detected in muscle tissue and in all sections of the gastrointestinal tract in this work. Moreover, MTMR7 mRNA is expressed in several colorectal cancer cell lines, indicating a potential role of the phosphatase in the disease of colorectal carcinoma.

In line with the findings on mRNA level and in contrast to Majerus et al. 2003, the protein expression pattern of MTMR7 could be extended by heart, lung, liver, kidney, muscle, and all parts of the gastrointestinal tract in murine tissue. Furthermore, MTMR7 expression is found in human cell lines of colorectal cancer.

Subcellular localization of MTMR7 revealed a colocalization with RAB9, a late endosomal marker. This result corroborated the suggestion of Majerus et al. 2003, that MTMR7 is enriched in endosomes or the Golgi apparatus, since RAB9 functions in transport between late endosomes and the trans Golgi network (Lombardi, Soldati et al. 1993), proposing a role of MTMR7 in membrane trafficking. Another indication that MTMR7 influences membrane trafficking, is the fact that it uses PI(3)P as substrates (Weidner, Söhn et al. 2016) and these, but not PI(3,5)P₂, are found in multivesicular bodies (Hnia, Vaccari et al. 2012).

Furthermore, MTMR7 contains a conserved region of about 70 amino acids, the GRAM domain, which also exists in glucosyltransferases, GTPase-activating proteins of the RAB small GTPases, and other proteins associated with membrane-coupled processes (Doerks, Strauss et al. 2000). Interestingly, localization of MTMR7 was dependent on the number of cells on the slide: Nuclear localization for single cells and cytosolic localization for cells grown to confluency. This observation may further corroborate a possible role of MTMR7 in membrane trafficking. However, this hypothesis has to be further elucidated.

The peroxisome proliferator-activated receptor-gamma (PPAR γ) is a ligand-activated transcription factor. PPAR γ is involved in the regulation of several processes including, glucose and lipid metabolism (Polvani, Tarocchi et al. 2016), inflammation, wound healing, differentiation (e.g. of mesenchymal and epithelial cells) and cancer (Burgermeister and Seger 2007, Srivastava, Kollipara et al. 2014, Zurlo, Ziccardi et al. 2016). For instance, the expression of genes involved in differentiation and growth inhibition are controlled by PPAR γ , and it is reported to be a negative regulator of the cell cycle (Grommes, Landreth et al. 2004). The nuclear receptor can be activated by its agonists like rosi- and pioglitazone, belonging to the thiazolidinedione family (van Beekum, Fleskens et al. 2009, Peymani, Ghoochani et al. 2013). Its activation inhibits proliferation of tumor cells derived from liposarcoma, breast adenocarcinoma (Rubin, Zhao et al. 2000), prostate carcinoma, colorectal carcinoma, non-small-cell lung carcinoma, pancreatic carcinoma, bladder cancer, gastric carcinoma, and glial tumors of the brain (Chattopadhyay, Singh et al. 2000). Furthermore, the tumor suppressor PTEN and the cyclin-dependent kinase inhibitor P21 are induced by thiazolidinediones, which contributes to their antiproliferative activity. However, pharmacological activation of the nuclear receptor is not only beneficial for malignant and inflammatory diseases (Rubin, Zhao et al. 2000, Tyagi, Gupta et al. 2011). For example, cardiovascular side effects (Erdmann, Charbonnel et al. 2007) and a pro-carcinogenic impact in bladder cancer (Neumann, Weill et al. 2012, Bosetti, Rosato et al. 2013), but not in colorectal cancer has been demonstrated for therapy with pioglitazone. Interestingly, there was a modest risk reduction of colorectal cancer in relation to thiazolidinediones and an inverse association particularly with rosi (Bosetti, Rosato et al. 2013).

Hence, PPAR γ specific agonists are currently in clinical trials as a combination therapy with conventional chemotherapeutics (Peters, Shah et al. 2012). Efatutazone therapy, for example, significantly reduced the size of pancreatic, colon, anaplastic thyroid carcinoma (Shimazaki, Togashi et al. 2008), and esophageal carcinoma (Sawayama, Ishimoto et al. 2014) in xenograft models. However, the combination of efatutazone with FOLFIRI in a phase II study showed no evidence of clinical efficacy (Marshall, Shuster et al. 2014). Furthermore, a phase II study in chronic myeloid leukemia revealed that the combination of pioglitazone with imatinib was well tolerated and yielded a favorable 56% response rate (Prost, Relouzat et al. 2015, Rousselot, Prost et al. 2017).

To better understand the discrepancy between preclinical and clinical efficacies of PPAR γ , we studied its molecular regulation mechanisms. Its regulation is dependent of its subcellular localization (Zhang, Berger et al. 1996, Camp and Tafuri 1997, van Beekum, Fleskens et al. 2009). It has been shown that the export of PPAR γ to the cytosol is due to mitogenic stimulations. These stimulations were correlated with the nuclear export signal (NES) in the mitogen-activated protein kinase kinase 1/2 (MEK1/2). This nuclear export leads to the reduced ability of PPAR γ to activate nuclear target genes and thus inhibits its genomic function (Burgermeister, Chuderland et al. 2007).

All these data and the fact that PPAR γ is forming a cytosolic complex with MTMR7 in human *KRAS*-mutated colorectal cancer cell lines (Söhn, Weidner et al., unpublished) gave evidence that this complex might be a druggable target in anti-cancer therapy.

Therefore, this thesis followed the investigations of P. Weidner (Weidner, Söhn et al. 2016) to further examine the molecular mechanism of PPAR γ -MTMR7 complex formation and its consequences.

CoIP experiments confirmed that the MTMR7-PPAR γ complex is located in the cytosol and it is being formed endogenously in HCT116 as well as in HEK293T cells after MTMR7 overexpression. These results were verified by immunofluorescence microscopy and proximity ligation assay, where endogenous PPAR γ and overexpressed MTMR7 were localized in the cytoplasm. This finding was unexpected, as PPAR γ alone is usually found in the nucleus.

We previously showed a reduced ERK 1/2 phosphorylation after MTMR7 overexpression (Weidner, Söhn et al. 2016) and assumed that this could be a new mechanism of a positive amplification loop of cytosolic PPAR γ on the transcriptional activity of the receptor in the nucleus. In detail, cytosolic PPAR γ seems to activate the lipid phosphatase MTMR7, which inhibits ERK 1/2 signaling and thereby activates PPAR γ activity in the nucleus (Söhn, Weidner et al., unpublished).

To test this hypothesis, subcellular fractionation was performed in the present work to analyze the nuclear and cytosolic distribution of the nuclear receptor PPAR γ . There was no cytosolic change in PPAR γ after MTMR7 overexpression, even after stimulation with 20 % FCS and rosi. In contrast, a decrease in phosphorylated (inhibited) PPAR γ in the nuclear fraction could be detected after MTMR7 transfection, while the unphosphorylated nuclear receptor amount remained unaltered.

However, an increased activity of the PPAR γ -response-element was found, which indicates activation of the nuclear receptor by MTMR7. This fact could also be underlined by upregulation of TFF3, a secretory protein in the gastrointestinal mucosa and a PPAR γ -target gene.

Thus, MTMR7 failed to evoke a massive translocation of PPAR γ to the nucleus, which was also demonstrated by immunofluorescence staining, suggesting that its positive effect on PPAR γ transcriptional activity might be via prevention of its inhibitory phosphorylation by the RAS-ERK 1/2 pathway.

Based on these data, the following mechanisms, how MTMR7 augments the transcriptional activity of PPAR γ , can be proposed: 1) by EGFR endocytosis routes or 2) by RAS down-regulation followed by reduced ERK 1/2 activity.

It is well known that the levels of EGFR (Keohavong, DeMichele et al.) at the cell surface are strictly regulated by a complex endocytotic machinery. After internalization, EGFR is either recycled back to the cell surface or transported to the late endosome or lysosome for degradation (Chi, Cao et al. 2011).

Phosphatidylinositol(3)phosphate (PI(3)P) also plays an important role in determining the flux of receptors toward the degradation and recycling pathways and is required for EGFR trafficking and degradation and, therefore, is a key regulator of endosomal morphology and function (Simonsen, Wurmser et al. 2001, Fili, Calleja et al. 2006). It has been shown that either the depletion of PI(3)P (Futter, Collinson et al. 2001, Lu, Hope et al. 2003, Petiot, Faure et al. 2003, Tsujita, Itoh et al. 2004) or increased levels of the phospholipids (Cao, Backer et al. 2008) impaired endosomal EGFR sorting, indicating that a tightly coordinated balance of overall PI(3)P is essential for proper growth factor receptor endocytosis and sorting.

Notably, these PI(3)Ps link the myotubularins to the EGF receptor. Cao et al. showed that the depletion of MTM1 or MTMR2 increased PI(3)P levels and slowed down EGFR degradation in two different keratinocyte cell lines, but EGFR internalization in response to ligand stimulation was unaffected by MTM depletion (Cao, Backer et al. 2008).

The present work showed that MTMR7 promoted membrane retention of EGFR in colorectal cancer cells and thereby reduced accumulation of EGFR in the nucleus (Burgermeister, Höde et al. 2017). The latter had been associated with highly proliferative tissue by Shiaw-Yih Lin et al., showing that nuclear EGFR is highly expressed in the uterus of mice on day 6 of pregnancy, in basal cells of human normal oral mucosa, and in breast cancer samples (Shiaw-Yih Lin 2001). In addition, nuclear EGFR expression has been associated with tumor progression and worse survival prognosis in cancer of the breast, ovary, oropharynx, esophagus, and non-small cell lung cancer (Lo, Xia et al. 2005, Psyrris, Yu et al. 2005, Hoshino, Fukui et al. 2007, Traynor, Weigel et al. 2013). Moreover, its nuclear expression is highly linked to an enhanced resistance to radiation, chemotherapy, and the anti-EGFR therapies gefitinib and cetuximab (Brand, Iida et al. 2013).

The data cited above suggest that MTMR7-mediated reduction of nuclear EGFR might lead to inhibition of proliferation and a better response to anti-EGFR therapies in colorectal cancer patients. Thus, MTMR7 may play an important role in colorectal cancer and EGFR sorting and it could be a possible future druggable target for overcoming therapy resistance in colorectal cancer patients.

As mentioned before, RAS-proteins (K-RAS, H-RAS and N-RAS) are the most frequently mutated proteins in cancers, including pancreatic (65 %), colorectal (33 %), and lung cancer (16 %) (Data from COSMIC v84 release, (Forbes, Bindal et al. 2011)). They are involved in the regulation of many cellular processes, including the control of cell proliferation, transformation, differentiation, and survival (Malumbres and Barbacid 2003, Ahearn, Haigis et al. 2011). The activity state of RAS proteins is in turn controlled by binding of growth factors to upstream receptor tyrosine kinases (RTKs), resulting in the recruitment of guanine nucleotide exchange factors which then catalyze the switch from the inactive, guanosine diphosphate (GDP)-bound to the active, guanosine triphosphate (GTP)-bound states (Downward 2003, Ahearn, Haigis et al. 2011). Mutations in RAS proteins occur predominantly at the amino acids in the CDS (coding sequence) at position G12, G13, and Q 61 (Buhrman, Holzapfel et al. 2010). Due to a defect in hydrolysis of GTP to GDP, these mutations result in a persistent GTP-bound state of RAS, leading to a constitutive activation of downstream signaling (Scheffzek, Ahmadian et al. 1997, Scheidig, Burmester et al. 1999).

In the present work, a reduced pan-RAS activity as well as a reduced total amount of pan-RAS protein, but not of mRNA, was found upon MTMR7 transfection in *KRAS* mutated colorectal cancer cell lines. However, no translocation to other cell compartments like the cytosol or the nucleus was detected.

Notably, the impact of MTMR7 on RAS down-regulation was higher in SW480 cells carrying the G12V, than in HCT116 carrying the G13D *KRAS* mutation. This might be due to the lower pan-RAS activity of the G13D mutation compared to the G12V, and the high endogenous expression level of MTMR7 in HCT116 cells compared to the low level in SW480 cells.

Thus, MTMR7 overexpression reduced the amount of pan-RAS protein in colorectal cancer cells. Since this was only observed on the protein level and not on the mRNA level, an effect on transcription or mRNA stability could be excluded. Thus, RAS protein might be down-regulated by MTMR7, e.g. by inhibition of translation or reduction of protein stability ("degradation").

RAS degradation was already described by others. However, the mode of RAS degradation remains controversial. Zeng et al. found that the E3 Ligase Nedd4-1 downregulates RAS in normal cells through the lysosomal pathway (Zeng, Wang et al. 2014). In addition, Shukla et al. reported, that the loss of Smad ubiquitination regulatory factor 2 (SMURF2) leads to mutant *KRAS* degradation by the lysosome and thereby inhibits survival and growth of lung and colorectal cancer cell lines, whereas wild type *KRAS* protein levels remained almost unaffected (Shukla, Allam et al. 2014). Furthermore, Lu et al. reported that *KRAS* degradation is carried out through the lysosome (Lu, Hope et al. 2003), which was also shown by others, reporting a lysosome-mediated degradation after 4-hydroxy-tamoxifen treatment (Kohli, Kaza et al. 2013).

In contrast, Jeong et al. provided evidence for a proteasomal mechanism of RAS degradation (Jeong, Yoon et al. 2012). Pan et al., developed a recombinant chimeric protein, which induces cell death in mutant KRAS-expressing pancreatic tumor cell lines and a tumor mouse model of pancreatic cancer exemplifying that RAS protein can also be degraded through the proteasomal system (Pan, Zhang et al. 2016).

Here, the two major mechanisms of degradation were considered, namely lysosomal protein degradation and the ubiquitin-proteasome system. The lysosome was discovered in rat liver in 1953 by Christian de Duve as vacuolar structure containing hydrolytic enzymes which function optimally in an acidic pH (De Duve, Gianetto et al. 1953, Gianetto and De Duve 1955). Lysosomal degradation starts with the intake of exogenous proteins and particles as well as endogenous proteins and cellular organelles. Exogenous proteins are digested via receptor-mediated endocytosis and pinocytosis, exogenous particle via phagocytosis, and endogenous proteins and cellular organelles via micro- and macro-autophagy.

The ubiquitin-proteasome system was discovered 30 years later by Aaron Ciechanover, Avram Hershko und Irwin Rose and rewarded for the Nobel Prize for chemistry in 2004. They found that proteins are continuously marked for degradation by ubiquitin, generating a polyubiquitin chain, which serves as the binding and degradation signal for the 26S proteasome, a multi subunit protease complex (Ciechanover 2005).

However, these two major pathways of protein degradation, i.e. lysosomal or proteasomal, did not clarify the mechanism of RAS down-regulation upon MTMR7 overexpression. In contrast, loss of RAS protein level was enhanced upon chloroquine treatment, meaning that RAS is not degraded via lysosomal acidification, but RAS can be further diminished using a lysosomal inhibitor. Furthermore, no regeneration of RAS protein was seen in MTMR7-transfected cells treated with MG132, indicating that RAS is not degraded via the proteasomal pathway.

Thus, alternative mechanism next to protein degradation may be involved here: For example, membrane association of KRAS is still not fully clarified and remains to be evaluated. Publications commonly suggest that RAS is attached to membranes by binding of its polybasic domain to the negatively charged phospholipids at the inner leaflet of the plasma membrane and the weak, lipophilic association through CAAX-sequence modulations. In addition, there must be other mechanisms to keep RAS attached to membranes (Willumsen, Christensen et al. 1984, Schmick, Vartak et al. 2014, Schmick, Kraemer et al. 2015). One described mechanism is the PDE δ -Arl-2 delivery system which continuously shuffles KRAS back to the plasma membrane. This process is as fast as the KRAS dissociation from membranes, leading to a constant steady-state level of KRAS at the plasma membrane (Schmick, Kraemer et al. 2015).

Since RAS seemed not to be degraded via the lysosome or the proteasome, literature research suggested a possible down-regulation through a biophysical mechanism.

Hancock et al. suggest an alternative mechanism of RAS post-translational regulation that involves changes in the membrane potential. They report membrane assembling of RAS proteins via nanoclusters, containing about six RAS proteins (Zhou and Hancock 2015). The stability of these clusters is enhanced by plasma membrane depolarization upon increased extracellular K⁺ concentrations and in contrast disrupted by hyperpolarization, achieved by expressing Kv2.1, a voltage-gated K⁺ channel (Zhou, Prakash et al. 2017).

Meanwhile, the results obtained in the present work showed the opposite effect. Instead of preventing loss of RAS using high extracellular K⁺ concentrations, down-regulation of RAS was promoted. In contrast, hyperpolarization blocking the influx of Na⁺ ions into the cytosol using amiloride prevented MTMR7-induced loss of RAS protein.

One possible explanation of RAS down-regulation upon MTMR7 transfection is its substrate specificity for PI(3)P. By dephosphorylation of PI(3)P to PI, the membrane also depolarizes, and RAS might get unstable due to the lost, negative charge of the inner leaflet of the plasma membrane. This idea, though, is not supported by available literature. Instead, there are two alternatives: 1) phosphatidylserine, but not PI(3)P is part of RAS nanoclusters (Zhou, Prakash et al. 2017), 2) the amount of all available PIPs at the plasma membrane is less than 10 % (Robinson and Dixon 2006). Thus, the contribution of MTMs to the overall membrane potential remains elusive.

Currently, the RAS down-regulation mechanism upon MTMR7 overexpression is still unclear. It might be due to multiple mode of actions including changes in translational initiation or protein stability. Another possibility could be autophagy, since several MTMs play a role here. Hence, more detailed analysis is needed to resolve this issue.

Nevertheless, the MTMR7-mediated activation of the nuclear receptor PPAR γ is still possible through the RAS down-regulation pathway. If that would be true, it could also be an explanation why MTMR7 did not facilitate nuclear import of PPAR γ like the inhibitors of RAS signaling Dok-1 and Caveolin-1 (Burgermeister, Friedrich et al. 2011). Instead, MTMR7 inhibits RAS (its activity and protein level), leading to a lower ERK 1/2 activity, which results in the reduction of inhibitory PPAR γ phosphorylation and in an increase of the transcriptional PPAR γ activity, and finally culminating in the activation of tumor suppressor genes like Dok-1 and Caveolin-1.

The mutual inhibition of the RAS-pathway and PPAR γ is well known from the literature. PPAR γ inhibition is due to constant active RAS, which leads to the permanent activation of MEK-1. This in turn inhibits PPAR γ in two ways: 1) MEK-1 leads to a constant export of PPAR γ from the nucleus to the cytosol (Burgermeister, Chuderland et al. 2007) and 2) MEK-1 leads to a constant phosphorylation of ERK 1/2, which phosphorylates PPAR γ at serine 84/114 (in humans) (Zhang, Berger et al. 1996, Camp and Tafuri 1997, van Beekum, Fleskens et al. 2009). The RAS-pathway is inhibited by PPAR γ -mediated up-regulation of tumor suppressors like PTEN and CDKIs (P21). Activated PTEN interrupts the PI3K-AKT/PKB- signaling pathway by dephosphorylating phosphatidylinositol phosphates (especially IP3) (Leslie, Kriplani et al. 2016). This negative feedback loops lead to inhibition of the RAS oncogenic driver pathways.

In conclusion, the tumor suppressor MTMR7 reduces the cellular amount of RAS, which prevents nuclear export of PPAR γ (Burgermeister, Chuderland et al. 2007), resulting in the activation of tumor suppressor genes (Burgermeister, Friedrich et al. 2011). Thus, the MTMR7-PPAR γ crosstalk might be a new target for the treatment of colorectal cancer, where constantly mutant *KRAS* leads to treatment failure of EGFR therapy in colorectal cancer patients.

There are currently no therapeutic approaches available to target mutant *KRAS* and there is a great need to identify effective druggable targets for *KRAS* mutated cancers.

Previously published results showed reduced growth rates upon MTMR7 overexpression compared with cells that received EV controls. Moreover, knockdown of endogenous MTMR7 showed an increase in tumor cell proliferation, consistent with the fact that MTMR7 is lost in colorectal cancer patients during tumor progression (Weidner, Söhn et al. 2016). Furthermore, our research evinced that proliferation is further inhibited by stimulating the cells with the PPAR γ ligand rosiglitazone (Friedrich 2013, Weidner 2016).

Thus, the intrinsic unresponsiveness of *KRAS* mutant cells to anti-EGFR therapy might be circumvented by the combination of PPAR γ -ligands, such as rosiglitazone with kinase inhibitors, downstream of mutant *KRAS*, like a multi-kinase inhibitor (sorafenib), inhibiting the RAF-kinase and several tyrosine kinases of the VEGF signaling pathway and mTOR-inhibitors (everolimus).

These inhibitors are already approved in the clinic, sorafenib for Hepatocellular carcinoma (HCC) (Lang 2008), and everolimus for neuroendocrine tumors (NET) of gastrointestinal or lung origin (Liu and Kunz 2017).

The results obtained showed that using MTMR7 together with either sorafenib or everolimus could not efficiently reduce the viability of colorectal cancer cells. Non-cancer cells, though, were sensitive to MTMR7 overexpression in combination with the inhibitors. In contrast, in presence of MTMR7 and the two drugs, proliferation of the cells was much slower as in respective monotherapies with each single drug, whereas resistance remained in the absence of MTMR7. The effect was also seen in non-cancer cells, but it was not as strong as in the two colorectal cancer cell lines. This indicates a potential specific effect of MTMR7 on RAS mutant cancer cell lines, consistent with the observation that MTMR7 down-regulates RAS protein. Another possibility might be the MTMR7-mediated inhibition of compensatory alternative signaling pathways (e.g. Wnt e.a.) that is activated if the RAF and mTOR signaling pathways are inhibited. However, the inhibiting effect of MTMR7 could not be further enhanced by additional treatment with the PPAR γ ligand rosiglitazone, which might be due to the already profound inhibition of tumor cell growth upon MTMR7 transfection and by the two kinase inhibitors.

Due to unwanted toxicity and side effects, the use of multiple inhibitors in clinical combination regimens often hinders therapy success. Concerning MTMR7 and its role in colorectal cancer patients, it is already published, that the lipid phosphatase is either present or completely absent in colorectal cancer tumor cells, which was shown in immunohistochemical staining on tissue microarrays (Weidner, Söhn et al. 2016). Additionally, MTMR7 positive tumor cells were associated with reduced local tumor growth, stage, and grade. This fact and the diminished *MTMR7* mRNA expression in colorectal cancer patient samples indicated that MTMR7 is lost during tumor development and tumor growth (Weidner, Söhn et al. 2016).

Hence, to resupply MTMR7 as a tumor suppressor and RAS-inhibitory protein to the cells might be a promising anti-tumor approach. Gene therapy in patients, though, is not feasible, and neither transgenic nor KO mice of MTMR7 are available to critically test this idea. Therefore, a docking site peptide corresponding to the coiled-coil domain of MTMR7 and a scrambled control-peptide were designed (by E. Burgermeister, unpublished) to test their effect on tumor cell proliferation. In fact, the peptide was effective and inhibited proliferation in a series of *KRAS*-mutated and *KRAS*-WT human cancer cell lines from the colon, stomach and pancreas, in the micromolar range (1-10 μ M). Notably, a tendency of RAS-inhibition upon MTMR7-peptide treatment was seen, however, it did not affect ERK 1/2 phosphorylation. In line with this data, SRE activation was diminished upon MTMR7-peptide treatment, indicating that the peptide is active and inhibits RAS-ERK 1/2 signaling. These data indicated that therapy with this MTMR7-peptide might be feasible also *in vivo*.

In general, peptides are highly effective and selective and therefore a good starting point for developing novel therapeutics (Fosgerau and Hoffmann 2015). In addition, they are associated with excellent safety and tolerability in humans, as well as with a shorter time to be developed and to get approved. Disadvantages in the past were their chemical and physical instability, their short half-time and their susceptibility to hydrolysis and oxidation (Fosgerau and Hoffmann 2015). Another obstacle is oral bioavailability, which is due to digestive enzymes that would break down amid bonds and thereby diminish the efficacy of the drug (Lau and Dunn 2017). Nevertheless, physicochemical properties of peptides could be improved by introducing chemical modifications like lactam bridges, stabilizing α -helices or salt bridge formations (Fosgerau and Hoffmann 2015). Presently, over 60 peptide drugs have been approved in Europe, the United States, and Japan, and there are about 150 in clinical development for several indications, including oncology (Lau

and Dunn 2017). For instance, Lupron™ from Abbott Laboratories is a peptide-based drug used for prostate cancer treatment (Kaspar and Reichert 2013, Fosgerau and Hoffmann 2015). Another one, Goserelin, targets the gonadotropin-releasing hormone receptor, and is used for palliative treatment of advanced prostate and breast cancer (Kaspar and Reichert 2013).

In sum, there are several peptide drugs available which closely mimic natural pathways by adding back or supplementing peptides in cases where they are missing or inadequate endogenously. The most prominent one might be insulin, first therapeutically used in 1922 (Banting, Best et al. 1922, Lau and Dunn 2017). If that could also be true for MTMR7 in the treatment of colorectal cancer patients, remains to be evaluated.

To investigate expression and regulation of PPAR γ and MTMR7 in vivo, we analyzed genetically modified mouse models (GEMMS) for CRC.

In vivo therapies were carried out in a *Apcmin/+ x Cav1-KO* mouse model established previously by our research group (Friedrich, Richter et al. 2013). These mice mostly develop highly vascularized, distal colorectal tumors. Genetically, these mice show a downregulation of genes related to the transcription factor PPAR γ and an upregulation of genes related to the RAS-signature like *Kras* and *Nras* (Friedrich 2013).

Since ColP experiments showed that MTMR7 is not only forming a complex with PPAR γ and MTMR9, but also with the Heat-shock protein 90 (Hsp90), *Apcmin/+ x Cav1-KO* mice were treated with 17-DMAG, a water-soluble derivative of the Hsp90 inhibitor geldanamycin, to investigate if Hsp90 is also involved in the stabilization of MTMR7.

In line with the previous data (Friedrich, Richter et al. 2013), highly vascularized, distal colorectal tumors were found in the untreated mice. Nevertheless, the tumor size could be diminished by treating the *Apcmin/+ x Cav1-KO* mice with the Hsp90 inhibitor. Furthermore, *Kras* gene expression was higher in the untreated tumor *Apcmin/+ x Cav1-KO* mice than in the untreated WT mice, as expected (Friedrich 2013). Under therapy a downregulation of *Kras* was seen in the tumor group compared to the WT mice. This held true on protein level, where pan-RAS expression was diminished in the treated *Apcmin/+ x Cav1-KO* mice compared to the untreated *Apcmin/+ x Cav1-KO* mice. This effect could also be seen in the decrease in P-ERK 1/2 expression in tissue of treated WT and treated *Apcmin/+ x Cav1-KO* mice compared to the untreated WT control mice. In addition, *Mtmr7* gene expression was higher in the treated WT and *Apcmin/+ x Cav1-KO* mice indicating a stabilization of *Mtmr7* in the WT mice upon 17-DMAG treatment and an indirect impact of MTMR7 on KRAS expression. The therapy effect on protein-level could not be assessed due to a lack of commercially available antibody against mouse MTMR7 suitable for IHC. However, this would be of great importance since MTMR7 was shown to be regulated on the protein and not on the mRNA level (Weidner, Söhn et al. 2016).

To evaluate the impact of pharmacological PPAR γ -activation on KRAS expression, a cohort of rosiglitazone-treated *Apcmin/+ x Cav1-KO* mice was used (Friedrich, Richter et al. 2013). A decrease of KRAS protein was seen in tumor tissue compared with adjacent normal tissue in the untreated and the treated *Apcmin/+ x Cav1-KO* mice which was in accordance to previous obtained data on *Kras* mRNA level. Due to the lack of freshly frozen tissue, *Mtmr7* expression could not be assessed in these mice, and, thus, no correlation between *Mtmr7* and *Kras* expression could be established. However, upregulation of the RAS-inhibitory proteins and tumor suppressors *Cav1* and *Dok1* might suggest that this could also true for *Mtmr7* (Friedrich 2013).

Taken together, this thesis delineated the expression and function of the lipid phosphatase MTMR7 and its relation to the RAS signaling pathway and the therapy resistance in colorectal carcinoma.

Through down-regulation of total and active RAS protein, MTMR7 reduces the activity of ERK 1/2, a negative regulator of PPAR γ , and thereby enhances transcriptional activity of the nuclear receptor (Figure 42, adapted from the DKFZ-MOST Ca158 proposal and progress reports by Dr. Elke Burgermeister).

MTMR7 inhibited active mutant and total RAS protein and on the other hand enhanced transcriptional activity of PPAR γ elevated the expression of PPAR γ target genes. Furthermore, MTMR7 promoted membrane retention of EGFR in colorectal cancer cells and thereby reduced nuclear EGFR expression, which is associated with tumor progression in patients (Shiaw-Yih Lin 2001). Its sensitizing effect on kinase inhibitor therapy and the fact that a synthetic MTMR7-peptide inhibited proliferation of colorectal carcinoma cell lines proposed it as a potent target for therapeutic strategies against CRC in patients. Nevertheless, the exact mechanism of MTMR7-mediated RAS-inhibition needs to be clarified in the future. Due to its absence in many colorectal carcinomas, which is independent of patient's KRAS mutation status, MTMR7 could also be a potential marker for therapy resistance, although it would be important to clarify precisely at which stage the tumor suppressor is lost during carcinogenesis.

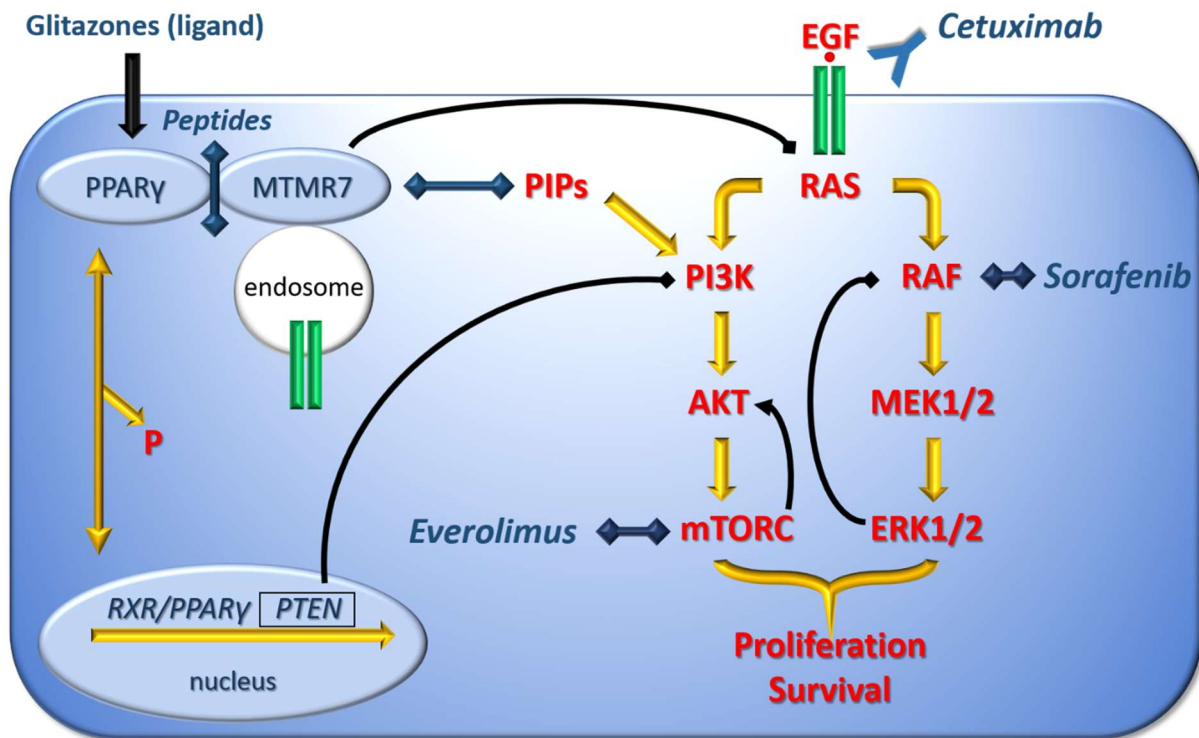


Figure 42: Model for RAS inhibition by MTMR7. Oncogenic RAS leads to a constant export of the nuclear transcription factor PPAR γ to the cytosol where it binds to MTMR7. MTMR7 down-regulates RAS, leading to the reduced ERK 1/2 activity, which results in the reduction of PPAR γ phosphorylation, a decrease in PPAR γ inhibition and in the activation of tumor suppressor genes like PTEN and finally in the inhibition of proliferation of KRAS-mutated CRC cells. Legend: Blue: tumor inhibitors; Red: tumor promoters; Yellow arrows-activation; Black arrows-inhibition. (adapted from Burgermeister (DKFZ-MOST, Ca158))

4.1. Outlook

The current thesis investigated the possible molecular and cellular mechanisms of MTMR7-mediated RAS down-regulation on multiple levels and by means of a series of experimental approaches. However, it has not been achievable to conclusively clarify the exact mode of action. Therefore, it will be necessary in the future to investigate functional cross-talk of MTMR7 and RAS in depth. One approach would be to specifically block either the PI3K class 2 or the PI3K class 3 kinases to assess whether RAS down-regulation is indeed associated with the disappearance of the PI(3)P molecule from internal cellular membranes (e.g. endosomes). Moreover, successful cloning of a mutant KRAS plasmid tagged with RFP would be helpful to detect GFP-MTMR7 and RFP-RAS protein in normal cycling colorectal cancer cells using live cell imaging or immunofluorescence co-staining. Nethertheless, the understanding of MTMR7 as a KRAS regulator is indispensable to further validate and develop it as a potential future target for colorectal cancer therapy.

In addition, it would be very important to examine the MTMR7-peptide efficacy in a *Kras* mutated mouse model *in vivo*, which was beyond the scope of this thesis, but might be an important milestone to elaborate the proof of concept if MTMR7 may be a druggable target to overcome therapy resistance in colorectal carcinoma patients.

5. Abbreviations

AB	Antibody
ACO	Acyl-CoA oxidase
APC	Adenomatous polyposis coli
ARC	Arcuate nucleus
Bp	Base pairs
BSA	Bovine serum albumin
CAV-1	Caveolin-1
cDNA	Complementary DNA
CD36	Cluster of differentiation 36
CDS	Coding sequence
CIN	Chromosomal instability
CIMP	CpG island methylator phenotype
c-like	Caspase-like activity
CMS	Consensus molecular subtypes
CoIP	Coimmunoprecipitation
COX	Cyclooxygenase
CRC	Colorectal cancer
Ct-like	Chymotrypsin-like activity
CT-values	cycle thresholds
DAB	3,3'-Diaminobenzidine
DAPI	4',6-diamidino-2-phenylindole
DMEM	Dulbecco's modified eagles medium
DMSO	Dimethylsulfoxid
DNA	Deoxyribonucleic acid
DOK-1	Docking protein-1
EDTA	ethylenediaminetetraacetic acid
EGF	Epidermal growth factor
EGFR	Epidermal growth factor receptor
ENaC	Epithelium sodium channel
ER	Endoplasmic reticulum
ERK	Extracellular signal related kinase
EtOH	Ethanol
EV	Empty vector
FAB	Familial adenomatous polyposis
FCS	Fetal calf serum
FL	Full-length
FOLFIRI	Folinic acid, fluorouracil, irinotecan
FOLFOX	Folinic acid, fluorouracil, oxaliplatin
5-FU	5-Fluoruracil
GDP	Guanosine diphosphate

GEF	Guanine nucleotide exchange factor
GFP	Green fluorescent protein
GTP	Guanosine triphosphate
HEK	Human embryonic kidney
HEPES	4-(2-hydroxyethyl)-1-piperazineethanesulfonic acid
HNPCC	Hereditary non-polyposis colorectal cancer
H-RAS	Harvey RAS
HSP90	Heat shock protein 90
IHC	Immunohistochemistry
INS	insoluble
IP	Immunoprecipitation
KCl	Potassium chloride
kD	Kilo dalton
K-RAS	Kirsten Ras
LB medium	lysogeny broth medium
LHA	Lateral hypothalamic area
LOH	Loss of heterozygosity
LV	Leucovorin
MEK	mitogen-activated protein
MMR	Mismatch repair
mRNA	Messenger ribonucleic acid
MSI	Microsatellite instability
MTMR	Myotubularin-related
MTT	3-(4,5-dimethylthiazol-2-yl)-2,5-diphenyltetrazolium
NES	Nuclear export signal
NRAS	Neuroblastoma RAS
NTC	Non-template control
NUC	Nuclear
OS	Overall survival
PBS	Phosphate buffered saline
PCR	Polymerase chain reaction
PEPCK	Phosphoenolpyruvate carboxykinase
PH-GRAM	Pleckstrin homology domain
PI3P	Phosphatidylinositol-3-phosphate
PLA	Proximity ligation assay
PPAR γ	Peroxisome proliferator activated receptor gamma
PPRE	PPAR γ response element
PI	Phosphatidylinositol

Abbreviations

pT	p-target (expression vector)
PTEN	Phosphatase and tensin homolog
PVN	Paraventricular nucleus
RAF	Rapidly accelerated fibrosarcoma
RBD	RAS binding domain
RNA	Ribonucleic acid
Rosi	rosiglitazone
RT	Room temperature
RTK	Receptor tyrosine kinases
RXR	9-cis retinoid x receptor
SDS	sodium dodecyl sulfate
shRNA	Small hairpin RNA
SID	Set interaction domain
SRE	Serum response element
TCL	Total cell lysate
TFF3	Trefoil factor 3
T-like	Trypsin-like activity
TP53	Tumor protein 53
TYS	Thymidylate synthase
Ub	ubiquitin
VEGF	Vascular endothelial growth factor
VAT	Visceral adipose tissue
WT	Wild-type
X-Gal	5-bromo-4-chloro-3-indolyl- β -D-galactopyranoside

6. References

- Ahearn, I. M., K. Haigis, D. Bar-Sagi and M. R. Philips (2011). "Regulating the regulator: post-translational modification of RAS." Nat Rev Mol Cell Biol **13**(1): 39-51.
- Ahuja, N., A. L. Mohan, Q. Li, J. M. Stolker, J. G. Herman, S. R. Hamilton, S. B. Baylin and J. P. Issa (1997). "Association between CpG island methylation and microsatellite instability in colorectal cancer." Cancer Res **57**(16): 3370-3374.
- Al-Sohaily, S., A. Biankin, R. Leong, M. Kohonen-Corish and J. Warusavitarne (2012). "Molecular pathways in colorectal cancer." J Gastroenterol Hepatol **27**(9): 1423-1431.
- Andre, T., A. de Gramont, D. Vernerey, B. Chibaudel, F. Bonnetain, A. Tijeras-Raballand, A. Sciva, T. Hickish, J. Tabernero, J. L. Van Laethem, M. Banzi, E. Maartense, E. Shmueli, G. U. Carlsson, W. Scheithauer, D. Papamichael, M. Moehler, S. Landolfi, P. Demetter, S. Colote, C. Tournigand, C. Louvet, A. Duval, J. F. Flejou and A. de Gramont (2015). "Adjuvant Fluorouracil, Leucovorin, and Oxaliplatin in Stage II to III Colon Cancer: Updated 10-Year Survival and Outcomes According to BRAF Mutation and Mismatch Repair Status of the MOSAIC Study." J Clin Oncol **33**(35): 4176-4187.
- Arends, J. W. (2000). "Molecular interactions in the Vogelstein model of colorectal carcinoma." J Pathol **190**(4): 412-416.
- Azzedine, H., A. Bolino, T. Taieb, N. Birouk, M. Di Duca, A. Bouhouche, S. Benamou, A. Mrabet, T. Hammadouche, T. Chkili, R. Gouider, R. Ravazzolo, A. Brice, J. Laporte and E. LeGuern (2003). "Mutations in MTMR13, a new pseudophosphatase homologue of MTMR2 and Sbf1, in two families with an autosomal recessive demyelinating form of Charcot-Marie-Tooth disease associated with early-onset glaucoma." Am J Hum Genet **72**(5): 1141-1153.
- Balla, T., M. Wymann and J. D. York (2012). Phosphoinositides I enzymes of synthesis and degradation. Subcellular biochemistry. Dordrecht ; New York, Springer: 1 online resource (xv, 352 p.).
- Banting, F. G., C. H. Best, J. B. Collip, W. R. Campbell and A. A. Fletcher (1922). "Pancreatic Extracts in the Treatment of Diabetes Mellitus." Can Med Assoc J **12**(3): 141-146.
- Baron, J. A., M. Beach, J. S. Mandel, R. U. van Stolk, R. W. Haile, R. S. Sandler, R. Rothstein, R. W. Summers, D. C. Snover, G. J. Beck, J. H. Bond and E. R. Greenberg (1999). "Calcium supplements for the prevention of colorectal adenomas. Calcium Polyp Prevention Study Group." N Engl J Med **340**(2): 101-107.
- Begley, M. J. and J. E. Dixon (2005). "The structure and regulation of myotubularin phosphatases." Current Opinion in Structural Biology **15**(6): 614-620.
- Begley, M. J., G. S. Taylor, M. A. Brock, P. Ghosh, V. L. Woods and J. E. Dixon (2006). "Molecular basis for substrate recognition by MTMR2, a myotubularin family phosphoinositide phosphatase." Proc Natl Acad Sci U S A **103**(4): 927-932.
- Begley, M. J., G. S. Taylor, S. A. Kim, D. M. Veine, J. E. Dixon and J. A. Stuckey (2003). "Crystal structure of a phosphoinositide phosphatase, MTMR2: insights into myotubular myopathy and Charcot-Marie-Tooth syndrome." Mol Cell **12**(6): 1391-1402.
- Bennett, A. and M. Del Tacca (1975). "Proceedings: Prostaglandins in human colonic carcinoma." Gut **16**(5): 409.
- Berger, P., I. Berger, C. Schaffitzel, K. Tersar, B. Volkmer and U. Suter (2006). "Multi-level regulation of myotubularin-related protein-2 phosphatase activity by myotubularin-related protein-13/set-binding factor-2." Hum Mol Genet **15**(4): 569-579.
- Berger, P., S. Bonneick, S. Willi, M. Wymann and U. Suter (2002). "Loss of phosphatase activity in myotubularin-related protein 2 is associated with Charcot-Marie-Tooth disease type 4B1." Hum Mol Genet **11**(13): 1569-1579.

References

- Berger, P., C. Schaffitzel, I. Berger, N. Ban and U. Suter (2003). "Membrane association of myotubularin-related protein 2 is mediated by a pleckstrin homology-GRAM domain and a coiled-coil dimerization module." *Proc Natl Acad Sci U S A* **100**(21): 12177-12182.
- Berger, P., K. Tersar, K. Ballmer-Hofer and U. Suter (2011). "The CMT4B disease-causing proteins MTMR2 and MTMR13/SBF2 regulate AKT signalling." *J Cell Mol Med* **15**(2): 307-315.
- Bergstraesser, C., S. Hoeger, H. Song, L. Ermantraut, M. Hottenrot, T. Czymai, M. Schmidt, M. Goebeler, N. Ponelies, C. Stich, R. Loesel, G. Molema, M. Seelen, W. van Son, B. A. Yard and N. Rafat (2012). "Inhibition of VCAM-1 expression in endothelial cells by CORM-3: the role of the ubiquitin-proteasome system, p38, and mitochondrial respiration." *Free Radic Biol Med* **52**(4): 794-802.
- Bertotti, A., E. Papp, S. Jones, V. Adleff, V. Anagnostou, B. Lupo, M. Sausen, J. Phallen, C. A. Hruban, C. Tokheim, N. Niknafs, M. Nesselbush, K. Lytle, F. Sassi, F. Cottino, G. Migliardi, E. R. Zanella, D. Ribero, N. Russolillo, A. Mellano, A. Muratore, G. Paraluppi, M. Salizzoni, S. Marsoni, M. Kragh, J. Lantto, A. Cassingena, Q. K. Li, R. Karchin, R. Scharpf, A. Sartore-Bianchi, S. Siena, L. A. Diaz, Jr., L. Trusolino and V. E. Velculescu (2015). "The genomic landscape of response to EGFR blockade in colorectal cancer." *Nature* **526**(7572): 263-267.
- Bolino, A., M. Muglia, F. L. Conforti, E. LeGuern, M. A. Salih, D. M. Georgiou, K. Christodoulou, I. Hausmanowa-Petrusewicz, P. Mandich, A. Schenone, A. Gambardella, F. Bono, A. Quattrone, M. Devoto and A. P. Monaco (2000). "Charcot-Marie-Tooth type 4B is caused by mutations in the gene encoding myotubularin-related protein-2." *Nat Genet* **25**(1): 17-19.
- Bonithon-Kopp, C., O. Kronborg, A. Giacosa, U. Rath and J. Faivre (2000). "Calcium and fibre supplementation in prevention of colorectal adenoma recurrence: a randomised intervention trial. European Cancer Prevention Organisation Study Group." *Lancet* **356**(9238): 1300-1306.
- Bosetti, C., V. Rosato, D. Buniato, A. Zambon, C. La Vecchia and G. Corrao (2013). "Cancer risk for patients using thiazolidinediones for type 2 diabetes: a meta-analysis." *Oncologist* **18**(2): 148-156.
- Botteri, E., S. Iodice, V. Bagnardi, S. Raimondi, A. B. Lowenfels and P. Maisonneuve (2008). "Smoking and colorectal cancer: a meta-analysis." *JAMA* **300**(23): 2765-2778.
- Boyle, P. and J. S. Langman (2000). "ABC of colorectal cancer: Epidemiology." *BMJ* **321**(7264): 805-808.
- Brand, T. M., M. Iida, N. Luthar, M. M. Starr, E. J. Huppert and D. L. Wheeler (2013). "Nuclear EGFR as a molecular target in cancer." *Radiother Oncol* **108**(3): 370-377.
- Brinkmann, B., M. Klintschar, F. Neuhuber, J. Huhne and B. Rolf (1998). "Mutation rate in human microsatellites: influence of the structure and length of the tandem repeat." *Am J Hum Genet* **62**(6): 1408-1415.
- Buhrman, G., G. Holzapfel, S. Fetis and C. Mattos (2010). "Allosteric modulation of Ras positions Q61 for a direct role in catalysis." *Proc Natl Acad Sci U S A* **107**(11): 4931-4936.
- Burgermeister, E., D. Chuderland, T. Hanoch, M. Meyer, M. Liscovitch and R. Seger (2007). "Interaction with MEK causes nuclear export and downregulation of peroxisome proliferator-activated receptor gamma." *Mol Cell Biol* **27**(3): 803-817.
- Burgermeister, E., T. Friedrich, I. Hitkova, I. Regel, H. Einwachter, W. Zimmermann, C. Rocken, A. Perren, M. B. Wright, R. M. Schmid, R. Seger and M. P. A. Ebert (2011). "The Ras Inhibitors Caveolin-1 and Docking Protein 1 Activate Peroxisome Proliferator-Activated Receptor through Spatial Relocalization at Helix 7 of Its Ligand-Binding Domain." *Molecular and Cellular Biology* **31**(16): 3497-3510.
- Burgermeister, E., P. Höde, J. Betge, T. Gutting, A. Merkel, W. Wu, M. Tanzer, M. Mossner, D. Nowak, J. Magdeburg, F. Ruckert, C. Sticht, K. Breitkopf-Heinlein, N. Schulte, N. Hartel, S. Belle, S. Post, T. Gaiser, B. I. Heppner, H. M. Behrens, C. Rocken and M. P. A. Ebert (2017). "Epigenetic silencing of tumor suppressor candidate 3 confers adverse prognosis in early colorectal cancer." *Oncotarget* **8**(49): 84714-84728.

- Burgermeister, E. and R. Seger (2007). "MAPK kinases as nucleo-cytoplasmic shuttles for PPARgamma." *Cell Cycle* **6**(13): 1539-1548.
- Calvo, F., L. Agudo-Ibanez and P. Crespo (2010). "The Ras-ERK pathway: understanding site-specific signaling provides hope of new anti-tumor therapies." *Bioessays* **32**(5): 412-421.
- Camp, H. S. and S. R. Tafuri (1997). "Regulation of peroxisome proliferator-activated receptor gamma activity by mitogen-activated protein kinase." *J Biol Chem* **272**(16): 10811-10816.
- Canavan, C., K. R. Abrams and J. Mayberry (2006). "Meta-analysis: colorectal and small bowel cancer risk in patients with Crohn's disease." *Aliment Pharmacol Ther* **23**(8): 1097-1104.
- Cao, C., J. M. Backer, J. Laporte, E. J. Bedrick and A. Wandinger-Ness (2008). "Sequential Actions of Myotubularin Lipid Phosphatases Regulate Endosomal PI(3)P and Growth Factor Receptor Trafficking." *Molecular Biology of the Cell* **19**(8): 3334-3346.
- Cao, C., J. Laporte, J. M. Backer, A. Wandinger-Ness and M. P. Stein (2007). "Myotubularin lipid phosphatase binds the hVPS15/hVPS34 lipid kinase complex on endosomes." *Traffic* **8**(8): 1052-1067.
- Chattopadhyay, N., D. P. Singh, O. Heese, M. M. Godbole, T. Sinohara, P. M. Black and E. M. Brown (2000). "Expression of peroxisome proliferator-activated receptors (PPARS) in human astrocytic cells: PPARgamma agonists as inducers of apoptosis." *J Neurosci Res* **61**(1): 67-74.
- Chi, S., H. Cao, Y. Wang and M. A. McNiven (2011). "Recycling of the epidermal growth factor receptor is mediated by a novel form of the clathrin adaptor protein Eps15." *J Biol Chem* **286**(40): 35196-35208.
- Cho, E., S. A. Smith-Warner, D. Spiegelman, W. L. Beeson, P. A. van den Brandt, G. A. Colditz, A. R. Folsom, G. E. Fraser, J. L. Freudenheim, E. Giovannucci, R. A. Goldbohm, S. Graham, A. B. Miller, P. Pietinen, J. D. Potter, T. E. Rohan, P. Terry, P. Toniolo, M. J. Virtanen, W. C. Willett, A. Wolk, K. Wu, S. S. Yaun, A. Zeleniuch-Jacquotte and D. J. Hunter (2004). "Dairy foods, calcium, and colorectal cancer: a pooled analysis of 10 cohort studies." *J Natl Cancer Inst* **96**(13): 1015-1022.
- Chojnowski, A., N. Ravise, C. Bachelin, C. Depienne, M. Ruberg, B. Brugg, J. Laporte, A. Baron-Van Evercooren and E. LeGuern (2007). "Silencing of the Charcot-Marie-Tooth associated MTMR2 gene decreases proliferation and enhances cell death in primary cultures of Schwann cells." *Neurobiol Dis* **26**(2): 323-331.
- Christoforidis, S., M. Miaczynska, K. Ashman, M. Wilm, L. Zhao, S. C. Yip, M. D. Waterfield, J. M. Backer and M. Zerial (1999). "Phosphatidylinositol-3-OH kinases are Rab5 effectors." *Nat Cell Biol* **1**(4): 249-252.
- Ciechanover, A. (2005). "Intracellular protein degradation: from a vague idea thru the lysosome and the ubiquitin-proteasome system and onto human diseases and drug targeting." *Cell Death Differ* **12**(9): 1178-1190.
- Clapper, M. L., W. C. Chang and N. J. Meropol (2001). "Chemoprevention of colorectal cancer." *Curr Opin Oncol* **13**(4): 307-313.
- Cross, A. J., S. Boca, N. D. Freedman, N. E. Caporaso, W. Y. Huang, R. Sinha, J. N. Sampson and S. C. Moore (2014). "Metabolites of tobacco smoking and colorectal cancer risk." *Carcinogenesis* **35**(7): 1516-1522.
- Cunningham, D., W. Atkin, H. J. Lenz, H. T. Lynch, B. Minsky, B. Nordlinger and N. Starling (2010). "Colorectal cancer." *Lancet* **375**(9719): 1030-1047.
- Cunningham, D., Y. Humblet, S. Siena, D. Khayat, H. Bleiberg, A. Santoro, D. Bets, M. Mueser, A. Harstrick, C. Verslype, I. Chau and E. Van Cutsem (2004). "Cetuximab monotherapy and cetuximab plus irinotecan in irinotecan-refractory metastatic colorectal cancer." *N Engl J Med* **351**(4): 337-345.
- Davies, R. J., R. Miller and N. Coleman (2005). "Colorectal cancer screening: prospects for molecular stool analysis." *Nat Rev Cancer* **5**(3): 199-209.

References

- Davies, R. L., V. A. Grosse, R. Kucherlapati and M. Bothwell (1980). "Genetic analysis of epidermal growth factor action: assignment of human epidermal growth factor receptor gene to chromosome 7." Proc Natl Acad Sci U S A **77**(7): 4188-4192.
- De Duve, C., R. Gianetto, F. Appelmans and R. Wattiaux (1953). "Enzymic content of the mitochondria fraction." Nature **172**(4390): 1143-1144.
- De Stefano, A. and C. Carlomagno (2014). "Beyond KRAS: Predictive factors of the efficacy of anti-EGFR monoclonal antibodies in the treatment of metastatic colorectal cancer." World J Gastroenterol **20**(29): 9732-9743.
- Doerks, T., M. Strauss, M. Brendel and P. Bork (2000). "GRAM, a novel domain in glucosyltransferases, myotubularins and other putative membrane-associated proteins." Trends Biochem Sci **25**(10): 483-485.
- Dowling, J. J., S. E. Low, A. S. Busta and E. L. Feldman (2010). "Zebrafish MTMR14 is required for excitation-contraction coupling, developmental motor function and the regulation of autophagy." Hum Mol Genet **19**(13): 2668-2681.
- Downward, J. (2003). "Targeting RAS signalling pathways in cancer therapy." Nat Rev Cancer **3**(1): 11-22.
- Eaden, J. A., K. R. Abrams and J. F. Mayberry (2001). "The risk of colorectal cancer in ulcerative colitis: a meta-analysis." Gut **48**(4): 526-535.
- El Zouhairi, M., A. Charabaty and M. J. Pishvaian (2011). "Molecularly targeted therapy for metastatic colon cancer: proven treatments and promising new agents." Gastrointest Cancer Res **4**(1): 15-21.
- Erdmann, E., B. Charbonnel, R. G. Wilcox, A. M. Skene, M. Massi-Benedetti, J. Yates, M. Tan, R. Spanheimer, E. Standl, J. A. Dormandy and P. R. Investigators (2007). "Pioglitazone use and heart failure in patients with type 2 diabetes and preexisting cardiovascular disease: data from the PROactive study (PROactive 08)." Diabetes Care **30**(11): 2773-2778.
- Fares, H. and I. Greenwald (2001). "Genetic analysis of endocytosis in *Caenorhabditis elegans*: coelomocyte uptake defective mutants." Genetics **159**(1): 133-145.
- Fearon, E. R. and B. Vogelstein (1990). "A genetic model for colorectal tumorigenesis." Cell **61**(5): 759-767.
- Feng, Y., B. Press, W. Chen, J. Zimmerman and A. Wandinger-Ness (2001). "Expression and properties of Rab7 in endosome function." Methods Enzymol **329**: 175-187.
- Fili, N., V. Calleja, R. Woscholski, P. J. Parker and B. Larijani (2006). "Compartmental signal modulation: Endosomal phosphatidylinositol 3-phosphate controls endosome morphology and selective cargo sorting." Proc Natl Acad Sci U S A **103**(42): 15473-15478.
- Firestein, R., P. L. Nagy, M. Daly, P. Huie, M. Conti and M. L. Cleary (2002). "Male infertility, impaired spermatogenesis, and azoospermia in mice deficient for the pseudophosphatase Sbf1." J Clin Invest **109**(9): 1165-1172.
- Forbes, S. A., N. Bindal, S. Bamford, C. Cole, C. Y. Kok, D. Beare, M. Jia, R. Shepherd, K. Leung, A. Menzies, J. W. Teague, P. J. Campbell, M. R. Stratton and P. A. Futreal (2011). "COSMIC: mining complete cancer genomes in the Catalogue of Somatic Mutations in Cancer." Nucleic Acids Res **39**(Database issue): D945-950.
- Fosgerau, K. and T. Hoffmann (2015). "Peptide therapeutics: current status and future directions." Drug Discov Today **20**(1): 122-128.
- Friedrich, T. (2013). Ras-driven mouse models of colorectal cancer: Interaction of MAPKs with the nuclear receptor PPAR γ , Technische Universität München. **naturwissenschaftliche Dissertation**. .

- Friedrich, T., B. Richter, T. Gaiser, C. Weiss, K. P. Janssen, H. Einwächter, R. M. Schmid, M. P. A. Ebert and E. Burgermeister (2013). "Deficiency of caveolin-1 in *Apcmin/+* mice promotes colorectal tumorigenesis." *Carcinogenesis* **34**(9): 2109-2118.
- Futter, C. E., L. M. Collinson, J. M. Backer and C. R. Hopkins (2001). "Human VPS34 is required for internal vesicle formation within multivesicular endosomes." *J Cell Biol* **155**(7): 1251-1264.
- Garland, C. F., F. C. Garland and E. D. Gorham (1999). "Calcium and vitamin D. Their potential roles in colon and breast cancer prevention." *Ann N Y Acad Sci* **889**: 107-119.
- Geigl, J. B., A. C. Obenauf, T. Schwarzbraun and M. R. Speicher (2008). "Defining 'chromosomal instability'." *Trends Genet* **24**(2): 64-69.
- Gelabert-Baldrich, M., D. Soriano-Castell, M. Calvo, A. Lu, A. Vina-Vilaseca, C. Rentero, A. Pol, S. Grinstein, C. Enrich and F. Tebar (2014). "Dynamics of KRas on endosomes: involvement of acidic phospholipids in its association." *FASEB J* **28**(7): 3023-3037.
- Gianetto, R. and C. De Duve (1955). "Tissue fractionation studies. 4. Comparative study of the binding of acid phosphatase, beta-glucuronidase and cathepsin by rat-liver particles." *Biochem J* **59**(3): 433-438.
- Gill, S., C. L. Loprinzi, D. J. Sargent, S. D. Thome, S. R. Alberts, D. G. Haller, J. Benedetti, G. Francini, L. E. Shepherd, J. Francois Seitz, R. Labianca, W. Chen, S. S. Cha, M. P. Heldebrant and R. M. Goldberg (2004). "Pooled analysis of fluorouracil-based adjuvant therapy for stage II and III colon cancer: who benefits and by how much?" *J Clin Oncol* **22**(10): 1797-1806.
- Gillooly, D. J., I. C. Morrow, M. Lindsay, R. Gould, N. J. Bryant, J. M. Gaullier, R. G. Parton and H. Stenmark (2000). "Localization of phosphatidylinositol 3-phosphate in yeast and mammalian cells." *EMBO J* **19**(17): 4577-4588.
- Gillooly, D. J., C. Raiborg and H. Stenmark (2003). "Phosphatidylinositol 3-phosphate is found in microdomains of early endosomes." *Histochem Cell Biol* **120**(6): 445-453.
- Gnjatic, S., C. Wheeler, M. Ebner, E. Ritter, A. Murray, N. K. Altorki, C. A. Ferrara, H. Hepburne-Scott, S. Joyce, J. Koopman, M. B. McAndrew, N. Workman, G. Ritter, R. Fallon and L. J. Old (2009). "Seromic analysis of antibody responses in non-small cell lung cancer patients and healthy donors using conformational protein arrays." *J Immunol Methods* **341**(1-2): 50-58.
- Grady, W. M. and J. M. Carethers (2008). "Genomic and epigenetic instability in colorectal cancer pathogenesis." *Gastroenterology* **135**(4): 1079-1099.
- Graham, J., M. Mushin and P. Kirkpatrick (2004). "Oxaliplatin." *Nat Rev Drug Discov* **3**(1): 11-12.
- Green, S. E., D. M. Bradburn, J. S. Varma and J. Burn (1998). "Hereditary non-polyposis colorectal cancer." *Int J Colorectal Dis* **13**(1): 3-12.
- Grommes, C., G. E. Landreth and M. T. Heneka (2004). "Antineoplastic effects of peroxisome proliferator-activated receptor gamma agonists." *Lancet Oncol* **5**(7): 419-429.
- Guinney, J., R. Dienstmann, X. Wang, A. de Reynies, A. Schlicker, C. Sonesson, L. Marisa, P. Roepman, G. Nyamundanda, P. Angelino, B. M. Bot, J. S. Morris, I. M. Simon, S. Gerster, E. Fessler, E. M. F. De Sousa, E. Missiaglia, H. Ramay, D. Barras, K. Homicsko, D. Maru, G. C. Manyam, B. Broom, V. Boige, B. Perez-Villamil, T. Laderas, R. Salazar, J. W. Gray, D. Hanahan, J. Tabernero, R. Bernards, S. H. Friend, P. Laurent-Puig, J. P. Medema, A. Sadanandam, L. Wessels, M. Delorenzi, S. Kopetz, L. Vermeulen and S. Tejpar (2015). "The consensus molecular subtypes of colorectal cancer." *Nat Med* **21**(11): 1350-1356.
- Hagan, S., M. C. Orr and B. Doyle (2013). "Targeted therapies in colorectal cancer-an integrative view by PPPM." *EPMA J* **4**(1): 3.
- Haggar, F. A. and R. P. Boushey (2009). "Colorectal cancer epidemiology: incidence, mortality, survival, and risk factors." *Clin Colon Rectal Surg* **22**(4): 191-197.

References

- Hnia, K., I. Vaccari, A. Bolino and J. Laporte (2012). "Myotubularin phosphoinositide phosphatases: cellular functions and disease pathophysiology." Trends Mol Med **18**(6): 317-327.
- Hoshino, M., H. Fukui, Y. Ono, A. Sekikawa, K. Ichikawa, S. Tomita, Y. Imai, J. Imura, H. Hiraishi and T. Fujimori (2007). "Nuclear expression of phosphorylated EGFR is associated with poor prognosis of patients with esophageal squamous cell carcinoma." Pathobiology **74**(1): 15-21.
- IARC Press (2014). World Cancer Report. B. Stewart and P. Kleihues.
- Jaffe, B. M. (1974). "Prostaglandins and cancer: an update." Prostaglandins **6**(6): 453-461.
- Janout, V. and H. Kollarova (2001). "Epidemiology of colorectal cancer." Biomed Pap Med Fac Univ Palacky Olomouc Czech Repub **145**(1): 5-10.
- Jemal, A., L. X. Clegg, E. Ward, L. A. Ries, X. Wu, P. M. Jamison, P. A. Wingo, H. L. Howe, R. N. Anderson and B. K. Edwards (2004). "Annual report to the nation on the status of cancer, 1975-2001, with a special feature regarding survival." Cancer **101**(1): 3-27.
- Jemal, A., M. J. Thun, L. A. Ries, H. L. Howe, H. K. Weir, M. M. Center, E. Ward, X. C. Wu, C. Ehemann, R. Anderson, U. A. Ajani, B. Kohler and B. K. Edwards (2008). "Annual report to the nation on the status of cancer, 1975-2005, featuring trends in lung cancer, tobacco use, and tobacco control." J Natl Cancer Inst **100**(23): 1672-1694.
- Jeong, W. J., J. Yoon, J. C. Park, S. H. Lee, S. H. Lee, S. Kaduwal, H. Kim, J. B. Yoon and K. Y. Choi (2012). "Ras stabilization through aberrant activation of Wnt/beta-catenin signaling promotes intestinal tumorigenesis." Sci Signal **5**(219): ra30.
- Johns, L. E. and R. S. Houlston (2001). "A systematic review and meta-analysis of familial colorectal cancer risk." Am J Gastroenterol **96**(10): 2992-3003.
- Johnson, L., A. Luke, A. Adeyemo, H. W. Deng, B. D. Mitchell, A. G. Comuzzie, S. A. Cole, J. Blangero, M. Perola and M. D. Teare (2005). "Meta-analysis of five genome-wide linkage studies for body mass index reveals significant evidence for linkage to chromosome 8p." Int J Obes (Lond) **29**(4): 413-419.
- Karapetis, C. S., S. Khambata-Ford, D. J. Jonker, C. J. O'Callaghan, D. Tu, N. C. Tebbutt, R. J. Simes, H. Chalchal, J. D. Shapiro, S. Robitaille, T. J. Price, L. Shepherd, H. J. Au, C. Langer, M. J. Moore and J. R. Zalberg (2008). "K-ras mutations and benefit from cetuximab in advanced colorectal cancer." N Engl J Med **359**(17): 1757-1765.
- Kaspar, A. A. and J. M. Reichert (2013). "Future directions for peptide therapeutics development." Drug Discov Today **18**(17-18): 807-817.
- Keohavong, P., M. A. DeMichele, A. C. Melacrinis, R. J. Landreneau, R. J. Weyant and J. M. Siegfried (1996). "Detection of K-ras mutations in lung carcinomas: relationship to prognosis." Clin Cancer Res **2**(2): 411-418.
- Kerbel, R. S., J. Yu, J. Tran, S. Man, A. Vioria-Petit, G. Klement, B. L. Coomber and J. Rak (2001). "Possible mechanisms of acquired resistance to anti-angiogenic drugs: implications for the use of combination therapy approaches." Cancer Metastasis Rev **20**(1-2): 79-86.
- Kim, S. A., P. O. Vacratis, R. Firestein, M. L. Cleary and J. E. Dixon (2003). "Regulation of myotubularin-related (MTMR)2 phosphatidylinositol phosphatase by MTMR5, a catalytically inactive phosphatase." Proc Natl Acad Sci U S A **100**(8): 4492-4497.
- Kohli, L., N. Kaza, T. Coric, S. J. Byer, N. M. Brossier, B. J. Klocke, M. A. Bjornsti, S. L. Carroll and K. A. Roth (2013). "4-Hydroxytamoxifen induces autophagic death through K-Ras degradation." Cancer Res **73**(14): 4395-4405.
- Lang, L. (2008). "FDA approves sorafenib for patients with inoperable liver cancer." Gastroenterology **134**(2): 379.

- Laporte, J., F. Bedez, A. Bolino and J. L. Mandel (2003). "Myotubularins, a large disease-associated family of cooperating catalytically active and inactive phosphoinositides phosphatases." Hum Mol Genet **12 Spec No 2**: R285-292.
- Laporte, J., F. Blondeau, A. Buj-Bello, D. Tentler, C. Kretz, N. Dahl and J. L. Mandel (1998). "Characterization of the myotubularin dual specificity phosphatase gene family from yeast to human." Hum Mol Genet **7**(11): 1703-1712.
- Laporte, J., F. Blondeau, A. Gansmuller, Y. Lutz, J. L. Vonesch and J. L. Mandel (2002). "The PtdIns3P phosphatase myotubularin is a cytoplasmic protein that also localizes to Rac1-inducible plasma membrane ruffles." J Cell Sci **115**(Pt 15): 3105-3117.
- Laporte, J., L. J. Hu, C. Kretz, J. L. Mandel, P. Kioschis, J. F. Coy, S. M. Klauck, A. Poustka and N. Dahl (1996). "A gene mutated in X-linked myotubular myopathy defines a new putative tyrosine phosphatase family conserved in yeast." Nat Genet **13**(2): 175-182.
- Lau, J. L. and M. K. Dunn (2017). "Therapeutic peptides: Historical perspectives, current development trends, and future directions." Bioorg Med Chem.
- Le, D. T., J. N. Uram, H. Wang, B. R. Bartlett, H. Kemberling, A. D. Eyring, A. D. Skora, B. S. Luber, N. S. Azad, D. Laheru, B. Biedrzycki, R. C. Donehower, A. Zaheer, G. A. Fisher, T. S. Crocenzi, J. J. Lee, S. M. Duffy, R. M. Goldberg, A. de la Chapelle, M. Koshiji, F. Bhajjee, T. Huebner, R. H. Hruban, L. D. Wood, N. Cuka, D. M. Pardoll, N. Papadopoulos, K. W. Kinzler, S. Zhou, T. C. Cornish, J. M. Taube, R. A. Anders, J. R. Eshleman, B. Vogelstein and L. A. Diaz, Jr. (2015). "PD-1 Blockade in Tumors with Mismatch-Repair Deficiency." N Engl J Med **372**(26): 2509-2520.
- Lee, M. S. and S. Kopetz (2015). "Current and Future Approaches to Target the Epidermal Growth Factor Receptor and Its Downstream Signaling in Metastatic Colorectal Cancer." Clin Colorectal Cancer **14**(4): 203-218.
- Lefebvre, A. M., I. Chen, P. Desreumaux, J. Najib, J. C. Fruchart, K. Geboes, M. Briggs, R. Heyman and J. Auwerx (1998). "Activation of the peroxisome proliferator-activated receptor gamma promotes the development of colon tumors in C57BL/6J-APCMin/+ mice." Nat Med **4**(9): 1053-1057.
- Leslie, N. R., N. Kriplani, M. A. Hermida, V. Alvarez-Garcia and H. M. Wise (2016). "The PTEN protein: cellular localization and post-translational regulation." Biochem Soc Trans **44**(1): 273-278.
- Levin, B., D. A. Lieberman, B. McFarland, R. A. Smith, D. Brooks, K. S. Andrews, C. Dash, F. M. Giardiello, S. Glick, T. R. Levin, P. Pickhardt, D. K. Rex, A. Thorson, S. J. Winawer, G. American Cancer Society Colorectal Cancer Advisory, U. S. M.-S. T. Force and C. American College of Radiology Colon Cancer (2008). "Screening and surveillance for the early detection of colorectal cancer and adenomatous polyps, 2008: a joint guideline from the American Cancer Society, the US Multi-Society Task Force on Colorectal Cancer, and the American College of Radiology." CA Cancer J Clin **58**(3): 130-160.
- Liechti-Gallati, S., B. Muller, T. Grimm, W. Kress, C. Muller, E. Boltshauser, H. Moser and S. Braga (1991). "X-linked centronuclear myopathy: mapping the gene to Xq28." Neuromuscul Disord **1**(4): 239-245.
- Lievre, A., J. B. Bachet, D. Le Corre, V. Boige, B. Landi, J. F. Emile, J. F. Cote, G. Tomasic, C. Penna, M. Ducreux, P. Rougier, F. Penault-Llorca and P. Laurent-Puig (2006). "KRAS mutation status is predictive of response to cetuximab therapy in colorectal cancer." Cancer Res **66**(8): 3992-3995.
- Liu, I. H. and P. L. Kunz (2017). "Biologics in gastrointestinal and pancreatic neuroendocrine tumors." J Gastrointest Oncol **8**(3): 457-465.
- Liu, Z. Q., T. Mahmood and P. C. Yang (2014). "Western blot: technique, theory and trouble shooting." N Am J Med Sci **6**(3): 160.
- Lloyd, S., S. Mead and J. Collinge (2011). "Genetics of prion disease." Top Curr Chem **305**: 1-22.
- Lo, H. W., W. Xia, Y. Wei, M. Ali-Seyed, S. F. Huang and M. C. Hung (2005). "Novel prognostic value of nuclear epidermal growth factor receptor in breast cancer." Cancer Res **65**(1): 338-348.

References

- Lombardi, D., T. Soldati, M. A. Riederer, Y. Goda, M. Zerial and S. R. Pfeffer (1993). "Rab9 functions in transport between late endosomes and the trans Golgi network." *EMBO J* **12**(2): 677-682.
- Lorenzo, O., S. Urbe and M. J. Clague (2006). "Systematic analysis of myotubularins: heteromeric interactions, subcellular localisation and endosome related functions." *J Cell Sci* **119**(Pt 14): 2953-2959.
- Lu, Q., L. W. Hope, M. Brasch, C. Reinhard and S. N. Cohen (2003). "TSG101 interaction with HRS mediates endosomal trafficking and receptor down-regulation." *Proc Natl Acad Sci U S A* **100**(13): 7626-7631.
- Lynch, H. T. and A. de la Chapelle (2003). "Hereditary colorectal cancer." *N Engl J Med* **348**(10): 919-932.
- Malumbres, M. and M. Barbacid (2003). "RAS oncogenes: the first 30 years." *Nat Rev Cancer* **3**(6): 459-465.
- Marin, J. J., M. R. Romero, P. Martinez-Becerra, E. Herraes and O. Briz (2009). "Overview of the molecular bases of resistance to chemotherapy in liver and gastrointestinal tumours." *Curr Mol Med* **9**(9): 1108-1129.
- Marin, J. J. G., F. Sanchez de Medina, B. Castaño, L. Bujanda, M. R. Romero, O. Martinez-Augustin, R. D. Moral-Avila and O. Briz (2012). "Chemoprevention, chemotherapy, and chemoresistance in colorectal cancer." *Drug Metabolism Reviews* **44**(2): 148-172.
- Marmol, I., C. Sanchez-de-Diego, A. Pradilla Dieste, E. Cerrada and M. J. Rodriguez Yoldi (2017). "Colorectal Carcinoma: A General Overview and Future Perspectives in Colorectal Cancer." *Int J Mol Sci* **18**(1).
- Marshall, J., D. E. Shuster, T. R. Goldberg, C. Copigneaux, S. Chen, H. Zahir, D. Dutta, M. N. Saleh, M. J. Pishvaian, M. S. Varela, F. Palazzo, N. Lazaretti, C. Costa, E. Loredó, J. Leon and R. W. V. Roemeling (2014). "A randomized, open-label phase II study of efatutazone in combination with FOLFIRI as second-line therapy for metastatic colorectal cancer (mCRC)." *Journal of Clinical Oncology* **32**(3_suppl): 535-535.
- Martinez-Useros, J. and J. Garcia-Foncillas (2016). "Obesity and colorectal cancer: molecular features of adipose tissue." *J Transl Med* **14**: 21.
- McCullough, M. L., A. S. Robertson, C. Rodriguez, E. J. Jacobs, A. Chao, J. Carolyn, E. E. Calle, W. C. Willett and M. J. Thun (2003). "Calcium, vitamin D, dairy products, and risk of colorectal cancer in the Cancer Prevention Study II Nutrition Cohort (United States)." *Cancer Causes Control* **14**(1): 1-12.
- Mochizuki, Y. and P. W. Majerus (2003). "Characterization of myotubularin-related protein 7 and its binding partner, myotubularin-related protein 9." *Proceedings of the National Academy of Sciences* **100**(17): 9768-9773.
- Mochizuki, Y. and P. W. Majerus (2003). "Characterization of myotubularin-related protein 7 and its binding partner, myotubularin-related protein 9." *Proc Natl Acad Sci U S A* **100**(17): 9768-9773.
- Mruk, D. D. and C. Y. Cheng (2011). "The myotubularin family of lipid phosphatases in disease and in spermatogenesis." *Biochem J* **433**(2): 253-262.
- Murray, J. T., C. Panaretou, H. Stenmark, M. Miaczynska and J. M. Backer (2002). "Role of Rab5 in the recruitment of hVps34/p150 to the early endosome." *Traffic* **3**(6): 416-427.
- Nandurkar, H. H., K. K. Caldwell, J. C. Whisstock, M. J. Layton, E. A. Gaudet, F. A. Norris, P. W. Majerus and C. A. Mitchell (2001). "Characterization of an adapter subunit to a phosphatidylinositol (3)P 3-phosphatase: identification of a myotubularin-related protein lacking catalytic activity." *Proc Natl Acad Sci U S A* **98**(17): 9499-9504.
- Nandurkar, H. H., M. Layton, J. Laporte, C. Selan, L. Corcoran, K. K. Caldwell, Y. Mochizuki, P. W. Majerus and C. A. Mitchell (2003). "Identification of myotubularin as the lipid phosphatase catalytic subunit associated with the 3-phosphatase adapter protein, 3-PAP." *Proc Natl Acad Sci U S A* **100**(15): 8660-8665.

- Naughtin, M. J., D. A. Sheffield, P. Rahman, W. E. Hughes, R. Gurung, J. L. Stow, H. H. Nandurkar, J. M. Dyson and C. A. Mitchell (2010). "The myotubularin phosphatase MTMR4 regulates sorting from early endosomes." *J Cell Sci* **123**(Pt 18): 3071-3083.
- Neumann, A., A. Weill, P. Ricordeau, J. P. Fagot, F. Alla and H. Allemand (2012). "Pioglitazone and risk of bladder cancer among diabetic patients in France: a population-based cohort study." *Diabetologia* **55**(7): 1953-1962.
- Nicot, A. S., H. Fares, B. Payrastre, A. D. Chisholm, M. Labouesse and J. Laporte (2006). "The phosphoinositide kinase PIKfyve/Fab1p regulates terminal lysosome maturation in *Caenorhabditis elegans*." *Mol Biol Cell* **17**(7): 3062-3074.
- Nicot, A. S. and J. Laporte (2008). "Endosomal phosphoinositides and human diseases." *Traffic* **9**(8): 1240-1249.
- Normanno, N., S. Tejpar, F. Morgillo, A. De Luca, E. Van Cutsem and F. Ciardiello (2009). "Implications for KRAS status and EGFR-targeted therapies in metastatic CRC." *Nature Reviews Clinical Oncology* **6**(9): 519-527.
- Ogino, S., K. Shima, Y. Baba, K. Nosho, N. Irahara, S. Kure, L. Chen, S. Toyoda, G. J. Kirkner, Y. L. Wang, E. L. Giovannucci and C. S. Fuchs (2009). "Colorectal Cancer Expression of Peroxisome Proliferator-Activated Receptor γ (PPARG, PPARgamma) Is Associated With Good Prognosis." *Gastroenterology* **136**(4): 1242-1250.
- Pan, T., Y. Zhang, N. Zhou, X. He, C. Chen, L. Liang, X. Duan, Y. Lin, K. Wu and H. Zhang (2016). "A recombinant chimeric protein specifically induces mutant KRAS degradation and potently inhibits pancreatic tumor growth." *Oncotarget* **7**(28): 44299-44309.
- Pancione, M., N. Forte, L. Sabatino, E. Tomaselli, D. Parente, A. Febbraro and V. Colantuoni (2009). "Reduced beta-catenin and peroxisome proliferator-activated receptor-gamma expression levels are associated with colorectal cancer metastatic progression: correlation with tumor-associated macrophages, cyclooxygenase 2, and patient outcome." *Hum Pathol* **40**(5): 714-725.
- Park, Y., D. J. Hunter, D. Spiegelman, L. Bergkvist, F. Berrino, P. A. van den Brandt, J. E. Buring, G. A. Colditz, J. L. Freudenheim, C. S. Fuchs, E. Giovannucci, R. A. Goldbohm, S. Graham, L. Harnack, A. M. Hartman, D. R. Jacobs, Jr., I. Kato, V. Krogh, M. F. Leitzmann, M. L. McCullough, A. B. Miller, P. Pietinen, T. E. Rohan, A. Schatzkin, W. C. Willett, A. Wolk, A. Zeleniuch-Jacquotte, S. M. Zhang and S. A. Smith-Warner (2005). "Dietary fiber intake and risk of colorectal cancer: a pooled analysis of prospective cohort studies." *JAMA* **294**(22): 2849-2857.
- Peters, J. M., Y. M. Shah and F. J. Gonzalez (2012). "The role of peroxisome proliferator-activated receptors in carcinogenesis and chemoprevention." *Nat Rev Cancer* **12**(3): 181-195.
- Petiot, A., J. Faure, H. Stenmark and J. Gruenberg (2003). "PI3P signaling regulates receptor sorting but not transport in the endosomal pathway." *J Cell Biol* **162**(6): 971-979.
- Peymani, M., A. Ghoochani, K. Ghaedi, F. Karamali, K. Karbalaie, A. Kiani-Esfahani, F. Rabiee, M. H. Nasr-Esfahani and H. Baharvand (2013). "Dual effects of peroxisome proliferator-activated receptor gamma on embryonic stem cell self-renewal in presence and absence of leukemia inhibitory factor." *Eur J Cell Biol* **92**(4-5): 160-168.
- Pino, M. S. and D. C. Chung (2010). "The chromosomal instability pathway in colon cancer." *Gastroenterology* **138**(6): 2059-2072.
- Polvani, S., M. Tarocchi, S. Tempesti, L. Bencini and A. Galli (2016). "Peroxisome proliferator activated receptors at the crossroad of obesity, diabetes, and pancreatic cancer." *World J Gastroenterol* **22**(8): 2441-2459.
- Poschl, G. and H. K. Seitz (2004). "Alcohol and cancer." *Alcohol Alcohol* **39**(3): 155-165.
- Pox, C., S. Aretz, S. C. Bischoff, U. Graeven, M. Hass, P. Heussner, W. Hohenberger, A. Holstege, J. Hubner, F. Kolligs, M. Kreis, P. Lux, J. Ockenga, R. Porschen, S. Post, N. Rahner, A. Reinacher-Schick, J.

References

F. Riemann, R. Sauer, A. Sieg, W. Scheppach, W. Schmitt, H. J. Schmoll, K. Schulmann, A. Tannapfel, W. Schmiegel, A. Leitlinienprogramm Onkologie der, V. Deutschen Krebsgesellschaft e and V. Deutschen Krebshilfe e (2013). "[S3-guideline colorectal cancer version 1.0]." Z Gastroenterol **51**(8): 753-854.

Prenen, H., S. Tejpar and E. Van Cutsem (2010). "New strategies for treatment of KRAS mutant metastatic colorectal cancer." Clin Cancer Res **16**(11): 2921-2926.

Prince, S. K. C. L. (2011). Molecular Chaperones.

Prost, S., F. Relouzat, M. Spentchian, Y. Ouzegdouh, J. Saliba, G. Massonnet, J. P. Beressi, E. Verhoeyen, V. Raggiueneau, B. Maneglier, S. Castaigne, C. Chomienne, S. Chretien, P. Rouselot and P. Leboulch (2015). "Erosion of the chronic myeloid leukaemia stem cell pool by PPARgamma agonists." Nature **525**(7569): 380-383.

Psyrrri, A., Z. Yu, P. M. Weinberger, C. Sasaki, B. Haffty, R. Camp, D. Rimm and B. A. Burtness (2005). "Quantitative determination of nuclear and cytoplasmic epidermal growth factor receptor expression in oropharyngeal squamous cell cancer by using automated quantitative analysis." Clin Cancer Res **11**(16): 5856-5862.

Robertson, D. (2012). "ABC of colorectal cancer." Gastroenterology.

Robinson, F. L. and J. E. Dixon (2006). "Myotubularin phosphatases: policing 3-phosphoinositides." Trends Cell Biol **16**(8): 403-412.

Robinson, F. L. and J. E. Dixon (2006). "Myotubularin phosphatases: policing 3-phosphoinositides." Trends in Cell Biology **16**(8): 403-412.

Rothenberg, M. L., J. R. Eckardt, J. G. Kuhn, H. A. Burris, 3rd, J. Nelson, S. G. Hilsenbeck, G. I. Rodriguez, A. M. Thurman, L. S. Smith, S. G. Eckhardt, G. R. Weiss, G. L. Elfring, D. A. Rinaldi, L. J. Schaaf and D. D. Von Hoff (1996). "Phase II trial of irinotecan in patients with progressive or rapidly recurrent colorectal cancer." J Clin Oncol **14**(4): 1128-1135.

Rouselot, P., S. Prost, J. Guilhot, L. Roy, G. Etienne, L. Legros, A. Charbonnier, V. Coiteux, P. Cony-Makhoul, F. Hugué, E. Cayssials, J. M. Cayuela, F. Relouzat, M. Delord, H. Bruzzoni-Giovanelli, L. Morisset, F. X. Mahon, F. Guilhot, P. Leboulch and C. M. L. G. French (2017). "Pioglitazone together with imatinib in chronic myeloid leukemia: A proof of concept study." Cancer **123**(10): 1791-1799.

Rubin, G. L., Y. Zhao, A. M. Kalus and E. R. Simpson (2000). "Peroxisome proliferator-activated receptor gamma ligands inhibit estrogen biosynthesis in human breast adipose tissue: possible implications for breast cancer therapy." Cancer Res **60**(6): 1604-1608.

Rudge, S. A., D. M. Anderson and S. D. Emr (2004). "Vacuole size control: regulation of PtdIns(3,5)P2 levels by the vacuole-associated Vac14-Fig4 complex, a PtdIns(3,5)P2-specific phosphatase." Mol Biol Cell **15**(1): 24-36.

Saltz, L. B., J. V. Cox, C. Blanke, L. S. Rosen, L. Fehrenbacher, M. J. Moore, J. A. Maroun, S. P. Ackland, P. K. Locker, N. Pirota, G. L. Elfring and L. L. Miller (2000). "Irinotecan plus fluorouracil and leucovorin for metastatic colorectal cancer. Irinotecan Study Group." N Engl J Med **343**(13): 905-914.

Samuels, Y. and V. E. Velculescu (2004). "Oncogenic mutations of PIK3CA in human cancers." Cell Cycle **3**(10): 1221-1224.

Sanchez-Juan, P., M. T. Bishop, Y. S. Aulchenko, J. P. Brandel, F. Rivadeneira, M. Struchalin, J. C. Lambert, P. Amouyel, O. Combarros, J. Sainz, A. Carracedo, A. G. Uitterlinden, A. Hofman, I. Zerr, H. A. Kretschmar, J. L. Laplanche, R. S. Knight, R. G. Will and C. M. van Duijn (2012). "Genome-wide study links MTMR7 gene to variant Creutzfeldt-Jakob risk." Neurobiol Aging **33**(7): 1487 e1421-1488.

Sawayama, H., T. Ishimoto, M. Watanabe, N. Yoshida, H. Sugihara, J. Kurashige, K. Hirashima, M. Iwatsuki, Y. Baba, E. Oki, M. Morita, Y. Shiose and H. Baba (2014). "Small molecule agonists of PPAR-gamma exert therapeutic effects in esophageal cancer." Cancer Res **74**(2): 575-585.

- Scheffzek, K., M. R. Ahmadian, W. Kabsch, L. Wiesmuller, A. Lautwein, F. Schmitz and A. Wittinghofer (1997). "The Ras-RasGAP complex: structural basis for GTPase activation and its loss in oncogenic Ras mutants." *Science* **277**(5324): 333-338.
- Scheidig, A. J., C. Burmester and R. S. Goody (1999). "The pre-hydrolysis state of p21(ras) in complex with GTP: new insights into the role of water molecules in the GTP hydrolysis reaction of ras-like proteins." *Structure* **7**(11): 1311-1324.
- Schmick, M., A. Kraemer and P. I. Bastiaens (2015). "Ras moves to stay in place." *Trends Cell Biol* **25**(4): 190-197.
- Schmick, M., N. Vartak, B. Papke, M. Kovacevic, D. C. Truxius, L. Rossmannek and P. I. H. Bastiaens (2014). "KRas localizes to the plasma membrane by spatial cycles of solubilization, trapping and vesicular transport." *Cell* **157**(2): 459-471.
- Seger, R. and E. G. Krebs (1995). "The MAPK signaling cascade." *FASEB J* **9**(9): 726-735.
- Senderek, J., C. Bergmann, S. Weber, U. P. Ketelsen, H. Schorle, S. Rudnik-Schoneborn, R. Buttner, E. Buchheim and K. Zerres (2003). "Mutation of the SBF2 gene, encoding a novel member of the myotubularin family, in Charcot-Marie-Tooth neuropathy type 4B2/11p15." *Hum Mol Genet* **12**(3): 349-356.
- Shiaw-Yih Lin, K. M., Weiya Xia (2001). "Nuclear localization of EGF receptor."
- Shimazaki, N., N. Togashi, M. Hanai, T. Isoyama, K. Wada, T. Fujita, K. Fujiwara and S. Kurakata (2008). "Anti-tumour activity of CS-7017, a selective peroxisome proliferator-activated receptor gamma agonist of thiazolidinedione class, in human tumour xenografts and a syngeneic tumour implant model." *Eur J Cancer* **44**(12): 1734-1743.
- Shisheva, A. (2008). "PIKfyve: Partners, significance, debates and paradoxes." *Cell Biol Int* **32**(6): 591-604.
- Shukla, S., U. S. Allam, A. Ahsan, G. Chen, P. M. Krishnamurthy, K. Marsh, M. Rumschlag, S. Shankar, C. Whitehead, M. Schipper, V. Basrur, D. R. Southworth, A. M. Chinnaiyan, A. Rehemtulla, D. G. Beer, T. S. Lawrence, M. K. Nyati and D. Ray (2014). "KRAS protein stability is regulated through SMURF2: UBCH5 complex-mediated beta-TrCP1 degradation." *Neoplasia* **16**(2): 115-128.
- Simonsen, A., A. E. Wurmser, S. D. Emr and H. Stenmark (2001). "The role of phosphoinositides in membrane transport." *Curr Opin Cell Biol* **13**(4): 485-492.
- Song, S. Y., M. R. Kang, N. J. Yoo and S. H. Lee (2010). "Mutational analysis of mononucleotide repeats in dual specificity tyrosine phosphatase genes in gastric and colon carcinomas with microsatellite instability." *APMIS* **118**(5): 389-393.
- Srivastava, N., R. K. Kollipara, D. K. Singh, J. Sudderth, Z. Hu, H. Nguyen, S. Wang, C. G. Humphries, R. Carstens, K. E. Huffman, R. J. DeBerardinis and R. Kittler (2014). "Inhibition of cancer cell proliferation by PPARgamma is mediated by a metabolic switch that increases reactive oxygen species levels." *Cell Metab* **20**(4): 650-661.
- Srivastava, S., Z. Li, L. Lin, G. Liu, K. Ko, W. A. Coetzee and E. Y. Skolnik (2005). "The phosphatidylinositol 3-phosphate phosphatase myotubularin-related protein 6 (MTMR6) is a negative regulator of the Ca²⁺-activated K⁺ channel KCa3.1." *Mol Cell Biol* **25**(9): 3630-3638.
- Stein, M. P., C. Cao, M. Tessema, Y. Feng, E. Romero, A. Welford and A. Wandinger-Ness (2005). "Interaction and functional analyses of human VPS34/p150 phosphatidylinositol 3-kinase complex with Rab7." *Methods Enzymol* **403**: 628-649.
- Stein, M. P., Y. Feng, K. L. Cooper, A. M. Welford and A. Wandinger-Ness (2003). "Human VPS34 and p150 are Rab7 interacting partners." *Traffic* **4**(11): 754-771.
- Taguchi-Atarashi, N., M. Hamasaki, K. Matsunaga, H. Omori, N. T. Ktistakis, T. Yoshimori and T. Noda (2010). "Modulation of local PtdIns3P levels by the PI phosphatase MTMR3 regulates constitutive autophagy." *Traffic* **11**(4): 468-478.

References

- Taheri, M., A. Salamian, K. Ghaedi, M. Peymani, T. Izadi, A. S. Nejati, A. Atefi, M. Nematollahi, F. Ahmadi Ghahrizjani, M. Esmaeili, A. Kiani Esfahani, S. Irani, H. Baharvand and M. H. Nasr-Esfahani (2015). "A ground state of PPAR γ activity and expression is required for appropriate neural differentiation of hESCs." *Pharmacol Rep* **67**(6): 1103-1114.
- Taylor, G. S., T. Maehama and J. E. Dixon (2000). "Myotubularin, a protein tyrosine phosphatase mutated in myotubular myopathy, dephosphorylates the lipid second messenger, phosphatidylinositol 3-phosphate." *Proc Natl Acad Sci U S A* **97**(16): 8910-8915.
- Thomas, N. S., H. Williams, G. Cole, K. Roberts, A. Clarke, S. Liechti-Gallati, S. Braga, A. Gerber, C. Meier, H. Moser and et al. (1990). "X linked neonatal centronuclear/myotubular myopathy: evidence for linkage to Xq28 DNA marker loci." *J Med Genet* **27**(5): 284-287.
- Tooze, S. A. and T. Yoshimori (2010). "The origin of the autophagosomal membrane." *Nat Cell Biol* **12**(9): 831-835.
- Traynor, A. M., T. L. Weigel, K. R. Oettel, D. T. Yang, C. Zhang, K. Kim, R. Salgia, M. Iida, T. M. Brand, T. Hoang, T. C. Campbell, H. R. Hernan and D. L. Wheeler (2013). "Nuclear EGFR protein expression predicts poor survival in early stage non-small cell lung cancer." *Lung Cancer* **81**(1): 138-141.
- Tsujita, K., T. Itoh, T. Ijuin, A. Yamamoto, A. Shisheva, J. Laporte and T. Takenawa (2004). "Myotubularin regulates the function of the late endosome through the gram domain-phosphatidylinositol 3,5-bisphosphate interaction." *J Biol Chem* **279**(14): 13817-13824.
- Tyagi, S., P. Gupta, A. S. Saini, C. Kaushal and S. Sharma (2011). "The peroxisome proliferator-activated receptor: A family of nuclear receptors role in various diseases." *J Adv Pharm Technol Res* **2**(4): 236-240.
- van Beekum, O., V. Fleskens and E. Kalkhoven (2009). "Posttranslational modifications of PPAR- γ : fine-tuning the metabolic master regulator." *Obesity (Silver Spring)* **17**(2): 213-219.
- Velichkova, M., J. Juan, P. Kadandale, S. Jean, I. Ribeiro, V. Raman, C. Stefan and A. A. Kiger (2010). "Drosophila Mtm and class II PI3K coregulate a PI(3)P pool with cortical and endolysosomal functions." *J Cell Biol* **190**(3): 407-425.
- Vergne, I., E. Roberts, R. A. Elmaoued, V. Tosch, M. A. Delgado, T. Proikas-Cezanne, J. Laporte and V. Deretic (2009). "Control of autophagy initiation by phosphoinositide 3-phosphatase Jumpy." *EMBO J* **28**(15): 2244-2258.
- Wactawski-Wende, J., J. M. Kotchen, G. L. Anderson, A. R. Assaf, R. L. Brunner, M. J. O'Sullivan, K. L. Margolis, J. K. Ockene, L. Phillips, L. Pottern, R. L. Prentice, J. Robbins, T. E. Rohan, G. E. Sarto, S. Sharma, M. L. Stefanick, L. Van Horn, R. B. Wallace, E. Whitlock, T. Bassford, S. A. Beresford, H. R. Black, D. E. Bonds, R. G. Brzyski, B. Caan, R. T. Chlebowski, B. Cochrane, C. Garland, M. Gass, J. Hays, G. Heiss, S. L. Hendrix, B. V. Howard, J. Hsia, F. A. Hubbell, R. D. Jackson, K. C. Johnson, H. Judd, C. L. Kooperberg, L. H. Kuller, A. Z. LaCroix, D. S. Lane, R. D. Langer, N. L. Lasser, C. E. Lewis, M. C. Limacher, J. E. Manson and I. Women's Health Initiative (2006). "Calcium plus vitamin D supplementation and the risk of colorectal cancer." *N Engl J Med* **354**(7): 684-696.
- Weidner, P. (2016). "Die Interaktion des Kernrezeptors PPAR γ mit der Lipidphosphatase MTMR7 im kolorektalen Karzinom." *Inauguraldissertation*.
- Weidner, P., M. Söhn, T. Gutting, T. Friedrich, T. Gaiser, J. Magdeburg, P. Kienle, H. Ruh, C. Hopf, H. M. Behrens, C. Rocken, T. Hanoch, R. Seger, M. P. Ebert and E. Burgermeister (2016). "Myotubularin-related protein 7 inhibits insulin signaling in colorectal cancer." *Oncotarget* **7**(31): 50490-50506.
- Weisenberger, D. J., K. D. Siegmund, M. Campan, J. Young, T. I. Long, M. A. Faasse, G. H. Kang, M. Widschwendter, D. Weener, D. Buchanan, H. Koh, L. Simms, M. Barker, B. Leggett, J. Levine, M. Kim, A. J. French, S. N. Thibodeau, J. Jass, R. Haile and P. W. Laird (2006). "CpG island methylator phenotype underlies sporadic microsatellite instability and is tightly associated with BRAF mutation in colorectal cancer." *Nat Genet* **38**(7): 787-793.
- Willett, W. C. (2005). "Diet and cancer: an evolving picture." *JAMA* **293**(2): 233-234.

- Willumsen, B. M., A. Christensen, N. L. Hubbert, A. G. Papageorge and D. R. Lowy (1984). "The p21 ras C-terminus is required for transformation and membrane association." *Nature* **310**(5978): 583-586.
- Wu, K., Y. Yang, D. Liu, Y. Qi, C. Zhang, J. Zhao and S. Zhao (2016). "Activation of PPARgamma suppresses proliferation and induces apoptosis of esophageal cancer cells by inhibiting TLR4-dependent MAPK pathway." *Oncotarget* **7**(28): 44572-44582.
- Xue, Y., H. Fares, B. Grant, Z. Li, A. M. Rose, S. G. Clark and E. Y. Skolnik (2003). "Genetic analysis of the myotubularin family of phosphatases in *Caenorhabditis elegans*." *J Biol Chem* **278**(36): 34380-34386.
- Yanagiya, T., A. Tanabe, A. Iida, S. Saito, A. Sekine, A. Takahashi, T. Tsunoda, S. Kamohara, Y. Nakata, K. Kotani, R. Komatsu, N. Itoh, I. Mineo, J. Wada, H. Masuzaki, M. Yoneda, A. Nakajima, S. Miyazaki, K. Tokunaga, M. Kawamoto, T. Funahashi, K. Hamaguchi, K. Tanaka, K. Yamada, T. Hanafusa, S. Oikawa, H. Yoshimatsu, K. Nakao, T. Sakata, Y. Matsuzawa, N. Kamatani, Y. Nakamura and K. Hotta (2007). "Association of single-nucleotide polymorphisms in MTMR9 gene with obesity." *Hum Mol Genet* **16**(24): 3017-3026.
- Yousefnia, S., S. Momenzadeh, F. Seyed Forootan, K. Ghaedi and M. H. Nasr Esfahani (2018). "The influence of peroxisome proliferator-activated receptor gamma (PPARgamma) ligands on cancer cell tumorigenicity." *Gene* **649**: 14-22.
- Yuvaniyama, J., J. M. Denu, J. E. Dixon and M. A. Saper (1996). "Crystal structure of the dual specificity protein phosphatase VHR." *Science* **272**(5266): 1328-1331.
- Zeng, T., Q. Wang, J. Fu, Q. Lin, J. Bi, W. Ding, Y. Qiao, S. Zhang, W. Zhao, H. Lin, M. Wang, B. Lu, X. Deng, D. Zhou, Z. Yin and H. R. Wang (2014). "Impeded Nedd4-1-mediated Ras degradation underlies Ras-driven tumorigenesis." *Cell Rep* **7**(3): 871-882.
- Zhang, B., J. Berger, G. Zhou, A. Elbrecht, S. Biswas, S. White-Carrington, D. Szalkowski and D. E. Moller (1996). "Insulin- and mitogen-activated protein kinase-mediated phosphorylation and activation of peroxisome proliferator-activated receptor gamma." *J Biol Chem* **271**(50): 31771-31774.
- Zhao, R., Y. Qi, J. Chen and Z. J. Zhao (2001). "FYVE-DSP2, a FYVE domain-containing dual specificity protein phosphatase that dephosphorylates phosphatidylinositol 3-phosphate." *Exp Cell Res* **265**(2): 329-338.
- Zhou, Y. and J. F. Hancock (2015). "Ras nanoclusters: Versatile lipid-based signaling platforms." *Biochim Biophys Acta* **1853**(4): 841-849.
- Zhou, Y., P. Prakash, H. Liang, K. J. Cho, A. A. Gorfe and J. F. Hancock (2017). "Lipid-Sorting Specificity Encoded in K-Ras Membrane Anchor Regulates Signal Output." *Cell* **168**(1-2): 239-251 e216.
- Zhou, Y., C. O. Wong, K. J. Cho, D. van der Hoeven, H. Liang, D. P. Thakur, J. Luo, M. Babic, K. E. Zinsmaier, M. X. Zhu, H. Hu, K. Venkatachalam and J. F. Hancock (2015). "SIGNAL TRANSDUCTION. Membrane potential modulates plasma membrane phospholipid dynamics and K-Ras signaling." *Science* **349**(6250): 873-876.
- Zurlo, D., P. Ziccardi, C. Votino, T. Colangelo, C. Cerchia, F. Dal Piaz, S. Dallavalle, S. Moricca, E. Novellino, A. Lavecchia, V. Colantuoni and A. Lupo (2016). "The antiproliferative and proapoptotic effects of cladospirals A and B are related to their different binding mode as PPARgamma ligands." *Biochem Pharmacol* **108**: 22-35.

7. Appendix

7.1. Interaction between MTMR7-PPAR γ and HSP90 (CoIP)

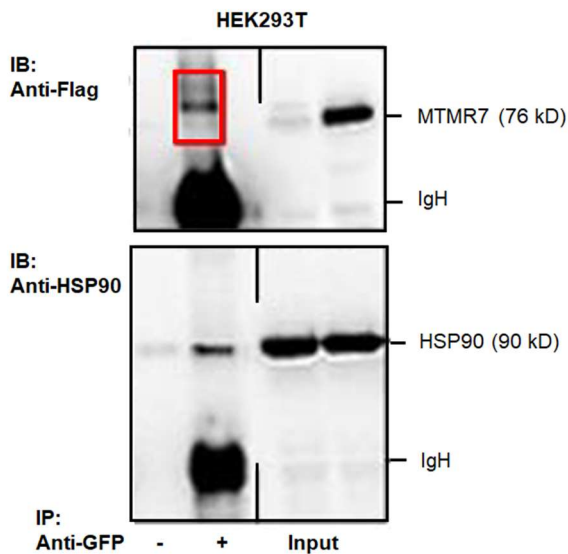
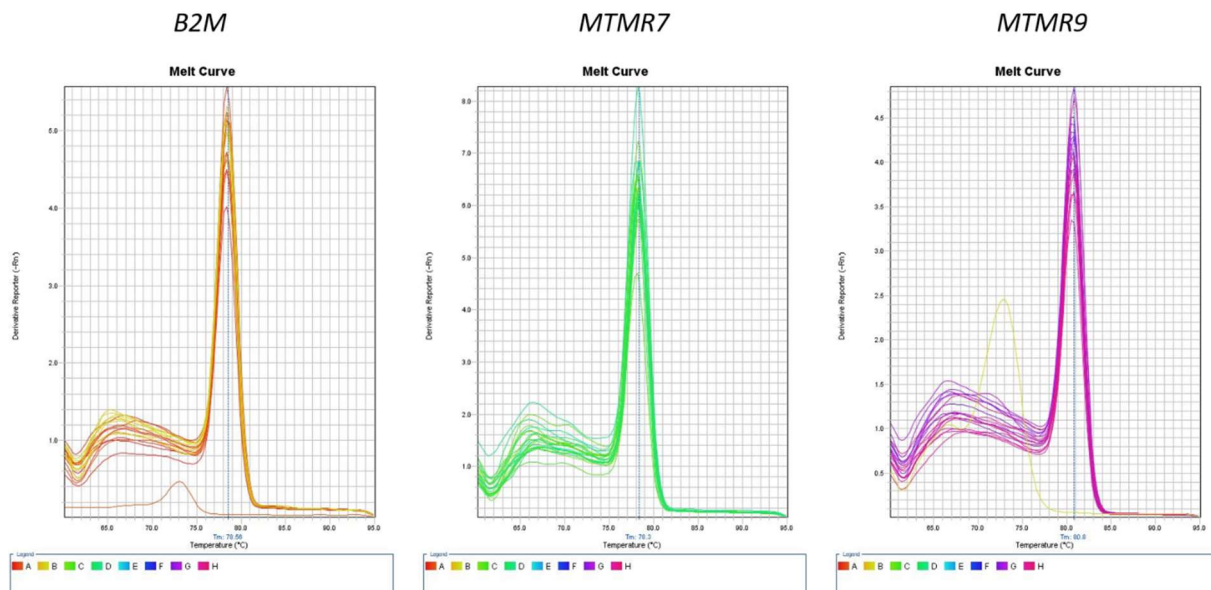


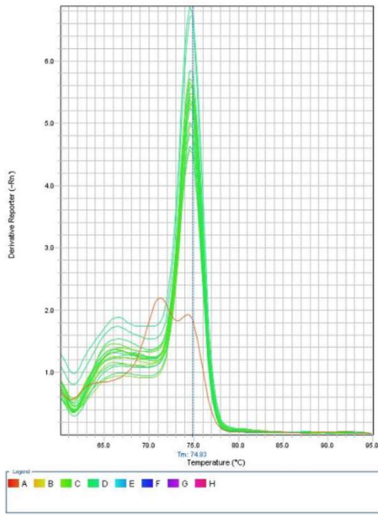
Figure 43: MTMR7 forms a complex with HSP90 and PPAR γ . CoIP of MTMR7 and PPAR γ from total cell lysates. HEK293T cells were transiently transfected with Flag-MTMR7 + GFP-PPAR γ . Immunoprecipitation ("IP") was performed using an anti-GFP Ab or no Ab (bead control). Coprecipitated proteins were detected by Western blot ("IB") using an antibody against anti-Flag or HSP90.

7.2. Melting curves of realtime PCRs

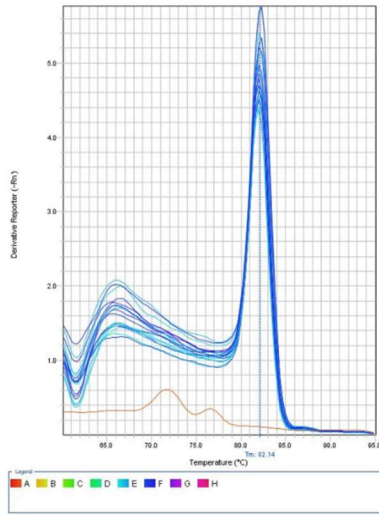
Melt curves celllines



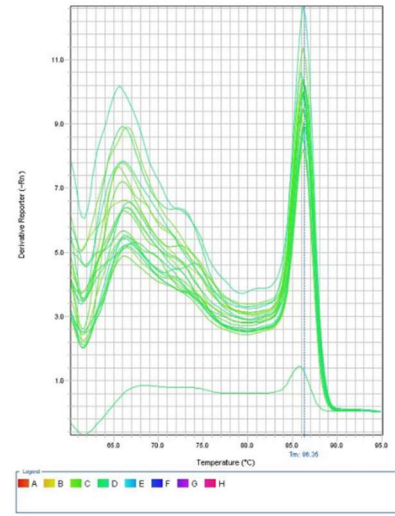
ACO
Melt Curve



PTEN
Melt Curve

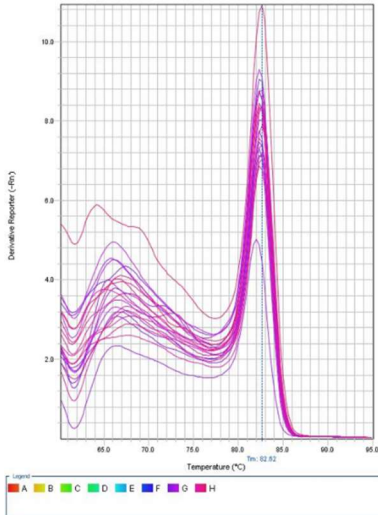


TFF3
Melt Curve



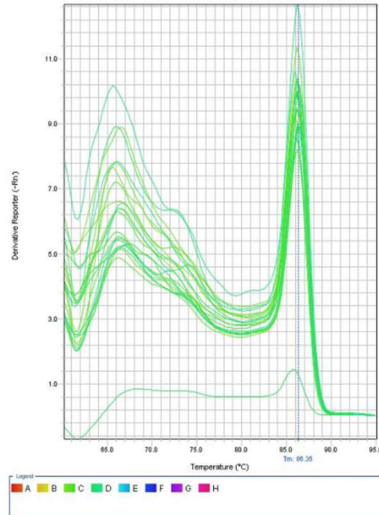
CyclinD1

Melt Curve



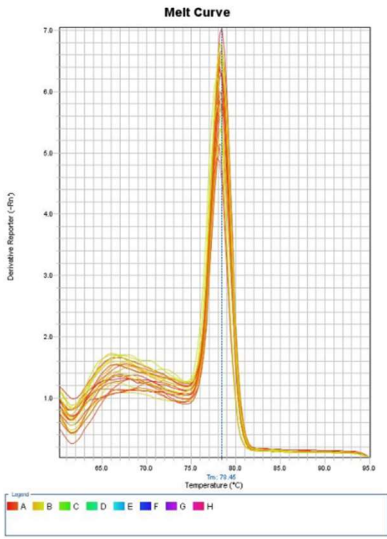
P21

Melt Curve

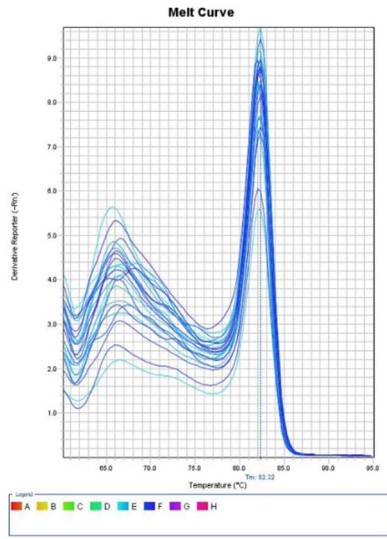


Melt curves 17-DMAG therapy

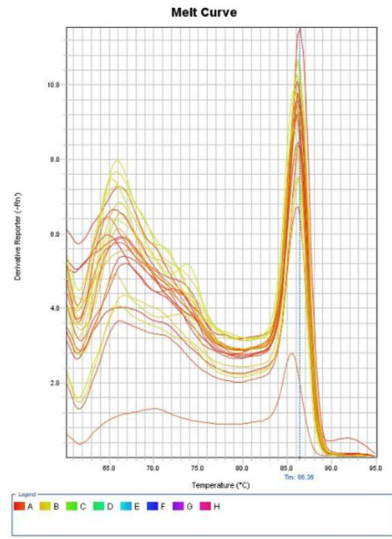
B2m



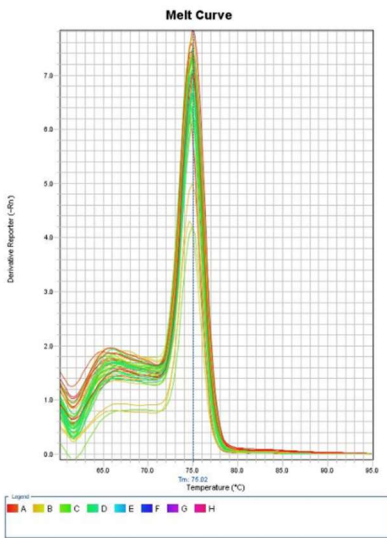
cyclind1



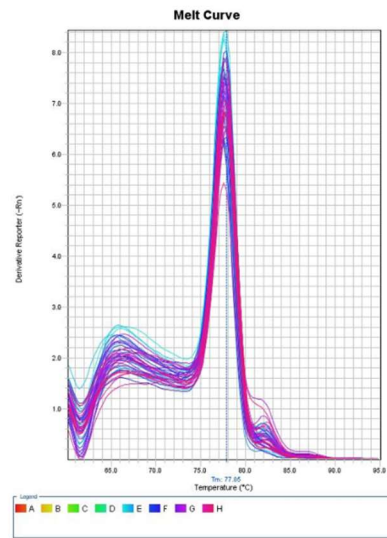
p21



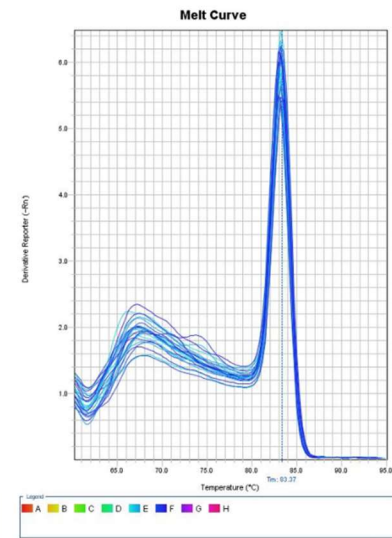
kras



mtmr7



tff3



7.3. RAS down-regulation does not take place on the mRNA level

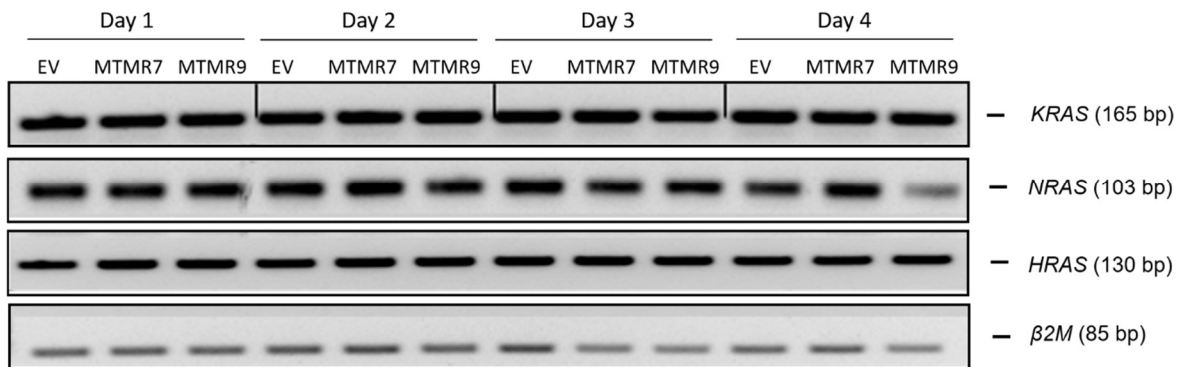


Figure 44: MTMR7-mediated RAS down-regulation is no transcriptional event. Detection of *KRAS*, *NRAS* and *HRAS* cDNA in total RNA extracted from SW480 cells. Representative agarose gels of RT-PCR (35 x cycles) are shown. Expected sizes of amplification products: *KRAS* = 165 bp, *NRAS* = 103 bp, *HRAS* = 130 bp and *B2M* = 85 bp.

7.4. Colocalization between MTMR7 and PH-domains of AKT and PLC δ

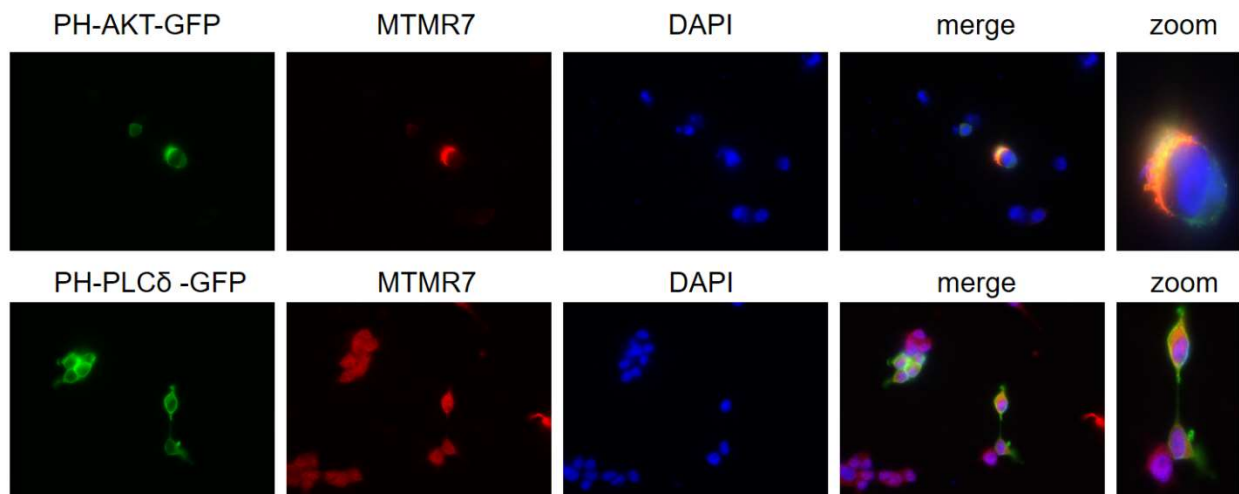


Figure 45: Costaining of MTMR7 and PH-domains of AKT and PLC δ . HEK293T cells were transiently transfected with MTMR7 together with PH-AKT-GFP plasmid or PH-PLC δ -GFP for 24 h. Immunofluorescence staining was done with anti-MTMR7 antibody. Colors: green = PH-AKT-GFP/ PH-PLC δ -GFP, red = MTMR7, blue = nuclei; magnification 400x.